Development and characterisation of a novel myotube-motoneuron 3D co-culture system.

Alec Simon Tulloch Smith

University College, London. Institute of Neurology

Medical Research Council (MRC) Doctoral Training Account

Supervisors: Professor Mark Lewis and Professor Linda Greensmith

Thesis submitted for the degree of Doctor of Philosophy.

University College, London.

2012.

Declaration

I, Alec Smith, confirm that the work presented in this Thesis is my own. Where information has been derived from other sources, I confirm that this has been indicated in the Thesis.

Acknowledgements

First of all, my heartfelt thanks to my supervisors Mark Lewis and Linda Greensmith for all their help, guidance and support during my studies. Thanks also to Vivek Mudera for his insight into the development of the model.

I have been very lucky to work with a great number of people during this project whose help and friendship have seen me through all the dramas and dilemmas I have faced. In no particular order, my thanks to Batool Kazmi, Karen Carlqvist, Bilal Malik, Barney Bryson, Amy Innes, Mhoriam Ahmed, Anna Gray, Phil McGoldrick, Ching-Hua Lu, Adrian Miller, Alex Rossor, Karli Montague, Emem Adet-Amana, Darren Player, Neil Martin, Adam Sharples, Jennifer Verhoekx, Umber Cheema, Kris Gellynk and Rishma Shah.

A special thank you must go to Sam Passey for all her help and for being my partner in crime on this project. Also to Jim Dick for running the lab so smoothly and making it so easy to get stuff done. Thanks to Bernadett Kalmar for her help and guidance with interpreting some of my collected data and to Virginie Bros for her help with the culture and transport of the embryonic stem cells.

A big thank you to Ivo Lieberam, Carolina Barcellos-Machado and Danielle Stevenson, at Kings College, London, for providing the stem cell derived motoneurons used in Chapter 5, and for their help in developing the protocol for using them in this model.

To all my family and friends, especially Calvin, Tracy, Ben and Charlie, thanks for always being there for me and making me who I am. To Natalie, thanks for putting up with me and for all the great times we had when I wasn't working!

Finally, to Mum and Dad, this is for you. Thanks for everything.

Abstract

The aim of this Thesis was to characterise the behaviour and interaction of primary muscle derived cells (MDCs) and motoneurons within a collagen-based 3D *in vitro* culture system.

Cells cultured under uniaxial tension within 3D collagen matrices are known to self-orientate along the lines of principle strain. In the case of skeletal muscle cells, this leads to the formation of aligned myotubes, thereby generating cultures which more closely recapitulate the architecture of *in vivo* muscle. Since maturation of muscle *in vivo* is dependent on functional innervation, integration of this model with a physiologically correct neural input would further improve both the accuracy and complexity of the *in vitro* construct. Furthermore, reliable neuromuscular junction formation in 3D culture could have substantial benefits for the study of neuromuscular disease and the testing of novel therapeutic agents.

The behaviour of primary rat MDCs within an established collagen-based 3D culture system was optimised and subsequently characterised. A comparison of this model to conventional 2D cell culture techniques was carried out using immunohistochemical and PCR analysis. Investigation of myogenin expression levels over a three week culture period in both 2D and 3D found no significant differences between the two systems, indicating a conserved ability for MDC differentiation in both models. Immunohistochemical data illustrated the alignment of uniaxial myotubes in 3D compared with randomly orientated and branched myotubes in conventional culture, demonstrating the improved biomimicity of myotubes developed in 3D and under directional tension.

The presence of motoneurons within the 3D co-culture was found to promote maturation of the MDCs as indicated by levels of macroscopic construct contraction and by quantitative PCR analysis. Co-localisation of pre- and post- synaptic markers in culture indicated the presence of putative synaptic contacts within the model.

The model presented in this Thesis represents a step forward in the development of physiologically accurate *in vitro* models of skeletal muscle, which may help in future investigations of skeletal muscle development, physiology and pathology.

Contents

List of abbreviations

2D	Two dimensional
3D	Three dimensional
ACh	Acetylcholine
AChE	Acetylcholinesterase
AChR	Acetylcholine receptor
ADFNK	Advanced DMEM, F12 and neurobasal media mix supplemented with knock-out serum replacement
ALS	Amyotrophic lateral sclerosis
ANOVA	Analysis of variance
ATP	Adenosine triphosphate
BAC	Bacterial artificial chromosome
BDNF	Brain derived neurotrophic factor
bp	Base pairs
BSA	Bovine serum albumin
Ca^{2+}	Calcium ion
CDK5	Cyclin dependent kinase 5
cDNA	Complementary DNA
CEE	Chick embryo extract
CFM	Culture force monitor
ChAT	Choline acetyltransferase
cm	Centimetre
CNB	Complete neurobasal

CNTF	Ciliary neurotrophic factor
CO_2	Carbon dioxide
DAPI	4,6-diamidino-2-phenylindole
DM	Differentiation medium
DMEM	Dulbecco's modified Eagle's medium
DNA	Deoxyribonucleic acid
Dvl	Dishevelled
ECM	Extracellular matrix
EDL	Extensor digitorum longus
EDTA	Ethylenediaminetetraacetic acid
eGFP	Enhanced green fluorescent protein
EGTA	Ethylene glycol tetraacetic acid
ELISA	Enzyme-linked immunosorbent assay
ESc	Embryonic stem cell
FCS	Fetal calf serum
GABA	γ-Aminobutyric acid
GDNF	Glial cell-derived neurotrophic factor
GGT	Geranylgeranyl transferase
GM	Growth medium
H_20	Water
HB	Homogenising buffer
HB9	Motor neuron and pancreas homeobox 1 (*MNX1*) or Homeobox-9
HBSS	Hank's balanced saline solution
HS	Horse serum

ICC	Immunocytochemistry
IGF-1	Insulin-like growth factor 1
K^+	Potassium ion
L	Litre
LRP4	Lipoprotein receptor-related protein 4
MACS	Magnetic-activated cell sorting
MAP-2	Microtubule-associated protein 2
MEM	Minimal essential medium
MEPP	Miniature endplate potential
MDC	Muscle derived cell
ml	Millilitre
mm	Millimetre
mM	Millimolar
µl	Microlitre
µm	Micromolar
mRNA	Messenger RNA
MuSK	Muscle-specific Kinase
MYHC	Myosin heavy chain
Na^+	Sodium ion
nm	Nanometre
ng	Nanogram
NMJ	Neuromuscular junction
PBS	Phosphate buffered saline
PCR	Polymerase chain reaction

PKC	Protein kinase C
P/S	Penicillin/ Streptomycin
pM	Picomolar
qPCR	Quantitative PCR
RA	Retinoic acid
RNA	Ribonucleic acid
RPII	RNA polymerase 2
SDS	Sodium dodecyl sulfate
Shh	Sonic hedgehog
SV-2	Synaptic vesicle protein 2
TA	Tiabialis anterior
TBE	TRIS/ borate/ EDTA buffer
TBS	TRIS buffered saline
V	Volts
VAChT	Vesicular acetylcholine transporter

List of Figures

Chapter 1

Chapter 2

Chapter 3

Chapter 4

Chapter 5

Appendices

List of Tables

Chapter 1

Chapter 2

Chapter 3

Chapter 5

1. General Introduction

The experiments described in this Thesis represent an attempt to develop, optimise and characterise a novel, three dimensional co-culture system for use in analysing neuromuscular interaction *in vitro*. The Introduction shall therefore focus on the physiology and development of skeletal muscle tissue and the neuromuscular junction (NMJ) *in vivo*, in order to provide an understanding of how these structures develop in living systems. The possibilities and limitations of standard *in vitro* techniques for use in investigating these tissues and structures shall also be discussed, to highlight the necessity for more biomimetic culture models in future research.

1.1. Skeletal muscle physiology and development

Skeletal muscle is a striated, contractile tissue that facilitates conscious movement of the body (Lumley *et al.*, 1980). Connection of this tissue to the skeleton (either directly or indirectly via tendons) across a joint, and interaction with other muscle groups, allows for the voluntary movement of joints and therefore complete control of the body's movement and locomotion (Lumley *et al.*, 1980).

1.1.1. Structure and function of skeletal muscle cells

Skeletal muscle consists of highly orientated, unbranched, contractile fibres arranged to bring about contraction of the tissue in a single plane (Lumley *et al.*, 1980). Each muscle fibre is a single cell, a syncytium of multiple myonuclei sharing a common cytoplasm (Alberts *et al.*, 2002). These fibres run parallel to the line of muscle action and range in length from 1 mm to several cm, often running the length of the muscle (Sciote & Morris, 2000). Nuclei, mitochondria and other organelles within these cells are pushed to the periphery since most of the intracellular space is

occupied by the myofibrils (Sciote & Morris, 2000). Myofibrils are cylindrical structures, 1-2 μm in diameter, made up of a long repeating chain of contractile units termed sarcomeres (Alberts *et al.*, 2002). Each sarcomere consists of a network of longitudinal filaments arranged in a regular pattern that gives the fibre its transversely striated appearance (Bell *et al.*, 1980). The different "bands" visible in the muscle fibre are due to variations in the refractive index of its, structurally highly regulated, myofibrils and the separation of the different filament types within (Bell *et al.*, 1980). The isotropic bands largely consist of thin filaments of actin arranged to run spirally along a tropomyosin protein (Bell *et al.*, 1980; Alberts *et al.*, 2002). The thin actin filaments are bound at their "plus" ends to a z disc, while the capped "minus" ends extend into the anisotropic band where they interlock with thicker myosin filaments (Alberts *et al.*, 2002). Each myosin filament is surrounded by 6 actin filaments and lies approximately 45 nm apart from its neighbour (Bell *et al.*, 1980). Sarcomeric structure is detailed in Figure 1.1.

Sarcomere shortening, and therefore muscle contraction, is initiated by a rise in cytosolic Ca^{2+}, upon the arrival of an action potential at the NMJ and the subsequent depolarisation of the post synaptic cell (Alberts *et al.*, 2002). Invaginations of the sarcolemma, termed transverse (T) tubules, run perpendicular to the length of the fibre and allow for depolarisation of the membrane to penetrate rapidly to the centre of the cell. T-tubules are heavily populated with L-type Ca^{2+} channels in order to ensure synchronous activation of sarcomere shortening across all the myofibrils in the cell (Alberts *et al.*, 2002). Influx of Ca^{2+} into the cell triggers the reconformation of the actin-tropomyosin structure by the troponin complex (Figure 1.2), allowing the myosin heads to cyclically bind to previously unavailable sites on the actin molecule and essentially "walk" along the filament, dragging the two z discs together (Alberts *et al.*, 2002; Gomes *et al.*, 2002). Rapid sequestration of cytosolic Ca^{2+} then returns the actin-tropomyosin structure to its original conformation, blocking myosin

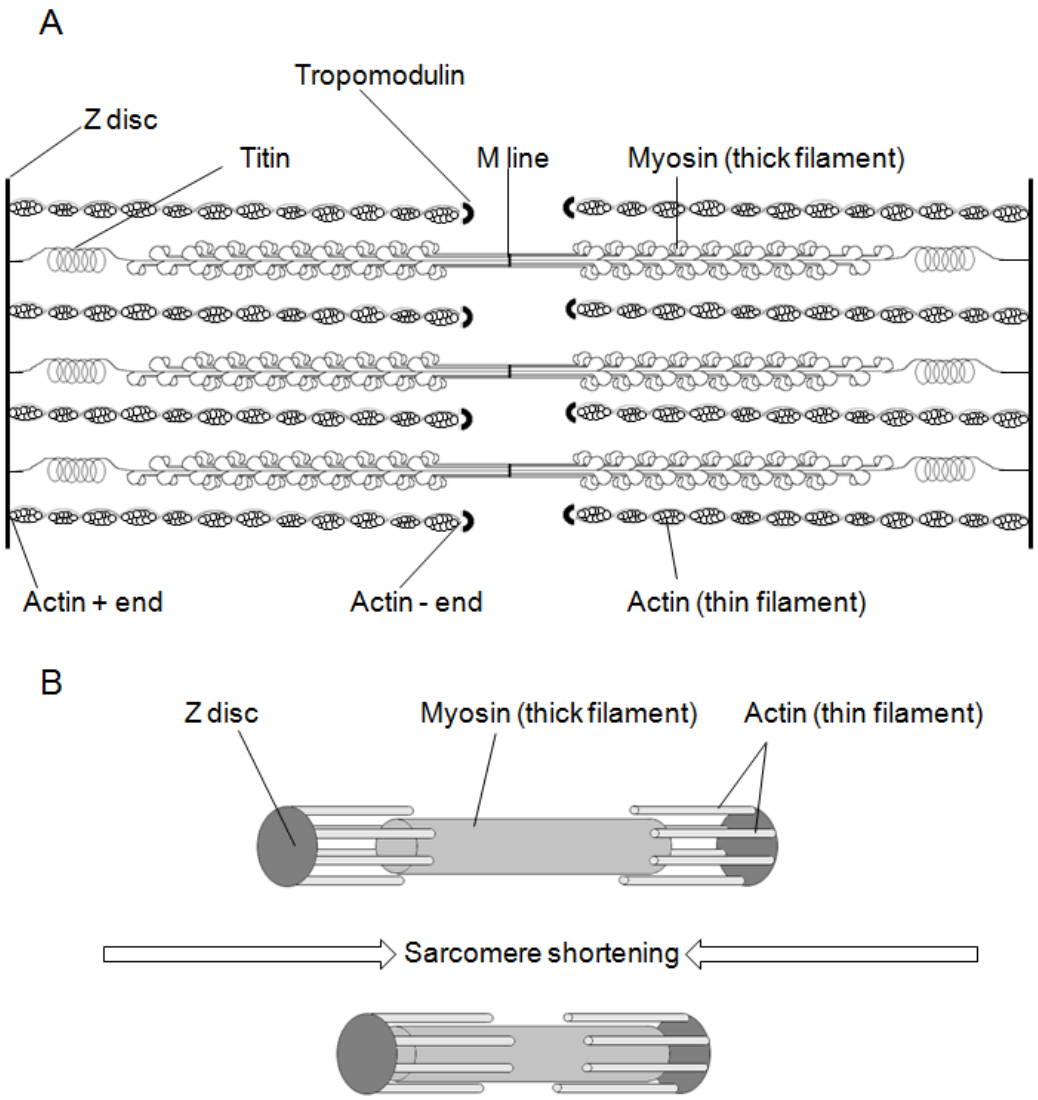

Figure 1.1: Diagram illustrating the skeletal muscle sarcomere. (A) Sarcomeric structure in mammalian skeletal muscle. Contraction is achieved through interaction of thick myosin filaments with thin actin filaments (Figure 1.2). Actin filaments are capped at their minus end by Tropomodulin and interact with CapZ at their plus end to bind the filament to the Z disc. Titin is a highly elastic protein which connects the myosin filaments to the Z disc and changes length to allow contraction and relaxation of the sarcomere. (B) Interaction of actin and myosin enables sarcomeric shortening. Synchronised shortening of thousands of sarcomeres lying end to end in each myofibril facilitates rapid contraction of the skeletal muscle tissue. Diagrams adapted from Alberts *et al.* (2002).

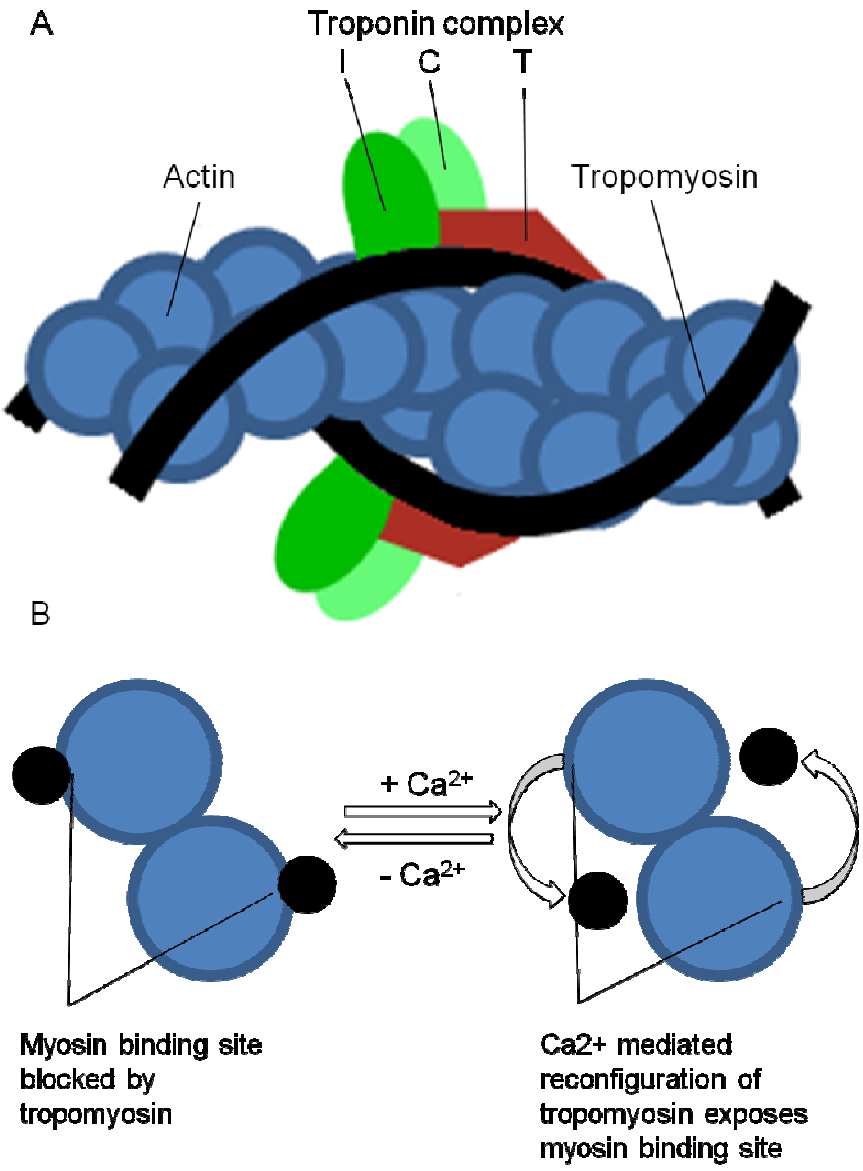

Figure 1.2: Diagram illustrating actin-myosin interaction within the skeletal muscle sarcomere. (A) The thin filament of the sarcomere consists of an actin polymer bound at regular intervals to tropomyosin. The troponin I-T complex holds tropomyosin in a conformation which prevents myosin binding. (B) Ca^{2+} binds to troponin-C, forcing troponin-I to release tropomyosin which in turn slips away from the myosin binding site. Myosin heads then bind cyclically to actin, pulling the thin filament past the thick filament. Removal of Ca^{2+} ions from the sarcoplasm reverses this interaction, blocking myosin binding and allowing the sarcomere to relax. Diagrams adapted from Alberts *et al.* (2002).

head binding and thus allowing for the relaxation of the sarcomere (Gomes *et al.*, 2002).

1.1.2. Muscle fibre phenotype

The contractile properties of a given muscle fibre are determined by the isoforms of myosin they contain within their myofibrils (Sciote & Morris, 2000). Myosin is a large molecule comprising 6 amino acid chains; 2 myosin heavy chains (MYHCs) and 2 pairs of non-identical myosin light chains (MYLCs) (Gershman *et al.*, 1966; Lowey & Risby, 1971; Weiss & Leinwand, 1996). MYHCs have both a structural role in muscle contraction as well as being responsible for enzymatically hydrolysing ATP (Pette & Staron, 2000). The latter function means that MYHCs play a key role in determining the nature of the excitation-contraction coupling during sarcomere shortening (Weiss *et al.*, 1999; Sciote & Morris, 2000). MYHC isoforms therefore determine the force-velocity characteristics of the muscle fibre and this role has led to the classification of muscle fibre types being based on the MYHC isoform they possess (Bárány, 1967; Sciote & Morris, 2000).

Nine fibre types have been identified in mammalian skeletal muscle using this method; β/I, α, extra-ocular, neonatal, embryonic, IIA, IIB, IIX and IIM. The neonatal and embryonic forms are obviously prevalent during development while adult skeletal muscle predominantly expresses the β/I, IIA, IIB and IIX subtypes (Weiss & Leinwand, 1996; Sciote & Morris, 2000). β/I fibres are slow contracting and referred to as type I fibres in skeletal muscle, the β used in reference to the same phenotype in cardiac muscle, while type II fibres are fast contracting isoforms with sarcomeric shortening speed relative to each other so that IIB>IIX>IIA (Weiss & Leinwand, 1996; Sciote & Morris, 2000). Hybrid fibres also exist, expressing multiple MYHC isoforms, and are believed to be involved in fibre phenotype switching so as to

better prepare the fibre to meet its functional demands (di Maso *et al.*, 2000; Baldwin & Haddad, 2001).

MYHC proteins are encoded by a super family of myosin genes (Table 1.1.), encoding striated muscle MYHCs as well as smooth muscle and non-muscle myosins (Weiss & Leinwand, 1996). The MYHC genes are highly conserved, likely arising from multiple duplications of a single ancestral gene, and are large, containing 40 - 41 exons (Weiss & Leinwand, 1996). Expression of specific MYHC genes contributes strongly to the overall fibre phenotype, however, other proteins involved in contraction, such as MYLCs and troponins, also have a number of isoforms which are known to be differentially expressed, and therefore also contribute to fibre phenotype within the muscle (Spangenburg & Booth, 2003). The dynamic nature of MYHC isoform switching and hybrid fibre formation, coupled with a multitude of differentially expressed proteins, suggests skeletal muscle possesses a complex control over contraction characteristics, allowing it to better adapt to changes in environmental stimuli (Baldwin & Haddad, 2001; Spangenburg & Booth, 2003). It should therefore be noted that, while a MYHC classification system is vital for means of communication, it in no way completely covers the complex regulatory control that skeletal muscle exerts over its contractile characteristics (Baldwin & Haddad, 2001; Spangenburg & Booth, 2003).

1.1.3. The extracellular matrix (ECM) of skeletal muscle

Macroscopically, skeletal muscle is organised into a hierarchy of fibres and matrix layers. The basal lamina of individual muscle fibres is surrounded by a layer of randomly aligned collagen fibres termed the endomysium which allow for movement during contraction (Lumley *et al.*, 1980; Kjær, 2004). Fibres are bundled into groups (fascicles) surrounded by a transverse, multilayered, fibrous structure called

Protein	Gene
MYHC Type I (β, slow)	MYH7
MYHC Type IIA (fast)	MYH2
MYHC IIX (faster)	MYH1
MYHC Type IIB (fastest)	MYH4
Embryonic MYHC	MYH3
Neonatal MYHC	MYH8

Table 1.1: The major skeletal muscle fibre phenotypes and the genes that encode the associated myosin heavy chain proteins. Note that skeletal muscle fibre phenotype is determined by expression of a complex array of contractile machinery protein isoforms. Expression of these myosin heavy chain genes is therefore not sufficient to promote the development of a specific phenotype in the muscle fibre, however, expression of a specific gene over all others provides a strong indicator of the overall fibre type expressed (Spangenburg & Booth, 2003).

the perimysium, which holds the fibres in place (Lumley *et al.*, 1980; Kjær, 2004). Fascicles are grouped together to form the complete muscle tissue which is itself surrounded by a sheet-like, double layer of collagen fibrils called the epimysium (Lumley *et al.*, 1980; Kjær, 2004) (Figure 1.3).

Components of the ECM are divided into 4 classes: collagenous glycoproteins, non-collagenous glycoproteins, proteoglycans and elastin (see Lewis *et al.* (2001) and Smith *et al.* (2010) for reviews). The specific content of the ECM varies depending on the muscle type and is believed to be linked to its functional role in that tissue (Kjær, 2004). Adhesion of muscle fibres to the ECM is facilitated by the membrane-bound, α7β1 integrin and the Dystrophin-Dystroglycan complex, a multi-subunit protein complex which traverses the sarcolemma (Lewis *et al.*, 2001; Smith *et al.*, 2010). Interaction of muscle cells with the ECM via these structures is essential for allowing both the muscle fibres and supporting cell types (e.g. fibroblasts) to respond to changes in external mechanical cues (Burridge & Chrzanowska-Wodnicka, 1996). It is also necessary to ensure the maintenance of spatial organisation during contraction and is thought to aid the generation of a uniform contraction profile across the entire muscle tissue (Kjær, 2004; Smith *et al.*, 2010).

1.1.3.1. Collagen

Collagens are the most abundant proteins in mammals, accounting for roughly 25% of the body's total protein mass (Alberts *et al.*, 2002). They are by far the most ubiquitous ECM protein within intramuscular connective tissue and therefore essential for both fascicle organisation and force transmission (Kjær, 2004).

The basic structure of collagen is a triple helix (Prockop & Kivirikko, 1995). Three polypeptide chains (α-chains), each wound into a left-handed helix, are together coiled into a right-handed super-helix, creating a rope-like structure (Bell *et al.*,

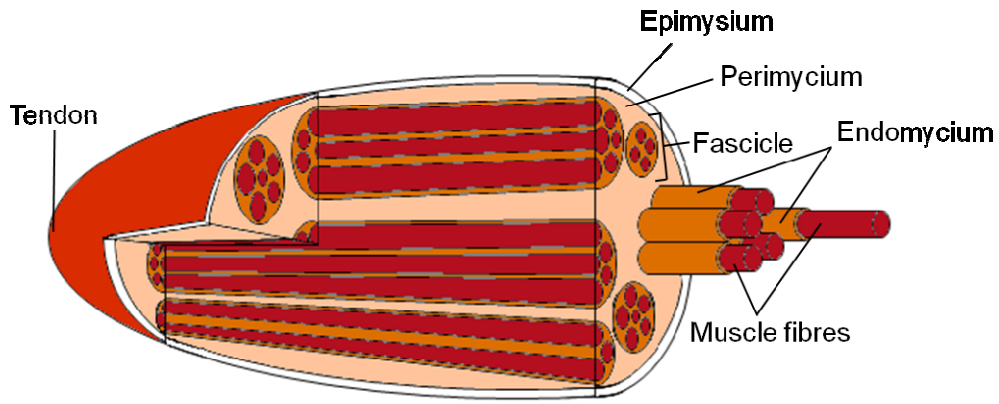

Figure 1.3: Diagram illustrating the hierarchical structure of the skeletal muscle ECM. Adapted from Leeson *et al.* (1988).

1980; Prockop & Kivirikko, 1995; Alberts *et al.*, 2002). Every third amino acid in a collagen polypeptide is glycine, a feature necessary to facilitate the tight winding of the triple helix (Prockop & Kivirikko, 1995; Alberts *et al.*, 2002). The other 2 amino acids are more varied but are frequently proline and 4-hydroxyproline (Bell *et al.*, 1980; Prockop & Kivirikko, 1995) which aid α-chain stabilisation and interaction with neighbouring molecules (Alberts *et al.*, 2002). More than 20 distinct collagen α-chains exist and each is encoded by a separate gene (Alberts *et al.*, 2002). Different combinations of α-chains in the triple helix alter the properties of the resulting collagen fibril and collagens are divided on the basis of the structures they form or on related structural features they possess (Prockop & Kivirikko, 1995).

Fibrillar collagens (types I, II, III, V and XI) are secreted into the ECM by fibroblasts where they assemble into larger collagen fibrils roughly 10 – 300 nm in diameter (Bell *et al.*, 1980; Alberts *et al.*, 2002). These fibrils often then aggregate into larger collagen fibres several μm in diameter (Bell *et al.*, 1980; Alberts *et al.*, 2002). While the basal lamina of skeletal muscle is dominated by the network-forming, type IV collagen, fibrillar collagens constitute the majority of ECM proteins in the epi-, peri- and endomysium (Bailey *et al.*, 1979; Kjær, 2004). Type I collagen is particularly prevalent, itself constituting between 30 and 97% of the total collagen content of skeletal muscle connective tissue depending on the muscle examined (Kjær, 2004).

Regulation of ECM composition and collagen turnover is dynamic and highly responsive to changes in mechanical loading (Savolainen *et al.*, 1988; Kjær, 2004). Increased levels of endurance training leads to the upregulation of collagen synthesis and its subsequent accumulation within the muscle ECM (Kovanen *et al.*, 1980). Fibroblasts are responsible for modelling the collagen network in response to external mechanical cues, ensuring the ECM network is capable of responding to the demands of the physical activity being undertaken (Alberts *et al.*, 2002).

1.1.4. Embryonic development of skeletal muscle

The mammalian skeletal musculature of the trunk and limbs originally derives from the somites, paraxial mesoderm segments that form on either side of the neural tube (Buckingham & Relaix, 2007). Correct development of skeletal muscle is critically dependent on a family of basic helix-loop-helix transcription factors, Myf5, MyoD, Mrf4 and myogenin (collectively termed the myogenic regulatory factors (MRFs)), as well as the paired box (Pax) transcription factors Pax 3 and Pax 7 (Rudnicki *et al.*, 1993; Kassar-Duchossoy *et al.*, 2004; Buckingham & Relaix, 2007). Initially, delaminating cells from the edges of the dermomyotome, the Pax 3/7 positive dorsal region of the somite, down-regulate Pax 3, becoming myoblasts through Myf5 and Mrf4 activation (Grefte *et al.*, 2007). Mrf4, MyoD and myogenin activity then promote differentiation of myoblasts into myocytes, which in turn fuse into multinuclear myotubes. These myotubes mature into muscle fibres, forming a continuous layer within the embryo termed the “myotome” (Grefte *et al.*, 2007) (Figure 1.4).

Once formed, the myotome is post mitotic since the muscle fibres present within it are multinuclear (Grefte *et al.*, 2007). Further growth of the skeletal muscle tissue is therefore facilitated by Pax 3/7 positive cells migrating out from the centre of the dermomyotome as it loses its epithelial structure during somite maturation (Relaix *et al.*, 2005; Buckingham & Relaix, 2007). A substantial sub-population of these proliferating cells gives rise to myogenic cells positive for Myf5 and MyoD which are then capable of fusing with existing fibres as well as with each other, creating new fibres, and thereby facilitating further growth of the skeletal musculature (Relaix *et al.*, 2005; Grefte *et al.*, 2007; Buckingham & Relaix, 2007).

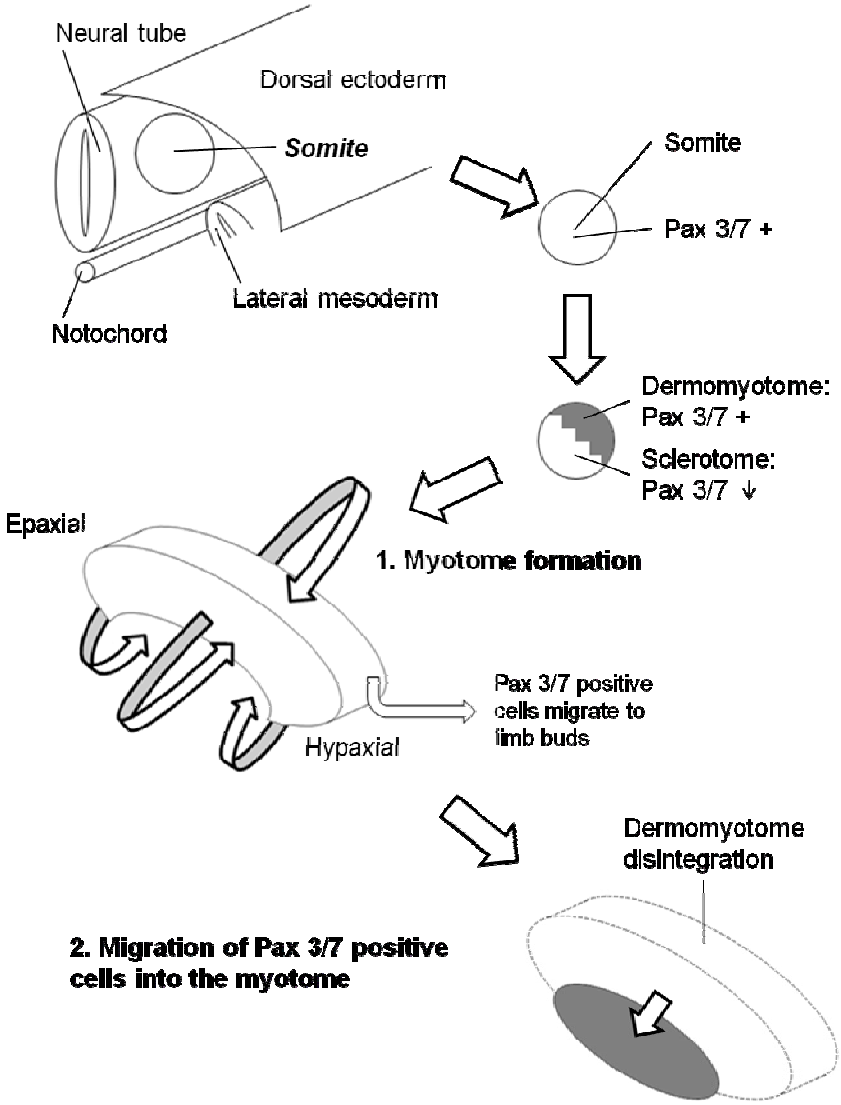

Figure 1.4 Diagram illustrating the formation of the myotome during mammalian development. Somites are located either side of the neural tube. *Pax 3/7* expression is maintained in the dorsal region of the somite, dictating formation of the dermomyotome distinct from the ventral sclerotome. Muscle progenitor cells undergo delamination from all 4 edges of the dermomyotome (1), up-regulating MRF expression and down regulating *Pax3.* These cells then fuse and mature, forming the myotome. The dermomyotome disintegrates (2), allowing Pax 3/7 positive cells to migrate to the myotome. These cells then facilitate further muscle growth and development of the embryonic musculature. Diagram adapted from Grefte *et al.* (2007) and Cossu & Borello (1999).

During myotome formation, migratory Pax 3/7 positive cells also travel from the lateral edges of the delaminating dermomyotome to the limb buds, mediated by activity of the tyrosine kinase receptor, c-Met, and its ligand, scatter factor/ hepatocyte growth factor (SF/HGF), as well as the homeobox gene *Lbx1* and the cell adhesion molecule N-cadherin (Bladt *et al.*, 1995; Jagla *et al.*, 1995; Brand-Saberi *et al.*, 1996). These infiltrating muscle precursors multiply and eventually fuse to form the pre-muscular masses of the developing limbs (Christ & Brand-Saberi, 2002). As with the central myotome, subsequent growth of these muscle groups is facilitated by fusion of migrating myoblasts derived from the disintegrating dermomyotome (Relaix *et al.*, 2005; Christ & Brand-Saberi, 2002).

1.1.5. Postnatal growth and regeneration of skeletal muscle

Towards the end of fetal muscle development, proliferating Pax 3/7 positive cells, migrating from the central dermomyotome in trunk muscles and the hypaxial dermomyotome in limb muscles, become enveloped in a basal lamina which forms around the maturing muscle fibres (Relaix *et al.*, 2005). These cells form the mammalian postnatal satellite cell population.

Satellite cells are not considered true stem cells since they are known to constitutively express skeletal muscle markers such as Myf5 and M-cadherin, suggesting a commitment to the myogenic lineage prior to activation (Irintchev *et al.*, 1994; Beauchamp *et al.*, 2000). There is evidence that satellite cells possess a number of subpopulations which differ in phenotype and functionality however, indicating that certain satellite cells may possess a more “stem cell-like” pluripotency (Molnar *et al.*, 1996; Blanton *et al.*, 1999; Zammit & Beauchamp, 2001). Given this ambiguity, satellite cells are rarely referred to as stem cells and are perhaps best described as multi-potent muscle precursor cells.

Skeletal muscle satellite cells lie between the sarcolemma and basal lamina of skeletal muscle fibres and it is through activation of these cells that growth and repair of the postnatal muscle tissue is achieved (Gamble *et al.*, 1978; Charge & Rudnicki, 2004). Satellite cells are mitotically quiescent, Pax 7 positive cells which are stimulated into multiple rounds of division in response to growth, traumatic injury or disease (Charge & Rudnicki, 2004; Tajbakhsh, 2009). Damage to muscle fibres leads to increased serum levels of muscle proteins since the integrity of the plasma membrane is compromised. Increased levels of serum creatine kinase along with autolysis of the damaged fibres provide signals to the damaged tissue and lead to inflammatory cell recruitment and satellite cell activation (Charge & Rudnicki, 2004). Activated satellite cells migrate to the injury site, undergo multiple rounds of division and become myoblasts expressing Mrf4 and MyoD (Smith *et al.*, 1994; Yablonka-Reuveni & Rivera, 1994; Cornelison & Wold, 1997; Charge & Rudnicki, 2004). Down regulation of Pax7 and upregulation of Mrf4 and myogenin within this population of myoblasts promotes their fusion with the damaged fibre (hyperplasia), replacing nuclei lost to trauma (Smith *et al.*, 1994; Ten Broek *et al.*, 2010). If the damage to the fibre is too great to repair it is autolysed completely, satellite cell derived myoblasts are then capable of fusing with each other to create new muscle fibres to replace those lost to trauma (hypertrophy) (Charge & Rudnicki, 2004; Ten Broek *et al.*, 2010).

Asymmetric self-renewal of activated satellite cells ensures that not all daughter cells undergo differentiation. A small subset of these proliferating precursors remains undifferentiated, in order to replenish the fibre's satellite cell pool, thus ensuring the tissue is able to respond to future traumatic events (Ten Broek *et al.*, 2010).

Although satellite cells migrate to the injury site, migration of cells from adjacent muscles is rare since it requires the breakdown of the connective tissue separating the 2 muscles (Schultz *et al.*, 1986). In severe cases, when the connective tissue is damaged, such migration can occur. However, the reorganisation and contraction of damaged connective tissue can then result in scar tissue formation, leading to incomplete regeneration of skeletal muscle (Kääriäinen *et al.*, 2000; Ten Broek *et al.*, 2010). An overview of satellite cell activity is provided in Figure 1.5.

1.2. Motoneuron physiology and development

Motoneurons facilitate the contraction of skeletal muscle by conveying efferent signals from the central nervous system to the NMJ (Kanning *et al.*, 2010). Chemical transmission across this synapse triggers contraction of the muscle fibre and is discussed in more detail later (see **Section 1.3.**). Motoneuron structure, like that of all neuronal cell types, is characterised by the presence of an axon and dendritic tree (Lumley *et al.*, 1980). Incoming action potentials arrive via the dendrites, which surround the cell body, and are passed on to the target tissue via the axon (Lumley *et al.*, 1980). The axon splits into many branches at its terminus, forming synaptic contacts with thousands of other cells (Alberts *et al.*, 2002).

Somatic motoneurons directly innervate skeletal muscles of the trunk and limbs and are subdivided into α-, β- and γ-motoneurons. α-motoneurons are the most abundant of these subtypes and innervate the extrafusal muscle fibres, making them responsible for triggering muscle contraction (Kanning *et al.*, 2010). γ-motoneurons innervate the intrafusal fibres and are involved in motor control while β-motoneurons innervate both fibre types and have an, as yet, poorly understood role in regulating muscle contraction (Grill & Rymer, 1987; Kanning *et al.*, 2010). The collection of motoneurons responsible for innervating an individual muscle is

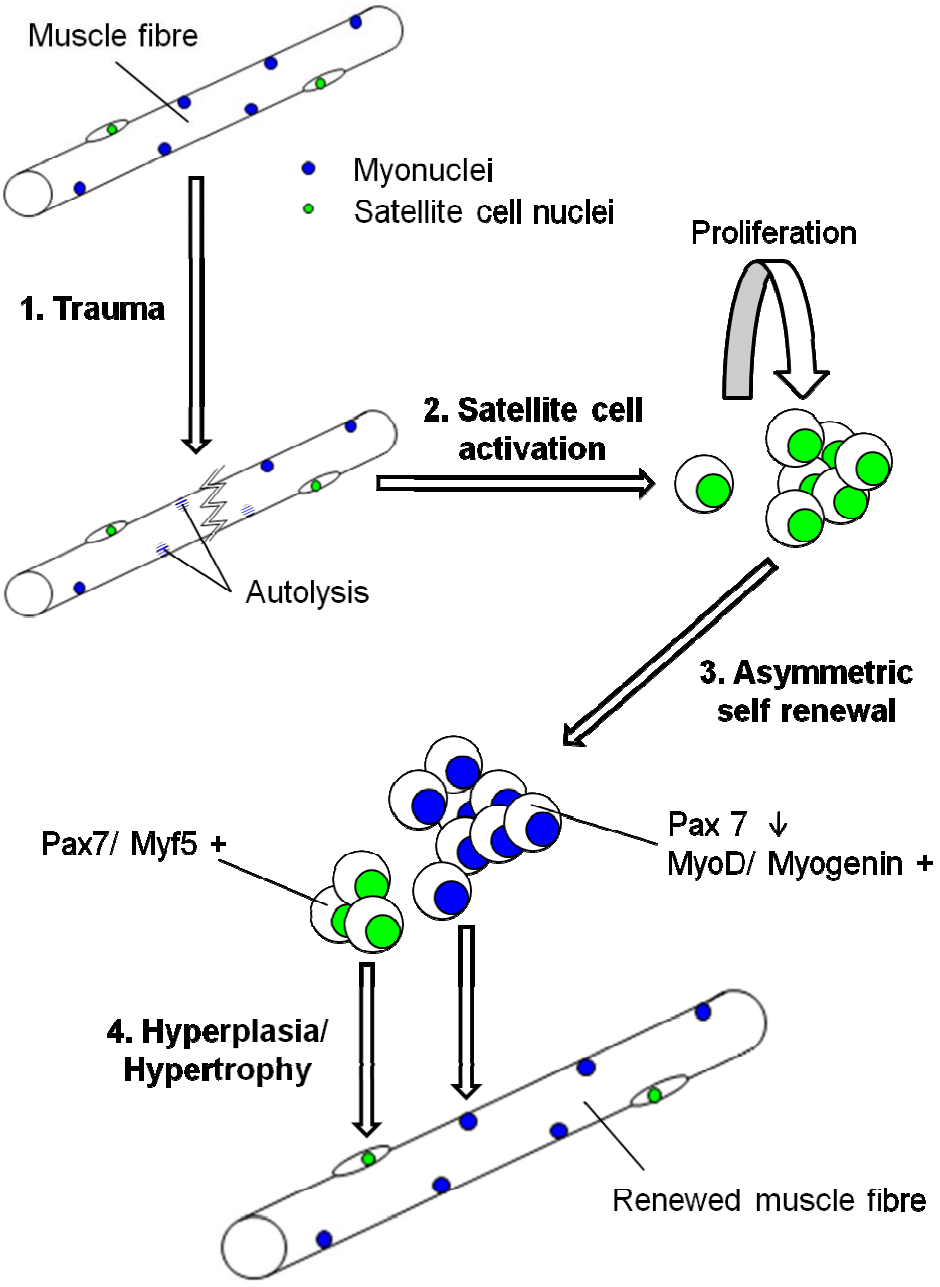

Figure 1.5: Diagram illustrating the satellite cell cycle in mammalian postnatal skeletal muscle tissue. Damage to the muscle fibre (1) triggers activation of the quiescent satellite cell population (2). These cells undergo multiple rounds of division, a small subpopulation remain Pax7 positive and are recycled to replenish the satellite cell pool (3). The majority of these cells differentiate however, upregulating MyoD and myogenin expression, fusing with damaged fibres or with each other (4) and leading to the complete restoration of the tissue. Diagram adapted from Yablonka-Reuveni *et al.* (2008).

termed a motor pool. The motor pools are collectively located within the ventral horn of the spinal cord, arranged topologically to match the muscular layout of the organism (Kanning *et al.*, 2010).

1.2.1. Embryonic development of motoneurons

Motoneurons are derived from the neuroepithelium and their embryonic differentiation is controlled by the notochord via Sonic hedgehog (Shh) activity (deLapeyrière & Henderson, 1997). Expression patterns of LIM homeodomain class transcription factors are believed to govern the developing motoneuron's subtype identity which in turn dictates axonal trajectory from the neural tube (deLapeyrière & Henderson, 1997; Eisen, 1998). Axonal growth is controlled by a complex interplay of chemo-attractants and repellents (reviewed by deLapeyrière & Henderson (1997)) and allows for the targeted movement of the developing growth cone towards its specific muscle group.

1.3. Neuromuscular interaction

Motoneurons reside in the motor columns of the ventral horn and each individual muscle fibre is innervated by the terminal branch of a single motoneuron (Vrbova *et al.*, 1995; Bell *et al.*, 1980). The regions of contact in both the nerve terminal and muscle fibre are specialised, forming the motor end-plate, and the area of apposition is roughly 2 mm^2 (Bell *et al.*, 1980).

In NMJs, synaptic transmission involves the release of the neurotransmitter acetylcholine (ACh) from the nerve terminal into the synaptic cleft and its subsequent binding to receptors on the post synaptic membrane (Bell *et al.*, 1980; Alberts *et al.*, 2002). The acetylcholine receptor (AChR) is a transmitter gated cation channel composed of 5 trans-membrane polypeptides (α_2, β, γ and δ) and encoded

by 4 separate genes (Grinnell, 1995; Alberts *et al.*, 2002). Upon innervation, in response to electrical activity and neural trophic factors, the γ-subunit is later substituted for a ε-subunit in the mature receptor of the NMJ (Grinnell, 1995). The 5 subunits are arranged in a ring, forming a narrow pore through the membrane lipid bi-layer, and clusters of negatively charged amino acids placed at either end of the pore help exclude negative ions from passing through the channel (Alberts *et al.*, 2002). When 2 molecules of ACh bind to the pentamer, it induces a conformational change in its structure which forces the pore open, allowing for the flow of positive ions (Na^+, K^+ and Ca^{2+}) down their respective concentration gradients in a non-specific manner (Alberts *et al.*, 2002). Hydrolysis of the bound ACh by acetylcholinesterase (AChE) reverts the receptor to its resting state, blocking further ion flow (Alberts *et al.*, 2002). Prolonged exposure to ACh due to excessive nerve stimulation leads to inactivation of the channel, temporarily preventing further depolarisation of the muscle membrane (Alberts *et al.*, 2002).

Ion flow through the opened AChR triggers the opening of associated cation channels which then leads to an influx of Na^+ ions and a local depolarisation of the membrane, termed a “miniature endplate potential” (MEPP) (Bell *et al.*, 1980; Alberts *et al.*, 2002). The arrival of an action potential at the nerve terminal results in the depolarisation of the presynaptic membrane and the release of large quantities of ACh into the synaptic cleft (Bell *et al.*, 1980; Alberts *et al.*, 2002). This in turn leads to a number of MEPPs occurring in quick succession which leads to greater depolarisation of the post synaptic membrane (Bell *et al.*, 1980; Alberts *et al.*, 2002). When the depolarisation reaches a specific threshold above baseline (-65 mV) it is sufficient to trigger an action potential in the muscle fibre (Bell *et al.*, 1980; Alberts *et al.*, 2002). Propagation of the action potential along the muscle fibre membrane and through the T-tubules leads to the opening of Ca^{2+} channels, triggering sarcomeric shortening as discussed previously (see **Section 1.1.1.**).

1.3.1. NMJ formation

The molecular mechanisms controlling NMJ formation are not fully characterised, but the process is believed to centre on the activity of the muscle membrane bound, receptor tyrosine kinase Muscle-Specific Kinase (MuSK) (Wu *et al.*, 2010; Ghazanfari *et al.*, 2011). The *MuSK* gene promoter contains a sequence targeted by myogenin, thereby ensuring it's upregulation during myoblast differentiation (Tang *et al.*, 2006). Subsequent controlled transcription patterns ensure targeted *MuSK* gene expression by specific myonuclei beneath the postsynaptic membrane of the muscle fibre (Ghazanfari *et al.*, 2011).

Before innervation, MuSK initially binds to Wnt signalling proteins, which play a role in early AChR clustering (Henríquez & Salinas, 2011; Budnik & Salinas, 2011). Wnts, secreted by the neuron growth cone, bind to MuSK and are thought to promote the activation of the cytoplasmic protein Dishevelled (Dvl) (Jing *et al.*, 2009). Dvl acts as a bridge molecule between MuSK and the p21 kinase PAK, allowing MuSK to regulate actin dynamics and thereby promote cytoskeletal changes to bring about AChR clustering (Jing *et al.*, 2009; Henríquez & Salinas, 2011).

In rodents, muscle fibres begin to promote AChR clustering as early as E12-14 in the developing embryo (Wu *et al.*, 2010). These early clustering events do not dictate the location of NMJ formation since incoming spinal motoneuron axons tend to ignore most pre-existing AChR clusters, instead forming synapses at new locations (Anderson & Cohen, 1977). These primitive, Wnt-MuSK mediated, aneural AChR clusters form around the central region of the fibre and, while not the exact target of the developing neurite, are believed to play a role in axon guidance, ensuring the growth cone is directed to the centre of the muscle fibre (Lin *et al.*,

2001; Wu *et al.*, 2010). By E16.5-18.5, aneural AChR clusters have completely disappeared and all remaining AChR clusters are apposed by nerve terminals (Lin *et al.*, 2001).

Agrin is synthesised in the motoneuron and secreted into the synaptic basal lamina, upon contact of the nerve with the muscle fibre membrane, where it binds to the lipoprotein receptor-related protein 4 (LRP4) (Zhang *et al.*, 2008). LRP4 and MuSK then interact through their extracellular domains, promoting MuSK phosphorylation and dimerisation (Wu *et al.*, 2010; Ghazanfari *et al.*, 2011). Downstream-of-tyrosine-kinase 7 (Dok7) also binds to MuSK at this early stage and is required for triggering the formation of the complete MuSK multi-protein complex which controls AChR cluster development and stabilisation (Bergamin *et al.*, 2010; Okada *et al.*, 2006).

Wnt3 binds to MuSK, promoting the formation of transient AChR micro-clusters in the muscle fibre membrane (Henriquez *et al.*, 2008; Henríquez & Salinas, 2011; Budnik & Salinas, 2011). Subsequent cytoskeletal reorganisation, facilitating AChR redistribution and anchoring in the muscle fibre membrane, then involves a complex agrin-MuSK mediated cascade of proteins including the tyrosine kinase Abl and geranylgeranyl transferase I (GGT), as well as Rac and Rho GTPases (Finn *et al.*, 2003; Luo *et al.*, 2003; Weston *et al.*, 2003). These proteins play crucial roles in regulating actin dynamics and MYLC phosphorylation, to stabilise these micro-clusters and further develop them into mature AChRs (see Wu *et al.* (2010) and Ghazanfari *et al.* (2011) for reviews).

The adaptor protein Rapsyn is subsequently essential for stabilisation of the AChR cluster and maturation of the postsynaptic terminal (Wu *et al.*, 2010; Ghazanfari *et al.*, 2011). Agrin-MuSK mediated activation of tyrosine kinases Abl and Src leads to the phosphorylation of the AChR β-subunit which recruits Rapsyn to the developing

AChR cluster (Mittaud *et al.*, 2004; Borges *et al.*, 2008). Agrin activity promotes Rapsyn interaction with both AChRs and the actin crosslinker α-actinin in order to link the AChR cluster to the underlying cytoskeleton (Dobbins *et al.*, 2008; Ghazanfari *et al.*, 2011). Rapsyn is a highly unstable protein, with a half life of 6 hours in muscle cells (Luo *et al.*, 2008). The agrin-MuSK complex interacts with the molecular chaperone heat-shock protein (HSP) 70 in order to mediate the activity of HSP90β on Rapsyn which is thought to help stabilise this protein at the synapse whilst simultaneously preventing AChR clustering in aneural areas (Luo *et al.*, 2008).

The Abl kinase also acts in a positive feedback manner to bolster further MuSK phosphorylation (Ghazanfari *et al.*, 2011). MuSK activation therefore triggers further MuSK activation, promoting the formation of larger AChR clusters from smaller ones. Conversely, MuSK mediated activation of Shp2 promotes a negative feedback loop which inhibits AChR clustering (Qian *et al.*, 2008). Neuronal release of ACh likewise promotes AChR disassembly through interaction with calpain and cyclin-dependent kinase 5 (CDK5) (Kummer *et al.*, 2006; Chen *et al.*, 2007). The agrin-MuSK-Rapsyn system inhibits this function by locally sequestering calpain, hence the development and maintenance of NMJs depends on a balance between local positive and negative signalling pathways (Chen *et al.*, 2007). The interactions of MuSK and its role in facilitating AChR clustering are illustrated in Figure 1.6.

Rapid changes in neurotransmitter release probability following growth cone contact with the muscle membrane suggests a role for retrograde signals from the muscle membrane having a positive effect on differentiation and activity of pre-synaptic structures (Grinnell, 1995; Vrbova *et al.*, 1995). The mechanism by which this retrograde signalling is achieved is currently poorly understood, however, there is

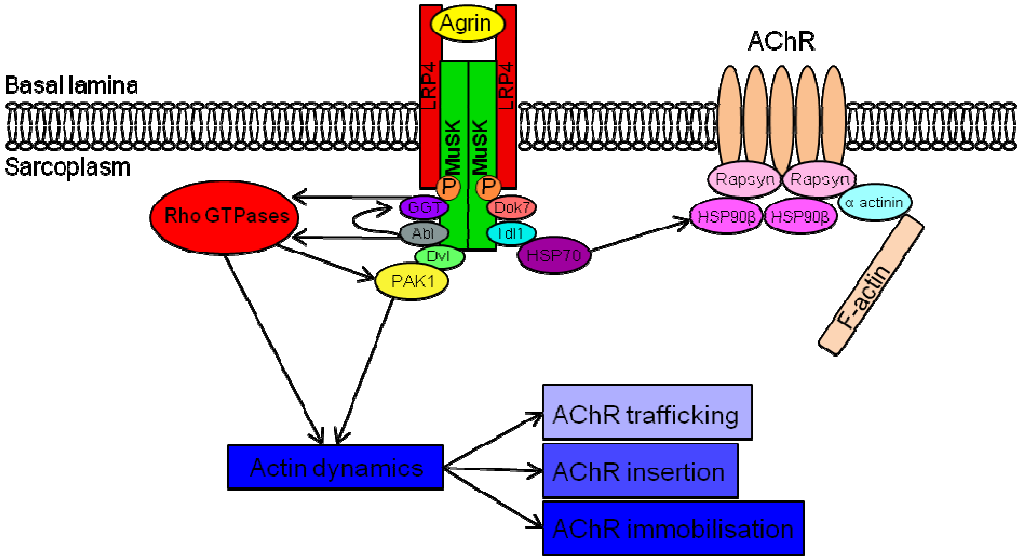

Figure 1.6: Diagram illustrating the basic activity of the agrin-MuSK complex on AChR clustering and stabilisation in the post-synaptic muscle fibre membrane. See 1.3.1 for details. Diagram adapted from Wu *et al.* (2010).

evidence for the involvement of a variety of growth factors including TGFβ, various FGFs and glial cell-derived neurotrophic factor (GDNF) (Wu *et al.*, 2010).

Activity of the Dvl pathway in muscle cells reduces spontaneous synaptic currents, indicating an ability of this postsynaptic pathway to affect pre-synaptic activity (Wu *et al.*, 2010). β-catenin is downstream of Dvl and suppression of this protein has been shown to be post-natally lethal due to pre-synaptic defects (Li *et al.*, 2008). Since Dvl is activated through MuSK in response to early binding by neuronal Wnt, it is possible that initial activation of the Wnt-MuSK pathway also activates a retrograde signal cascade, involving β-catenin, which promotes pre-synaptic development (Wu *et al.*, 2010).

1.3.2. Early synaptic activity at the NMJ

Initially, each muscle fibre develops synapses with multiple motoneuron axons but a process of elimination occurs during the neonatal period, leaving each fibre innervated by a single nerve (Sanes & Lichtman, 2001). The elimination of poly-neuronal innervation is achieved in an activity-dependent and competitive manner and is believed to involve the activation of Protein Kinase C (PKC), mediated by the serine protease Thrombin (Lanuza *et al.*, 2002).

The post-synaptic membrane in neonates is substantially different from that in adults and maturation of the junction apparatus is a complex process taking several weeks (Xie & Poo, 1986; Sanes & Lichtman, 2001). Alterations to the physical make-up of the NMJ include the invagination of the post-synaptic membrane in order to increase surface area between the nerve terminal and muscle membrane, the replacement of the γ-subunit of the AChR with the ε-subunit and the increased efficacy of pre-synaptic neurotransmitter release (Sanes & Lichtman, 2001).

Despite the high levels of NMJ maturation and development that occur post-natally, neuromuscular synapses are actually functional from before birth (Xie & Poo, 1986; Sanes & Lichtman, 2001). Moreover, chemical transmission begins practically as soon as the axon arrives at the muscle and the evoking of synaptic potentials has been shown within minutes of a growth cone making contact with a myotube (Xie & Poo, 1986; Vrbova *et al.*, 1995).

Before the establishment of robust NMJs, early ACh driven depolarisations of the muscle membrane vary in amplitude and can, in some cases, even trigger contraction of the myofibrils (Xie & Poo, 1986; Vrbova *et al.*, 1995). The release of ACh from the pre-synaptic terminal is increased significantly upon contact with the muscle membrane suggesting that contact between the two cell types may specifically induce neurotransmitter release (Navarrette & Vrbová, 1993; Vrbova *et al.*, 1995). The substantial release of ACh upon contact may play a role in the patterning of the post-synaptic membrane, including the removal of aneural AChR clustering (Xie & Poo, 1986). This initial chemical interaction appears to occur independently of action potentials and yet can induce myofibril contraction (Xie & Poo, 1986), therefore suggesting a possible influence on subsequent muscle fibre maturation (Navarrette & Vrbová, 1993; Vrbova *et al.*, 1995). The efficiency of neuromuscular transmission steadily improves over time, as both pre- and post-synaptic terminals mature, leading gradually to greater amplitudes and faster rise times in muscle fibre membrane endplate potentials during post-natal development (Navarrette & Vrbová, 1993; Vrbova *et al.*, 1995).

1.3.3. The effect of synaptic activity on muscle maturation and phenotype

The diversification of muscle fibres, as discussed previously (see **Section 1.1.2.**), is known to begin independently of innervation during development (Navarrette & Vrbová, 1993). The eventual fibre phenotype that myoblasts will adopt when incorporated into a muscle fibre is not pre-determined however, but rather reliant on a variety of extrinsic factors including mechanical loading and unloading, hormonal signalling, aging and, importantly, neuromuscular activity (Pette & Staron, 2000). Analysis of denervated and aneural muscles has provided substantial insight into the importance of neural stimulation for correct muscle fibre development and maturation (Midrio, 2006). Data regarding the effect of denervation on muscle maturation in neonatal tissue are somewhat contradictory, however the majority of work seems to suggest that innervation is required for the maintenance of the slow phenotype *in vivo* (Midrio, 2006). Aneural skeletal muscle has been shown to possess the same fibre types as controls, but a marked decrease in the appearance of slow fibres is observed (Condon *et al.*, 1990). Also of interest is the observation that neonatally denervated rat muscles show a significant reduction in the number of satellite cells present within that tissue, suggesting that innervation is also required for maintenance of the satellite cell population (Schmalbruch, 1990).

In denervated adult tissue, fast muscles tend to become slower and slow muscles tend to become faster, due to decreases in MYHCI and IIB expression and a concomitant increase in MYHCIIA, suggesting that neuronal activity is required to prevent “regression to the mean” with regards to specialised fibre phenotype (Pette & Staron, 2000). Moreover, it has been demonstrated that the re-innervation of slow fibres by nerves from fast motor pools results in the switching of the muscle fibre towards a faster phenotype (Navarrette & Vrbová, 1993; Pette & Staron, 2000).

Cross-innervation induced changes are believed to be due to the muscle responding to specific impulse patterns of the innervating neuron (Pette & Staron, 2000). This hypothesis is supported by electrical stimulation data which demonstrate that denervated fast muscles, such as the extensor digitorum longus (EDL) or tibialis anterior (TA), when subjected to low frequency electronic stimulation promote a switch towards a slow phenotype (Pette & Vrbová, 1999). This switch includes alterations in MYHC isoform expression as well as other proteins of the myofibrillar apparatus, changes in proteins regulating Ca^{2+} dynamics and mediating anaerobic and aerobic oxidative pathways, adaptations in synaptic specialisation, including alterations in AChE activity, changes to glucose and fatty acid metabolism, oxygen and fuel supply and increased capillary density, perfusion, myoglobin content and satellite cell presence (Pette & Vrbová, 1999). Conversely, a phasic, high-frequency stimulation regime promotes upregulation of fast MYHC phenotypes within denervated slow muscles (Gorza *et al.*, 1988).

Collectively, these data imply that muscle cells are able to mature to the point where they express adult MYHC isoforms without input from the nervous system. Innervation is required in order to dictate the fibre phenotype characteristic of that muscle through controlling the impulse pattern delivered to the muscle fibres. Since other extrinsic cues, such as hormone levels and mechanical tension are known to play roles in fibre phenotype switching (Pette & Staron, 2000), it is possible such cues also have roles in promoting muscle fibre maturation. However, specific neuronal stimulation patterns are clearly required to give this process direction. Without this control, alternative cues appear to exhibit far greater control over muscle fibre diversification, leading to severely altered and somewhat disorganised patterning of the skeletal muscle tissues.

Denervated muscles show a significant reduction in cross-sectional area, indicating the importance for innervation in promoting skeletal muscle growth (Condon *et al.*, 1990). Denervation is known to lead to a substantial decrease in the contractile strength of skeletal muscle due to significant levels of myofibril contractile protein degradation, indicating a role for neuronal stimulation in promoting myofibril assembly and maintenance (Goldspink, 1976; Furuno *et al.*, 1990). While a reduction in the size of denervated muscles is therefore partially attributable to a smaller average fibre diameter, it is also due largely to a substantial decrease in the number of fibres present within the tissue (Condon *et al.*, 1990; Schmalbruch, 1990). Innervation is therefore able to influence skeletal muscle growth both through encouraging new fibre formation and by promoting myofibril assembly within individual fibres.

1.4. Conventional cell culture techniques

1.4.1. Culture of muscle cells *in vitro*

Techniques for establishing *in vitro* cultures of primary muscle cells from both human and rodent sources have been available for over 30 years (Bischoff, 1974; Yasin *et al.*, 1977). While alternative methods have been developed (Sinanan *et al.*, 2004), enzymatic breakdown of the basal lamina, allowing for the release and subsequent isolation of mononuclear myoblasts, remains a common technique for attaining primary muscle cells for *in vitro* culture (Machida *et al.*, 2004; Das *et al.*, 2009; Hinds *et al.*, 2011). These myoblasts are derived from the satellite cell population discussed previously (see **Section 1.1.5.**), and are responsible for growth and repair of extant multinuclear, and therefore post-mitotic, muscle fibres *in vivo*. Cultured myoblasts retain a hypertrophic ability *in vitro* and, given the correct stimuli, are able to fuse, forming primary myotubes capable of spontaneous contractile activity (Yasin *et al.*, 1977). The formation of these multinuclear bodies is

fundamental to the *in vitro* study of skeletal muscle tissue. Such cultures allow for investigation of the metabolic and functional activity of muscle fibres and muscle precursor cells without interference from other tissues as normally occurs *in vivo*. Skeletal muscle is heavily influenced by external stimuli and interactions with other cell types (Forcales & Puri, 2005; Cosgrove *et al.*, 2009; Smith *et al.*, 2010). *In vitro* culture removes any such external or systemic cues, thereby allowing for a clearer investigation of the specific effect of chemical, physical or pathological challenges on the physiology and metabolism of skeletal muscle cells.

Enzymatic digestion of skeletal muscle tissue results in a heterogeneous population of cells including myogenic and non-myogenic/ fibroblastic cell types (Machida *et al.*, 2004). A number of techniques have been developed in order to purify the myogenic fraction from these mixed isolates including flow cytometry (Baroffio *et al.*, 1993), differential plating (Rouger *et al.*, 2007) and magnetic cell sorting (Brady *et al.*, 2008). Such techniques are invaluable in attempting to gain pure cell populations, especially considering that myogenic cells tend to be out competed in culture by non-myogenic fibroblasts, leading to significant reductions in the myogenic cell population over time (Machida *et al.*, 2004). However, fibroblasts are essential for maintenance of the skeletal muscle ECM and for modulating tissue responses to external physical cues *in vivo* (see **Section 1.1.3.1.**). There is therefore a danger that purification of the myogenic fraction will hinder the cultured cell's ability to respond to extrinsic stimuli. This is of little importance for conventional cell culture techniques, where the physical environment is already far removed from the *in vivo* niche, but becomes of increasing significance as technology moves towards more biomimetic models of the *in vivo* tissue (Brady *et al.*, 2008).

Although satellite cell derived myoblasts can be isolated from skeletal muscle tissue and cultured *in vitro*, a number of factors impact on both the size of the attainable

myoblast population and the activity of the isolated cells. Age is known to have a substantial impact on the number of satellite cells present *in situ* in both fast and slow muscle fibres (Shefer *et al.*, 2006). Significant reduction in satellite cell number over the life of an animal indicates that the number of myoblasts attainable from digests of their tissue likewise deteriorates with age.

Sexual dimorphism exists in skeletal muscle in terms of muscle mass, maximum force and fatigue resistance (Manzano *et al.*, 2011). While it remains unclear to what degree this diversity is due to inherent differences in the satellite cell population of males and females, *in vitro* studies have suggested differences in both the rate of proliferation and differentiation in myoblasts from donors of different sexes (Manzano *et al.*, 2011).

Finally, whether the muscle in question is predominantly “slow” or “fast” has a significant impact on the number of associated satellite cells it possesses. Slow-twitch muscle, containing fibres expressing mainly the MYHCI isoform, have a larger pool of satellite cells associated with them than the equivalent fast-twitch fibres (Manzano *et al.*, 2011). This is believed to be because slow muscle fibres are more rapidly and more frequently recruited during muscle activity and are therefore more likely to suffer damage (Manzano *et al.*, 2011).

Age, sex and fibre type all impact significantly on the satellite cell population of a given muscle. This is of great importance when planning *in vitro* studies of skeletal muscle cells, since it greatly increases the likelihood of there being substantial variation between *in vitro* myoblast cultures isolated from different donor sources.

1.4.2. Culture of motoneurons *in vitro*

The study of motoneurons *in vitro* is vital since it represents the only method by which the direct action of a molecule on motoneuron survival or development may be investigated (Camu *et al.*, 1993). As such, suitable methods for the isolation, enrichment and purification of motoneurons from the ventral spinal cord have been in development since the 1970s (Masuko *et al.*, 1979; Henderson *et al.*, 1995). Methods almost always focus on the use of cells from embryonic spinal cords taken just prior to the onset of naturally occurring cell death in the motoneuron population (Houenou *et al.*, 1991; Camu *et al.*, 1993). Since motoneurons are among the first post-mitotic neurons in the spinal cord, culture of cells from early time points, as early as E13 in rats, is known to considerably enrich the population of motoneurons obtained and reduce contamination from other neuronal cell types (Camu *et al.*, 1993).

Motoneurons are notoriously difficult to maintain *in vitro* (Henderson *et al.*, 1995; Arce *et al.*, 1998). Evidence suggests that motoneurons *in vivo* need to make contact with their target muscle fibre as well as with Schwann cells, glial cells and interneurons in order to receive the necessary positive signals to survive (Arce *et al.*, 1998). Conventional *in vitro* cultures obviously lack this complexity and as such, cultured motoneurons do not receive the necessary secreted factors to promote their survival in the long term. Even when maintained in heavily supplemented media, survival of motoneurons *in vitro* is difficult to extend beyond 10 days (Henderson *et al.*, 1995).

Conversely, maintenance of motoneurons *in vitro* for at least 6-7 days is necessary to ensure adequate levels of maturation have occurred within the cultured cells. Primary rat motoneurons are known to require this length of time in culture to form

distinct axonal and dendritic processes and to develop an electrophysiological profile representative of *in situ* motoneurons (Alessandri-Haber *et al.*, 1999). These factors indicate that a narrow window of several days (between roughly days 6 and 8 *in vitro*) represents the time frame in which most effective analysis of primary motoneurons can occur *in vitro*.

1.4.3. Muscle-motoneuron interaction *in vitro*

The ability for dissociated primary muscle cells and motoneurons to generate functional neuromuscular transmission *in vitro* was first reported using chick cells by Fischbach (1970). In such cultures, electrical stimulation led to action potentials recorded in the neuron which were followed by a brief depolarizing potential in the associated myotube membrane (Fischbach, 1972). Early work on neuromuscular interaction *in vitro* focused on the chick and *Xenopus* model systems due to the ease and rapidity associated with using these cells (Daniels *et al.*, 2000). Studies utilising rodent cells were later developed and seen as advantageous for three reasons as described by Daniels *et al.* (2000). Firstly, NMJ development *in vivo* has been studied in more detail in the rat than in any other mammalian species. Secondly, a greater number of antibodies and gene expression probes are available for rodents than for avian or amphibian species. Finally, established techniques for culturing rodent cells allowed for the development of cultures derived from transgenic or knock-out mice, even in cases where the mutation is lethal in late fetal development.

A number of relatively recently published papers focus on the use of primary rodent cells and discusses their ability to form NMJs *in vitro* (Daniels *et al.*, 2000; Faraut *et al.*, 2004; Lanuza *et al.*, 2006; Das *et al.*, 2007; Das *et al.*, 2010). Electrophysiological recordings from such cultures suggest the existence of

functional neuromuscular transmission between the 2 cultured cell types, with voltage-clamped motoneurons and myotubes producing characteristic Na^+ and K^+ currents and action potentials (Das *et al.*, 2007). Spontaneous contraction of the cultured myotubes is also observed and is shown to be blocked by treatment with the non-depolarising neuromuscular blocker D-tubocurarine (Das *et al.*, 2007). However, most immunocytochemical (ICC) data from such studies highlights the relatively immature morphology of these contacts, in terms of maturation of the post-synaptic membrane and development of a branched pre-synaptic terminal (Faraut *et al.*, 2004; Das *et al.*, 2010). Typically in these studies, AChR clusters are small and undefined and release of pre-synaptic markers, such as synaptophysin, is diffuse over large areas of the underlying myotubes (Daniels *et al.*, 2000; Das *et al.*, 2007; Das *et al.*, 2010).

As discussed previously (see **Section 1.3.2.**), neurotransmitter release increases substantially upon contact with a muscle fibre membrane, leading to miniature endplate potentials in the muscle fibre capable of eliciting a contractile response (Vrbova *et al.*, 1995). The immature nature of the neuromuscular contacts in the published work suggests that this may be the type of neurotransmission observed in these *in vitro* co-culture systems.

A lack of robust NMJs *in vitro* may be due to the age of the donor tissue used in these studies. Since maturation of the NMJ *in vivo* is known to occur over several weeks in post-natal tissue (Sanes & Lichtman, 2001), the use of fetal tissue in these cultures may hinder the formation of more mature and robust synaptic contacts.

The simplified nature of the culture environment may also inhibit NMJ formation. Lack of supporting cell types such as Schwann cells, normally required for axon

guidance and trophic support *in vivo* (Sanes & Lichtman, 2001), may further hinder effective motoneuron-myotube interaction.

Finally, the lack of centrally co-ordinated firing of neurons and established impulse patterns may well prevent the establishment of mature NMJs since maintenance and development of these structures *in vivo* is known to be activity dependent (Akaaboune *et al.*, 1999).

So far, a number of systems have been developed for the effective co-culture of primary motoneurons and myotubes. While these culture models display significant levels of neuromuscular interaction, the published data to date fall short of demonstrating an ability for these 2 cell types to form robust, mature and long lasting NMJs *in vitro*.

1.4.4. Limitations of conventional cell culture for use in studies of the neuromuscular system

Given the contractile nature of skeletal muscle cells, adherence to a rigid surface has long been recognised as problematic. The spontaneous contraction of these multinuclear structures usually leads to the detaching of the seeded cells from the tissue culture plastic following several days in culture (Vandenburgh *et al.*, 1988; Cooper *et al.*, 2004). The plating of muscle cells onto an elastic surface largely addresses this problem, since the substrate facilitates the spontaneous contraction of the myotubes (Cooper *et al.*, 2004). Of greater significance is the fact that the removal of any cells from their biological niche, and placing them in an environment wholly unrepresentative of the *in vivo* tissue, isolates them from a wide variety of extrinsic stimuli required to mediate their differentiation and maturation (Vandenburgh *et al.*, 1988). In the case of skeletal muscle, this includes the removal of innervation, endocrine signals and increasing mechanical tension throughout

development; stimuli required for the continued maturation of fetal skeletal muscle into adult muscle fibres (Vandenburgh *et al.*, 1988; Pette & Staron, 2000).

In order to facilitate directed contraction, skeletal muscle fibres *in vivo* need to be oriented in a parallel alignment (Khodabukus *et al.*, 2007). Conventional two-dimensional cell culture techniques are unable to provide suitable signals to promote the formation of spatially organised and orientated myotubes. The myotubes that develop in 2D cultures are usually randomly orientated and possess branched fibres, a feature wholly uncharacteristic of the *in vivo* tissue (Fear, 1977). Furthermore, the culture of myotubes on a rigid surface negates any attempt to measure the contractile force they generate, thereby drastically reducing the analysis of functional capacity that can be performed on these cells *in vitro* (Khodabukus *et al.*, 2007).

Given these limitations, it seems sensible to look towards new cell culture technologies when developing more biomimetic systems for studying neuromuscular interaction. Co-culture of primary myoblasts and motoneurons in a biologically representative environment capable of promoting organised myotube development and long term maintenance would represent a step forward in current cell culture techniques. The formation of NMJs in such a system would allow for future studies into the effect of innervation on the contractile capacity of primary myotubes and the development of a biomimetic culture system with which to study the physiology and development of NMJs in both health and disease.

1.5. Aims of this Thesis

The primary aim of this Thesis is to develop a three-dimensional, biomimetic co-culture system with which to study the interactions of myotubes and motoneurons *in vitro*. The behaviour of primary rat myoblasts within an established collagen-based 3D culture system will be optimised and characterised first. A comparison of this model to conventional 2D cell culture techniques will then be carried out, demonstrating the improvement this system represents over conventional cell culture techniques.

The effect of co-culturing primary spinal motoneurons with myoblasts in this system will then become the focus of the study. Whether or not motoneuron presence has a positive effect on the maturation and development of muscle cells in this 3D *in vitro* environment will have important implications for the future of skeletal muscle tissue engineering research.

1. Is it possible to adapt a published 3D culture system to generate a collagen based model that is representative of *in vivo* skeletal muscle tissue and capable of being maintained *in vitro* in the medium to long term?
2. If so, does this model represent an improvement over standard *in vitro* culture techniques?
3. Can the 3D model be adapted to promote motoneuron survival in co-culture with primary myotubes?
4. If so, do the co-cultured motoneurons interact with the differentiated myotubes, and to what degree?

2. Materials and Methods

2.1. Cell Culture

Unless otherwise stated, all cell culture work was carried out in a Class II microbiological flow hood under sterile conditions. All incubations were undertaken at 37^{o}C in a humidified 5% CO_2 incubator.

2.1.1. Isolation of primary muscle derived cells (MDCs)

In these experiments, MDC cultures were established from neonatal rats. One day old, postnatal (P1) Sprague-Dawley rat pups were killed by cervical dislocation, in accordance with the code of practice for the humane killing of animals under Schedule 1 of the Animals (Scientific Procedures) Act 1986.

The pups were then pinned out (ventral side prone) on a cork board and the tail removed with dissection scissors. The skin surrounding the hind limbs was removed and the legs cut though at the hip and ankle and transferred to a Petri dish containing phosphate buffered saline solution (PBS) (Sigma-Aldrich, Dorset UK) supplemented with 2% penicillin (100 units/ ml)/ streptomycin (100 µg/ ml) (P/S) (GIBCO/ Invitrogen, Paisley UK).

Using sterile curved forceps, the muscle tissue was separated from the bone. Bone fragments and cartilage were then removed from the Petri dish and discarded. The muscle tissue fragments were divided and transferred to two 15 ml centrifuge tubes (BD Biosciences, Oxford UK) and spun at 180 g for 1 minute. The supernatant was removed and the muscle fragments resuspended in 3 ml 0.1% collagenase (GIBCO/ Invitrogen) in PBS.

The tubes were secured within a shaking incubator set to 300 rpm and left for 25 minutes. The tubes were removed and the muscle fragments triturated vigorously, in order to break up any aggregations that had formed. The tubes were then returned to the shaking incubator for a further 25 minutes or until the tissue fragments had fully dissociated.

The resulting cell solution was passed through a 100 µm and then a 40 µm mesh (BD Biosciences), in order to remove any debris or undigested tissue fragments, before being spun at 450 g for 10 minutes. The cells were then resuspended in 500 µl standard growth medium (GM) (High glucose Dulbecco's Modified Essential Medium (DMEM) (GIBCO/ Invitrogen), 20% fetal calf serum (FCS) (PAA, Somerset UK) and 1% P/S).

2.1.2. Isolation of primary mixed ventral horn cells

Primary rat motoneurons were isolated from rat embryos at gestational age E14 using a method modified from that described by Henderson *et al.* (1995) (Kalmar & Greensmith, 2009). Pregnant Sprague-Dawley females were killed by exposure to a rising concentration of carbon dioxide gas, in accordance with the code of practice for the humane killing of animals under Schedule 1 of the Animals (Scientific Procedures) Act 1986.

Embryos within the uterine horn were removed following hysterectomy and transferred to a Petri dish containing Hank's Balanced Saline Solution (HBSS) (Sigma-Aldrich, Dorset, UK) supplemented with 2% P/S. Under a dissecting microscope, spinal cords were separated from the surrounding tissue using fine curved forceps. The meninges were carefully removed and the dorsal horn cut away from the ventral portion of the spinal cord and discarded. The ventral horns from individual embryos were pooled in fresh HBSS + 2% P/S on ice and transferred to a

Class II microbiological flow hood; all further steps were performed under sterile conditions.

The spinal cords were incubated in a 0.025% trypsin solution (type XII-S) (Sigma-Aldrich) in HBSS for 10 minutes. They were then transferred to a fresh solution containing 800 µl L-15 medium (GIBCO/ Invitrogen), 100 µl 4% bovine serum albumin (BSA) (Sigma-Aldrich) and 100 µl DNAse (1 mg/ ml) (Sigma-Aldrich). The spinal cords were agitated vigorously until they had disaggregated and were then triturated using a P1000 tip and left to settle. After 2 minutes the solution was transferred to a fresh 15 ml centrifuge tube (care was taken to avoid transferring any un-dissociated fragments). This process was repeated twice and the three supernatants were pooled before being spun through a 1 ml 4% BSA cushion for 5 minutes at 370 g.

Once the supernatant had been removed, the pellet was resuspended in complete neurobasal medium (CNB) containing neurobasal medium (GIBCO/ Invitrogen), B27 supplement (1 unit/ ml) (GIBCO/ Invitrogen), 2% horse serum (HS) (PAA, Somerset UK), 0.5 mM L-glutamine (GIBCO/ Invitrogen), 0.05% 2-mercaptoethanol (GIBCO/ Invitrogen), ciliary neurotrophic factor (CNTF) (500 pg/ ml) (Alomone labs, Bucks UK), glial cell-line derived neurotrophic factor (GDNF) (100 pg/ ml) (Alomone labs), brain derived neurotrophic factor (BDNF) (100 pg/ ml) (Alomone labs) and 1% P/S.

2.1.3. Cell counting

Since specific seeding densities were required for experiments in this study, the number of cells in solution was calculated using a haemocytometer. 10 µl of the cell suspension was added to 10 µl 0.4% Trypan Blue solution (Sigma-Aldrich) in order to help distinguish between dead and living cells. This was the case for all cultures except when isolating MDCs for use in 3D culture; in this case 10 µl of the cell

suspension was added to 190 µl Trypan Blue solution. This dilution was necessary since the volume of GM used to resuspend the cells was so small that it would have been impossible to accurately count the cells under a light microscope at this concentration.

10 µl of the cell/ Trypan Blue solution was released under each end of the haemocytometer's coverslip and allowed to fill the 2 chambers by capillary action. Under a light microscope at x10 magnification the number of cells present in each corner and the centre square of each chamber were counted. The number was divided in half, to give an average for the 2 chambers, and then multiplied by the dilution factor. The result was multiplied by $5x10^4$ and then by the original volume (in millilitres) to give an estimation of the total number of cells present.

2.1.4. Culture of primary MDCs in 2D

MDCs were isolated from the hind limbs of P1 neonatal rat pups as detailed above (see **Section 2.1.1.**). Sterile glass coverslips (13 mm; VWR, Leicestershire, UK) were put into standard 24 well plates (BD Biosciences) and treated with 0.2% gelatin (Sigma-Aldrich, Dorset, UK) in PBS 30 minutes prior to seeding cells. MDCs were then seeded at varying densities onto these cover slips and maintained in growth media (GM; 20% FCS and 1% P/S in high glucose DMEM) until they reached confluency. At this point the media was replaced with differentiation media (DM) in order to promote fusion of the myogenic cells. In certain cases, DM was supplemented with either IGF-1 (AbD Serotec, Oxford, UK), at 10ng/ ml, or 0.5% chick embryo extract (CEE) (Sera Laboratories, West Sussex, UK). Unless specifically stated otherwise, DM consisted of 2% HS and 1% P/S in high glucose DMEM.

2.1.5. Culture of primary mixed ventral horn cells in 2D

13 mm glass cover slips were put into standard 24 well plates, treated with poly-ornithine (1.5 mg/ ml in sterile, distilled H_20) (Sigma-Aldrich) and stored in an incubator the night before culturing. Before isolation of the motoneurons, the poly-ornithine was taken off of the plate and replaced with laminin (1 mg/ ml in L-15 medium) (Sigma-Aldrich); the plate was then returned to the incubator for the duration of the isolation protocol.

Once the laminin solution had been removed, the mixed ventral horn cells (see **Section 2.1.2.**) were seeded on to the treated coverslips at a density of 25,000 cells/ cm^2. The plate was returned to the incubator and the cultures maintained for 7 days before being fixed in a methanol/ acetone solution for staining. During this culture period, the feeding media was changed every 2-3 days.

2.1.6. Co-culture of MDCs and mixed ventral horn cells in 2D

2D MDC cultures were established as described above (see **Section 2.1.4.**), at a seeding density of 50,000 cells/ cm^2, and maintained in GM until they reached confluency. At this point, GM was replaced with CNB+IGF-1 and 50,000 mixed ventral horn cells (isolated using the protocol described above) were pipetted directly on top of the seeded MDCs. The co-cultures were returned to the incubator and maintained for a further 4 days before being prepared for analysis.

2.1.7. Establishing collagen-based 3D cultures of primary MDCs

The establishment of aligned *in vitro* cultures of myotubes relies on the seeded cells' ability to reorganise themselves in line with a directional signal (Cheema *et al.*, 2005). Cell mediated matrix contraction against two fixed points in culture leads to

the development of uniaxial tension within the system, providing a mechanical signal to the seeded cells sufficient to promote their realignment along the lines of principal strain (Eastwood *et al.*, 1998). Creation of 3D cultures of aligned myotubes therefore requires the construction of anchors that can be used to provide the fixed points in culture for the seeded cells to pull against. In this study, custom built flotation bars were used in conjunction with commercially available, single well chamber slides (NUNC, New York, USA) to provide the conditions necessary to promote cellular alignment.

2.1.7.1. Flotation bar assembly

Flotation bars were constructed from polyethylene meshwork (Darice Inc. Strongsville, Ohio, USA). Rectangles of the meshwork were cut from larger sheets to fit across the short plane of single well chamber slides. Three such pieces were then bound together using 0.3 mm stainless steel orthodontic wire (UCL Eastman Dental Institute, London, UK) in order to create a structure with sufficient anchorage to maintain gel attachment during cellular remodelling and tensioning of the matrix. In order to attach these flotation bars in position at either end of the chamber slide, a piece of 0.7 mm orthodontic wire was bent to form 3 sides of a rectangle and driven in between 2 of the bound polyethylene sheets. By bending this structure in half, a hook was created that was capable of holding the construct in place on the lip of the chamber slide. Details of the flotation bars constructed for use in this study can be found in Figure 2.1.

The use of polyethylene meshwork precluded the use of an autoclave for sterilisation of the flotation bars. Instead the structures were soaked for at least 24 hours in 70% ethanol (VWR, Leicestershire, UK) prior to use in any culture construct. Before use, flotation bars were allowed to dry fully within a class II

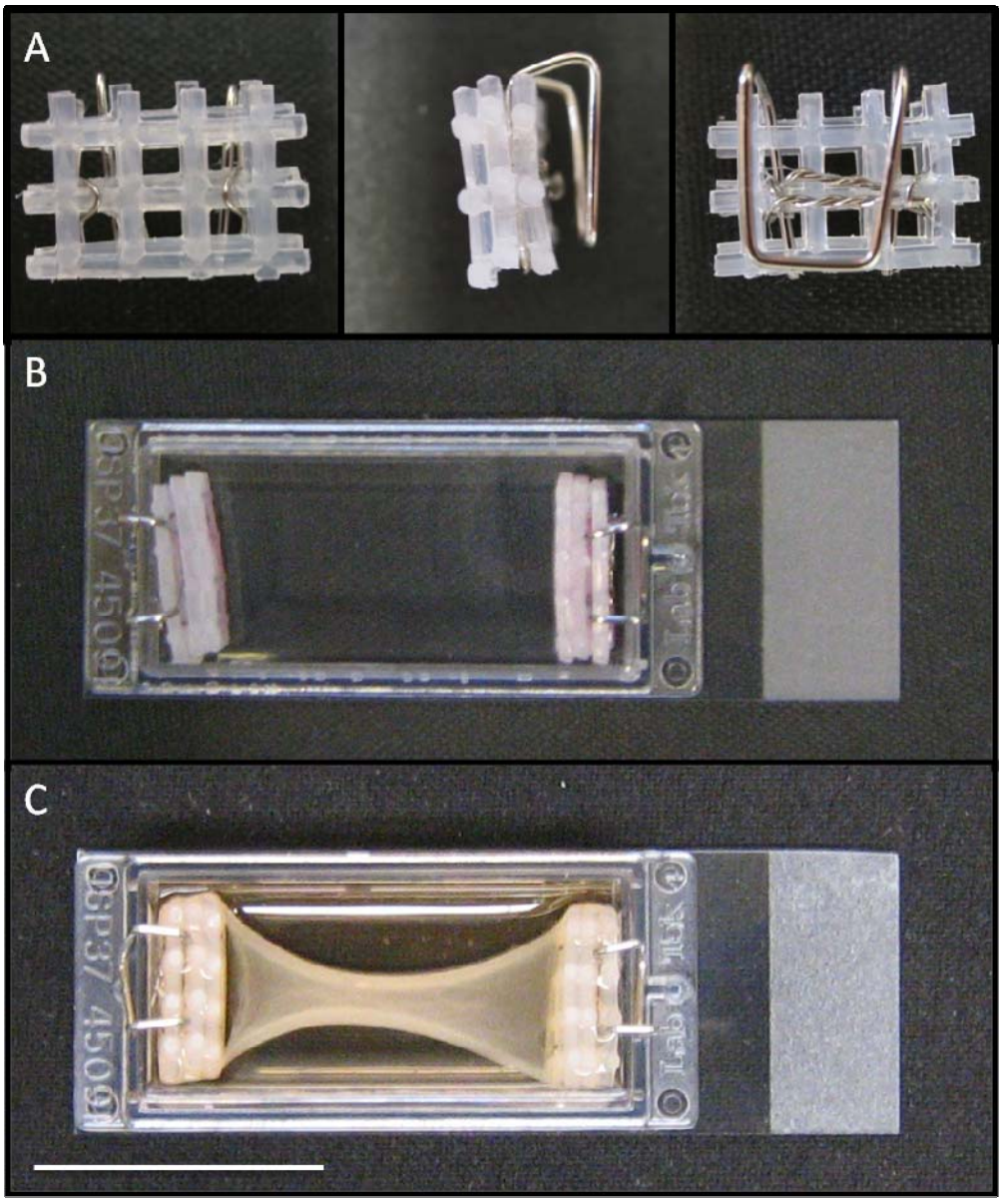

Figure 2.1: Examples of the flotation bars and chamber slides used throughout this study. (A) Front, side and back views of the custom built flotation bars used in this study. (B) Top view of a single well chamber slide fitted with flotation bars at either end. (C) Top view of the complete construct; a collagen matrix seeded with 5 million MDCs/ ml, cast between 2 flotation bars within a single well chamber slide and floated in media. Scale bar = 25 mm.

microbiological flow hood, to ensure no ethanol remained on the plastic which could interfere with the gelling of the collagen construct.

2.1.7.2. MDC 3D culture assembly

The protocol for establishing collagen constructs was adapted from those described previously (Mudera *et al.*, 2010). Significant adaptations made to the published culture environment are detailed later (see **Section 3.3.4.**).

Type 1 rat tail collagen (2.6 ml at 2.05 mg/ ml in 0.1M acetic acid; First Link, Wolverhampton UK) was mixed with 300 µl 10x minimal essential medium (MEM; GIBCO/ Invitrogen) to provide a pH indicator. 5M NaOH (VWR) was then added dropwise until a colour change from yellow to pink was observed, indicating the neutralisation of the acidic collagen solution. This solution was used to coat the flotation bars in order to aid the subsequent adhesion of the cell populated collagen gel. A second collagen solution was then prepared as described above and supplemented with 300 µl GM containing the desired number of freshly isolated primary rat MDCs (see **Section 2.1.1.**). This solution was then pipetted into a prepared single well chamber slide containing a collagen coated flotation bar fixed at either end. The construct was incubated for 30 minutes or until the collagen gel had set. After incubation, the construct was cut away from the sides of the chamber slide using a sterile needle and floated in GM. Care was taken to ensure the construct was fully detached from all surfaces except the flotation bars. The construct was returned to the incubator and media was subsequently changed daily.

2.1.8. Co-culture of MDCs and mixed ventral horn cells in 3D

3D muscle constructs were established as described above and maintained in GM for 4-7 days. At this point GM was replaced with CNB+IGF-1 and the desired

number of motoneurons (see **Section 2.1.2.**) were pipetted directly onto the upper surface of the collagen gel. Constructs were returned to the incubator and maintained for a further 7-14 days before being prepared for analysis; media was changed daily during this period. For certain cultures, CNB+IGF-1 was further supplemented with agrin recombinant protein, at a 200 pM concentration, and Wnt3 recombinant protein at 20ng/ µl.

2.2. Immunocytochemistry

2.2.1. Staining of 2D cultures

Cells on glass coverslips were aspirated and immersed in 500 µl ice cold PBS. 500 µl of an ice cold methanol/ acetone solution (100% methanol (VWR) and 100% acetone (VWR) in a 1:1 mix) was then added drop wise. The cells were left at 4^{o}C for 10 minutes before the wells were aspirated and a further 500 µl ice cold methanol/ acetone was carefully added to each. The cells were then left at 4^{o}C for 5 minutes before being washed twice with PBS and the glass coverslips transferred to stages using curved forceps. The stages were built using the lids from 1.5 ml Eppendorf tubes (Eppendorf, Cambridge UK) glued to a Petri dish. Placing the coverslip on such a stage made the manipulation and movement of the coverslips easier as well as reducing the volume of reagent required per coverslip.

Cells were immunostained with a panel of antibodies which differed depending on the experimental design. The details of the antibodies used throughout this study are provided in Table 2.1.

Each coverslip was treated with 100 µl of a standard blocking/ permeabilisation medium consisting of 5% serum (serum type was dependent on the antibodies used) and 0.2% Triton X-100 (Sigma-Aldrich) in 1x TRIS (0.05M) buffered saline

Primary Antibody	Primary Antibody Concentration	Secondary Antibody	Secondary Antibody Concentration	Blocking Serum Used
Desmin (Dako, Cambridgeshire, UK)	1 in 200	Alexa Fluor 488 goat anti-mouse IgG (GIBCO/ Invitrogen)	1 in 200	Goat
Microtubule-associated protein 2 (MAP-2) (Millipore)	1 in 1000	Alexa Fluor 568 donkey anti-rabbit IgG (GIBCO/ Invitrogen)	1 in 200	Donkey
2H3 neurofilament (DSHB, Iowa, USA)	1 in10	Alexa Fluor 488 goat anti-mouse IgG	1 in 200	Goat
Synaptic vesicle protein 2 (SV-2) (DSHB)	1 in 10	Alexa Fluor 488 goat anti-mouse IgG	1 in 200	Goat
Texas Red conjugated α-bungarotoxin (Sigma-Aldrich)	1 in 1000	N/A	N/A	N/A
DAPI (Sigma-Aldrich)	1 in 1000	N/A	N/A	N/A

Table 2.1: Details of antibodies/ immunocytochemical markers used in the analysis of cultured cells in this Thesis.

solution (TBS) (3.029 g TRIS base (Fisher Scientific), 4.5 g sodium chloride (VWR) and ~1.5 ml concentrated hydrochloric acid (VWR) (adjusted to pH~7.8) in distilled H_2O) for 15 minutes. Coverslips were washed 3 times with 100 µl TBS and then treated with the primary antibody diluted in TBS containing 2% serum and 0.2% Triton X-100. The cells were kept at room temperature for 1 hour before being washed 3 times with 100 µl TBS. They were then treated with a secondary antibody (dependent on the primary antibody) diluted in TBS + 2% serum and 0.2% Triton X-100. Nuclei were identified using the fluorescent minor-groove DNA binding probe DAPI (4,6-diamidino-2-phenylindole; 1.0 ng/ml; Sigma–Aldrich) which was incorporated into the secondary antibody incubation stage at a concentration of 1 in 1000. The cells were incubated at room temperature in a darkened chamber for 30 minutes before being washed 3 times with 100 µl TBS. Finally coverslips were dried and mounted on standard glass microscope slides (VWR) using a drop of MOWIOL mounting medium (Sigma-Aldrich).

2.2.2. Staining of 3D cultures

Culture chambers were aspirated and the 3D constructs immersed in 3 mls ice cold PBS plus 3 mls of an ice cold methanol/ acetone solution. Constructs were stored at 4^{o}C for 20 minutes, at which point the chambers were again aspirated and the constructs immersed in 3 mls of fresh, ice cold methanol/ acetone. The constructs were stored at 4^{o}C for another 20 minutes before being washed twice in PBS. Fixed constructs were stored in a solution of 10% sucrose in TBS for 24 hours and then a second solution of 20% sucrose in TBS for a further 24 hours. Dehydration of the collagen matrix using sucrose acted as a cryo-protectant and served to prevent the tissue from tearing during subsequent cryo-sectioning.

Dehydrated constructs were cut into 2 mm^2 tissue fragments using a sharp scalpel blade. Fragments were embedded in OCT media (Tissue Tek/ Sakura Finetek Europe, Hoge Rijndijk the Netherlands) within an aluminium foil mould and placed at -80^oC for several hours to freeze. Once frozen, OCT media was used to secure the embedded tissue to a chuck. This was then fixed in place within a Bright^{TM} cryostat and 30 µm sections were cut, collected on poly-lysine coated slides (VWR) and air-dried for 45 minutes.

Tissue sections and un-sectioned tissue fragments were both analysed using immunocytochemistry (ICC) during this study. Both were collected separately onto poly-lysine coated slides, ringed with a PAP pen (VWR) and allowed to dry for 15 minutes. The slides were then transferred to a humidified staining chamber at room temperature for the remainder of the protocol. The tissue was washed (3 x 5 minutes in TBS) and then blocked for 1 hour using TBS + 5% serum (dependent on the secondary antibody used) and 0.2% Triton X-100. The tissue was then washed (2 x 5 minutes in TBS) prior to treatment with the primary antibody diluted in TBS + 2% serum and 0.2% Triton X-100. The tissue was then incubated overnight at room temperature.

The tissue was again washed (2 x 5 minutes in TBS) before being treated with the secondary antibody diluted in TBS + 2% serum and 0.2% Triton X-100. Nuclei were again identified using DAPI which was incorporated into the secondary antibody incubation stage at a concentration of 1 in 1000. The tissue was incubated for 3 hours at room temperature in a darkened chamber before being washed (3 x 5 minutes in TBS), dried and mounted with glass coverslips (VWR) using a drop of MOWIOL mounting medium.

The antibodies used in the analysis of 3D cultures throughout this study are the same as those used in 2D cultures and are detailed in Table 2.1.

2.2.3. Image analysis

Images from 2D cultures were collected using an inverted Leica DMIRB microscope with Leica FW4000 image-processing software. Images from both 3D construct sections and un-sectioned construct fragments were collected using a Zeiss LSM510 Meta Confocal microscope and the accompanying software.

Analysis of percentage positivity for a given antigen in cultured cells was performed using Metamorph software (Universal Imaging Corporation, Downington, PA, USA). Images from cultured cells immunostained for a protein of interest, and counterstained with DAPI to mark nuclei, were processed by the software. Co-localisation of a nucleus with positive cytoplasmic immunostaining was marked as a positive cell. The total number of cells and the number of positive cells per image were totalled across all images taken and an average calculated from these values.

In each experiment using 2D culture, 10 random images at x20 magnification were taken per coverslip and 3 coverslips were examined per experiment. Using un-sectioned tissue fragments, 3D constructs were assessed at 5 random points in the tissue. Z stacks of 11 images were collected taking an image every 5 μm. 11 images at 5 μm intervals allowed complete resolution of the entire depth of the gel while simultaneously ensuring, as much as possible, that the same cell wasn't imaged and counted twice. In both 2D and 3D, the number of images taken was deemed sufficient to generate a truly representative mean as indicated by cumulative frequency analysis (see **Appendix A** and **B**).

2.3. Gene expression analysis of purified RNA using the Polymerase Chain Reaction (PCR)

All instruments and surfaces used in the processing of RNA samples were thoroughly cleaned using RNase Zap (Applied Biosystems, CA, USA) and rinsed in RNase free water (Qiagen, Crawley, UK) prior to use.

2.3.1. RNA purification

Wells containing cells for PCR analysis were aspirated, washed twice with PBS and treated with 500 µl TRIzol® (GIBCO/ Invitrogen). A P1000 tip was used to scrape the surface of the well in order to ensure the cells had fully detached before transferring the solution to an RNase free 1.5 ml Eppendorf tube.

3D constructs for PCR analysis were removed from culture, cut from their frames using a sharp scalpel blade and transferred to RNase free 1.5 ml Eppendorf tubes where they were immersed in 500 µl Trizol®. An IKA T10 basic homogenizer (IKA-Werke GmbH & Co., Staufen, Germany) was then used to break up the collagen construct; 3-6 second bursts on full power proved sufficient to completely break up the tissue.

Samples were treated with 100 µl chloroform (Sigma-Aldrich) and were shaken vigorously for 2-3 minutes at room temperature. Following this, the samples were spun for 15 minutes at 4^{o}C at a speed of 12,000 g. The upper aqueous phase from the resulting solution was transferred to fresh RNase free 1.5 ml Eppendorf tubes and treated with 250 µl isopropyl alcohol (VWR). The remainder of the original samples not transferred to a fresh tube was discarded at this point. The samples were incubated at room temperature for 10 minutes before being spun for 10 minutes at 4^{o}C at a speed of 12,000 g. The supernatant was removed and

discarded and the samples treated with 75% ethanol (diluted in nuclease-free water) and incubated at room temperature for 5 minutes. Samples were spun for 5 minutes at 4^{o}C at a speed of 7,500 g, the supernatant was then discarded and the samples left to dry for 15 minutes. The purified RNA was finally resuspended in 50 µl nuclease-free water. RNA yield was quantified using a Nanodrop ND1000 spectrophotometer (Nanodrop Products, Wilmington, DE, USA).

2.3.2. cDNA synthesis

Total mRNA was reverse transcribed to cDNA using a high capacity cDNA reverse transcription kit (Applied Biosystems). The following reaction mix was prepared: 2 µl 10x RT buffer, 0.8 µl dNTPs (100 mM), 2 µl 10x RT random primers, 1 µl multiscribe reverse transcriptase (50 U/ µl) and 4.2 µl nuclease-free water. A mastermix was made up with these volumes multiplied to cover the number of reactions to be carried out. The amount of RNA required was dependent on the number of genes to be analysed and the number of replicates to be performed. Each PCR reaction requires cDNA synthesised from 10 ng RNA, therefore 10 ng multiplied by the number of genes and again by the intended number of replicates gave the total required RNA volume for that sample. This value, divided by the current RNA concentration calculated on the Nanodrop (see **Section 2.3.1**), gave the required volume of the RNA solution to include in the cDNA synthesis reaction. The PCR reaction requires 2.5 µl cDNA per reaction, therefore 2.5 multiplied by the number of reactions gives the required final volume of the cDNA solution. The protocol requires the mastermix and RNA solutions to be mixed in a 1:1 ratio. Hence the total RNA required was diluted in nuclease-free water to make up a volume half that of the final volume required and the remainder was made up using the mastermix solution detailed above.

Each sample was made up in an RNase free 0.5 ml Eppendorf tube on ice and then transferred to a thermal cycler (Eppendorf). The samples were then incubated at 25^{o}C for 10 minutes, 37^{o}C for 120 minutes and then 85^{o}C for 5 seconds. At this point samples could be stored at -80^{o}C and analysis continued at a later date.

2.3.3. Conventional PCR analysis

Conventional PCR was performed using a Taq DNA Polymerase kit (GIBCO/ Invitrogen). Each reaction was set up in RNase free 0.2 µl eppendorf tubes on ice; the reaction mixture consisted of 2.5 µl 10x PCR buffer, 0.75 µl 50 mM $MgCl_2$, 0.5 µl dNTPs (Stratagene, CA USA), 0.25 µl forward primer, 0.25 µl reverse primer, 2.5 µl cDNA, 0.1 µl DNA polymerase and 18.15 µl nuclease-free water to create a total reaction volume of 25 µl.

The primers used throughout this study differed depending on the specific experimental design but were all specific for markers of myotube maturation and NMJ formation. A list of the primers used throughout this study is provided in Table 2.2.

The reaction tubes were transferred to a thermal cycler (Eppendorf) and the samples incubated at 94^{o}C for 3 minutes before being cycled 40 times at 94^{o}C for 30 seconds, 60^{o}C for 2 minutes and then 72^{o}C for 2 minutes. Following this cycling regime, samples were incubated at 72^{o}C for 10 minutes.

The products of these reactions were then used in a Southern blot analysis. A 2% agarose gel was made by dissolving 1 g of agarose (Sigma-Aldrich) in 50 ml 1x TRIS/ Borate/ EDTA (TBE) buffer (10x TBE buffer (GIBCO/ Invitrogen) diluted in

Gene	Forward Primer	Reverse Primer
RPII	ACATAACGAAGACGGTCAT	TAAGCCATTCAACAAGCAATA
β-actin	CCCCATTGAACACGGCATTG	ACGACCAGAGGCATACAGG
Myogenin	CAACCAGGAGGAGCGCGATCTCCG	AGGCGCTGTGGGAGTTGCATTCACT
MYH1 (adult fast)	CCTAAAGGCAGACTCTCCCACTGGG	GGCCATCTCGGCGTCGGAAC
MYH3 (embryonic)	GCCGGTGTGACTCAGCCAACACTAT	TCCTGGCGCTTTTTGCCTCGG
MYH7 (adult slow/ beta/ cardiac)	AAGAAGGTGCGCATGGACCTGG	CCTGCTCATCCTCAATCCTGGCG
MYH8 (neonatal)	TACGCCAGTGCTGAAGCAGGTA	CCATGGCACCGGGAGTTTTCG
Troponin T (slow, type 1)	GTCGGGAGATGAAACTCAGGAT	CAGGTCAAATTTCTCCGATTCC
AChRε	GGCAGTTTGGAGTGGCCTACGACT	GCAGGACGTTGATAGAGACCGTGC
ChAT	GCCTGGCCCTGCCAGTCAAC	AGGGAGTGGCTGTCCAGCAGA

Table 2.2: PCR primer sequences used in this Thesis to examine expression of genes associated with muscle maturation and neuromuscular interaction.

distilled H_20). The solution was heated in a microwave until the agarose had completely dissolved and was then treated with 5 µl Gel Red (Biotium, CA, USA) before being poured in to a mould containing a comb at one end; the solution was then left to gel for roughly 30 minutes. The comb was then removed to supply wells for the PCR products and the gel placed in an electrophoresis chamber and submerged in 1x TBE buffer.

The PCR products were mixed with 2.5 µl 10x Blue Juice DNA loading Dye (GIBCO/ Invitrogen) and 8 µl of each sample was then transferred to a separate well in the gel. 8 µl of the TrackIt 100 bp DNA ladder (GIBCO/ Invitrogen) was added to a single well to act as a guide before the lid was put on and the system set to run at 70 V for roughly 40 minutes. The results were imaged using a GeneGenius image analyser (Syngene, Cambridge, UK) and Genesnap image acquisition software.

2.3.4. Quantitative PCR analysis

Due to problems with access and availability to various qPCR hardware systems, a number of protocols were utilised during this study for the investigation of gene expression levels from these cultures. For the sake of simplicity, the protocol used in each Chapter is therefore detailed in the Materials and Methods section of that Chapter. Unless stated otherwise, the primers used in qPCR analysis were the same as for conventional PCR and are detailed in Table 2.2.

2.3.5. DNA sequencing of PCR products

PCR products were excised from polyacrylamide gels and purified using the QIAquick gel extraction kit (QIAgen, Crawley, UK) according to the manufacturer's protocol. They were then sent for sequencing at Geneservice (Geneservice, London, UK). The returned sequences were analysed using Finch TV software and

compared to the respective gene's known DNA sequence from an online database (www.ncbi.nlm.nih.gov) in order to confirm the validity of the primers used for amplifying sequences from the target gene (see **Appendix C**).

2.4. Western blotting

2.4.1. Sample preparation

3D collagen gels were transferred directly from the culture environment to 1.5 ml eppendorf tubes containing 500 µl of a homogenising buffer (HB) consisting of 2% sodium dodecyl sulfate (SDS) (Sigma-Aldrich), 2 mM ethylene diamine tetraacetic acid (EDTA) (Sigma-Aldrich) and 2 mM ethylene glycol tetraacetic acid (EGTA) (Sigma-Aldrich) in 5 mM TRIS (Thermo-Fisher Scientific, Leicestershire, UK) buffer. Prior to addition of the collagen construct, a protease inhibitor cocktail (Sigma-Aldrich) was added to the HB, diluted 1 in 100, in order to prevent protein degradation. Samples were homogenised using an IKA T10 basic handheld homogeniser (IKA-Werke GmbH & Co., Staufen, Germany) and stored on ice for 5 minutes before being spun down for 5 minutes at 14,000 rpm. The supernatant was then transferred to a fresh 1.5 ml tube and the pellet discarded. The protein solution was super concentrated using 10 KDa Amicon centrifugal filter units (Millipore, Watford, UK) and according to the manufacturer's protocol.

2.4.2. Gel electrophoresis and membrane transfer

Concentrated protein samples were diluted 1 in 10 in HB and 20 µl of the resulting solution was then mixed 1:1 with a laemmli buffer stock solution (0.5 M TRIS, 25 ml glycerol (Sigma-Aldrich), 20 ml 10% SDS and 20 ml 0.005% bromophenol-blue (Sigma-Aldrich) in 22.5 ml dH_2O). β-mercaptoethanol (Sigma-Aldrich) was also added 1 in 20 to the laemmli buffer prior to mixing with the samples. The diluted

samples were incubated at 95^{o}C for 5 minutes and 40 µl of each was then loaded into separate wells of a 7.5% polyacrylamide gel (Geneflow limited, Staffordshire, UK). 5 µl of Precision Plus Protein Western C standards (Bio-Rad Laboratories, Hercules, CA, USA) was loaded into a single well in order to provide a reference point for determining molecular weight of the separated proteins. Loaded gels were clamped into an electrode block and submerged in a running buffer consisting of 100 ml stock running buffer (Geneflow limited) diluted in 900 ml dH_2O. Electrodes were attached to the block and the samples subjected to a 160 V force for 60 minutes or until the samples had reached the bottom of the gel.

Once run, the polyacrylamide gel was removed from the apparatus and placed on top of a nitrocellulose membrane (Whatman, Kent, UK) soaked in an ice cold transfer buffer consisting of 100 ml stock transfer buffer (Geneflow limited), 200 ml methanol and 700 ml dH_2O. The gel and membrane were clamped into an electrode block positioned so that the nitrocellulose membrane was between the gel and the positive electrode, in order to facilitate the transfer of negatively charged protein from the gel onto the membrane. The block was immersed in ice cold transfer buffer and subjected to a 90 V force for 70 minutes. After this run time, successful transfer of protein to the membrane was visualised and confirmed using Ponceau solution (Sigma-Aldrich).

2.4.3. Immunoblotting

Presence of target proteins on the nitrocellulose membranes were confirmed through probing with specific antibodies for MYHC (mouse polyclonal anti-MYHC IgG clone A4.1025; Millipore), AChRε (goat polyclonal anti-AChRε IgG (C-20): sc-1454; Santa Cruz Biotechnology, Heidelberg, Germany) and β-actin (mouse monoclonal anti-β-actin IgG [AC15] (HRP); Abcam, Cambridge, UK). Membranes

were first washed 3x10 minutes in PBS to remove the Ponceau solution before being immersed in a blocking solution consisting of 0.1% TWEEN (Sigma-Aldrich) and 5% milk fat protein (Premier International Foods, Lincolnshire, UK) in PBS for 1 hour. The membranes were again washed 3x10 minutes with PBS and during this time primary antibodies were diluted in blocking solution (1 in 1000 for MYHC and AChRε and 1 in 5000 for actin). The primary antibody solution was then added and the membrane incubated at 4^{o}C overnight.

Following this incubation step, the membranes were washed 3x10 minutes in PBS while secondary antibody solutions were prepared. Secondary antibodies were diluted 1 in 1000 in blocking solution: rabbit polyclonal anti-mouse HRP conjugated IgG (Dako) was used on MYHC and β-actin blots and rabbit polyclonal anti-goat HRP conjugated IgG (Dako) was used on AChRε blots. StrepTactin (Bio-Rad) was also added to this solution at 1 in 10,000 in order to facilitate protein ladder visualisation. The membranes were incubated with the secondary antibody solution for 2 hours at room temperature. A final 3 washes in PBS were performed before the membrane was treated with 3 ml Supersignal (Thermo-Fisher Scientific) and incubated at room temperature for 5 minutes. Protein was visualised using a FluorChem SP imaging system (Alpha Innotech/ Cell Biosciences, Santa Clara, CA, USA) and the accompanying software.

3. Development and optimisation of a 3D collagen based model of skeletal muscle using primary rat cells

3.1. Introduction

Tissue engineered skeletal muscle has been highlighted in a number of publications as a possible future treatment for restoring tissue loss caused by traumatic injury, congenital defects, tumour ablation and prolonged denervation (Bian & Bursac, 2008; Liao & Zhou, 2009). Its use in the treatment of a wide variety of debilitating myopathies such as muscular dystrophy has also been suggested (Liao & Zhou, 2009).

While the ability to engineer fully functional skeletal muscle is not yet possible (Khodabukus *et al.*, 2007), current techniques in muscle engineering are thought to represent significant improvements to standard *in vitro* culture methodology (Khodabukus & Baar, 2009). Establishment of *in vitro* models that closely recapitulate the cellular architecture and functional capacity of the *in vivo* tissue are likely to play an important role in the future investigation of skeletal muscle development, physiology and pathology as well as cellular responses to pharmacological treatment and exercise.

As described previously (see **Section 1.1.1.**), skeletal muscle consists of bundles of highly differentiated, multinuclear fibres (myotubes) orientated uniaxially in order to facilitate contraction of the tissue in a single plane. This functional architecture therefore dictates the key factors for any *in vitro* model to emulate; namely the ability to promote the differentiation of muscle precursor cells (myoblasts) into myotubes and the orientation of these fibres into densely packed and highly orientated "fascicle-like" structures (Khodabukus *et al.*, 2007; Bian & Bursac, 2008).

Strategies to promote the formation of organised muscle cultures can broadly be divided into 2 sub-groups based on the nature of the scaffold used to support the cells in 3D: synthetic scaffolds and biopolymer matrices.

3.1.1. Skeletal muscle cells in synthetic tissue scaffolds

Manipulating the topography of artificial substrates and scaffolds in order to provide directional signals for the orientated growth of muscle derived cells (MDCs) is a technique that has been used extensively to generate aligned cultures of myotubes. Elastomers such as poly(dimethylsiloxane) provide a flexible substrate and can be patterned, using soft lithography, with high levels of reproducibility to control cell shape, size, proliferation, survival and, most importantly, spatial organisation (Whitesides *et al.*, 2001; Huang *et al.*, 2006). Such culture systems provide elastic substrates which promote the development of cells in a spatially organised manner. Their ability to promote MDC differentiation and maturation as measured by myotube length, striation and myoblast proliferation is greatly increased when compared to un-patterned control substrates (Huang *et al.*, 2006). The problem with such systems is that, although they generate organised *in vitro* cultures, their adherence to an essentially flat substrate precludes their incorporation into animal models or their use as a realistic model of the *in vivo* tissue.

In 1999, Saxena *et al.* demonstrated that sheets of poly-glycolic acid (PGA) fibres could be used to provide directional cues to seeded myoblasts, promoting organisation of the cells along strands of polymer matrix. Since then more organised sheets have been derived using electrospinning of polymers such as poly(lactide-co-glycolide) (McKeon-Fischer & Freeman, 2010; Aviss *et al.*, 2010) and polyaniline (McKeon *et al.*, 2010). MDCs seeded onto such matrices can be promoted to

elongate and fuse in an aligned manner (Huang *et al.*, 2006; McKeon-Fischer & Freeman, 2010) , thereby more closely mimicking the *in vivo* tissue.

Further advances in this field have led to the incorporation of various elements into the polymer matrix in order to further improve myoblast differentiation and maturation. Electrospun poly (L-lactide) sheets combined with gold nanoparticles significantly increase the conductivity of the resulting composite material, thereby allowing better transmission of electrical signals to the seeded cells and greater control over their electrical activation (McKeon-Fischer & Freeman, 2010). Primary myoblasts seeded onto polypyrole substrates dosed with the extracellular matrix (ECM) components hyaluronic acid or chondroitin sulphate A, show varying ability to proliferate and fuse *in vitro* (Gilmore *et al.*, 2009). These data demonstrate the ability for polymer-dopant chemistry to have a significant influence on the development of the seeded cells and may play a role in promoting cellular maturation in these constructs in future.

Cells seeded into such constructs and implanted *in vivo* survive and form aligned myotubes within the polymer matrix (Levenberg *et al.*, 2005). Vascularisation of the constructs is possible, and aided by co-culturing the seeded myoblasts with embryonic endothelial cells to promote endothelial vessel network formation (Levenberg *et al.*, 2005). Such cultures exhibit improved cell survival as well as improving the complexity of the extant model by incorporating multiple cell types; a step towards a more biomimetic culture system.

The use of external synthetic scaffolds such as these has been investigated as a possible method of myoblast transplantation in cases of significant tissue loss (Saxena *et al.*, 2001). The extensive matrix provides stability to the damaged tissue and helps recover its aesthetic form, while simultaneously promoting organised

myofibre growth throughout the damaged area (Saxena *et al.*, 1999). While there has been little clinical success using such constructs (McKeon-Fischer & Freeman, 2010), to date they remain a valid candidate for future investigation and therapeutic strategies (Aviss *et al.*, 2010).

3.1.2. Skeletal muscle cells in biopolymer matrices

Although synthetic polymer constructs represent exciting possibilities in wound healing and tissue replacement, their use as *in vitro* models of skeletal muscle are somewhat limited. Bian *et al.* (2009) described the problems inherently linked to the use of rigid scaffolds, such as those mentioned above, in effectively modelling *in vivo* skeletal muscle tissue. Firstly, the polymer presence makes it difficult to seed cells in a uniformly dense and spatially continuous manner and there is little scope to alter the scaffold structure in order to vary cell alignment and tissue thickness. Secondly, the rigidity of the scaffold prevents macroscopic contraction of the construct, thereby preventing evaluation of the engineered tissue's functional ability. Finally, if the scaffold polymer is degradable, it remains unclear how the eventual disintegration of the polymer will affect the established cellular alignment.

These problems are largely avoided when using naturally derived biopolymers. Collagen or fibrin hydrogels are capable of rapid polymerisation around seeded cells, allowing for the generation of uniformed and spatially constant cell densities (Bian *et al.*, 2009). Cell spreading throughout the construct is easily facilitated through multiple attachment sites. Furthermore, the significant reduction in construct rigidity allows for the use of tensile forces in facilitating the alignment of the seeded cells, as well as permitting macroscopic tissue contractions that can be effectively quantified (Bian *et al.*, 2009).

3.1.2.1. Fibrin constructs

In 1990, Strohman *et al.* demonstrated that collagen coated squares of Saran Wrap pinned onto a rubber gel layer (Sylgard; Dow Chemical Co., Billingham, UK) provided suitable culture conditions to promote advanced levels of MDC organisation and development in culture (Strohman *et al.*, 1990). MDCs seeded into this model induced the remodelling of the Saran Wrap layer as they began to contract, pulling the substrate away from the rubber underneath, and forming a tightly wrapped construct held in place by pins. Adherence of the construct to the pins allowed for the generation of tension within the system as the seeded cells pulled against them. The inherent tension in this model proved sufficient to promote the reorganisation of the seeded cells along the lines of strain, leading to the formation of aligned myotubes in culture. Staining of these cultures demonstrated expression of more developmentally mature myosin heavy chain (MYHC) proteins than were observed in standard 2D culture.

Dennis and colleagues (Dennis & Kosnik, 2000; Dennis *et al.*, 2001) built further on this innovation, developing a more accurate and biologically relevant model for the *in vitro* study of skeletal muscle. Laminin was used in place of Saran Wrap and 2 sets of adherence pins were used rather than the 7 used in the Strohman study. As the laminin was pulled off of the Sylgard by the contracting cells it rolled up around the uniaxial adherence pins to form a cylindrical culture of MDCs and supporting fibroblasts surrounded by a laminin matrix. As with the Saran Wrap construct, tension generated by the cells pulling against these fixed points promoted the alignment of the seeded MDCs along the lines of strain. The presence of only 2 pins in parallel led to the formation of uniaxially aligned myotubes in culture by 35 days *in vitro*. Attachment of one of the construct pins to a force transducer allowed for measurements of the contractile force generated by the myotubes in response to

broad field electrical stimulation to be obtained. Comparison in the force generated by laminin based constructs compared to muscles from 1 day old Wistar rats *ex vivo*, showed a 10-fold reduction in the specific force generated by the *in vitro* model when compared to *in vivo* tissue (Dennis & Kosnik, 2000). This difference was attributed by the authors to the presence of non-contractile material, the disordered sarcomeric structure and the greater presence of embryonic and neonatal contractile machinery in the laminin constructs compared with *in vivo* tissue. Although the culture did not produce levels of force generation comparable to the *in vivo* tissue, they did exhibit contraction profiles similar to neonatal skeletal muscle (Jones & Ridge, 1987), with time to peak tension at around 60 milliseconds and a half relaxation time of 60-100 milliseconds (Khodabukus *et al.*, 2007).

In order to improve on the 35 day construct maturation time frame, the model was later adapted to use fibrin instead of laminin (Khodabukus *et al.*, 2007); (Khodabukus & Baar, 2009). Such constructs developed in 7-10 days, required no supplementary fibroblasts to facilitate development and generated twice as much active force as the laminin model (Khodabukus *et al.*, 2007; Khodabukus & Baar, 2009). Prolonged electrical stimulation protocols for these constructs have been shown to improve the seeded cell's force production (Donnelly *et al.*, 2010) and serve to highlight the suitability of this system for generating models of skeletal muscle which can be used to evaluate the functional response of muscle to novel physical and chemical stimuli.

3.1.2.2. Collagen constructs

3D culture of MDCs was first reported in 1988 when Vandenburgh and colleagues (Vandenburgh *et al.*, 1988) populated a collagen gel matrix with partially differentiated avian myotubes. The matrix was attached to a circular ring which held

the gel size and promoted tension formation in the system as the seeded cells contracted. After several weeks in culture, the myotubes possessed a high concentration of organised myofibrillar proteins, peripheral nuclei and a well developed lamina layer; all indicators of substantial myogenic maturation. Incorporation of a mechanical stimulator into this model allowed for stretching of the cultured cells and subsequent analysis suggested improved myotube development when mechanically stimulated as measured by prostaglandin synthesis (Vandenburgh *et al.*, 1993).

The technique of embedding cells into a collagen matrix has since been developed further to provide uniaxial tension and thereby promote alignment of the seeded cells in a single orientation (Eastwood *et al.*, 1996; Vandenburgh *et al.*, 1996; Cheema *et al.*, 2003; Vandenburgh *et al.*, 2008; Langelaan *et al.*, 2010; Hinds *et al.*, 2011). MDC seeded collagen gels are set between two fixed points and then floated in media; an experimental setup derived from studies of the cytomechanics of fibroblasts in 3D collagen culture (Eastwood *et al.*, 1996). As with the fibrin model, contraction of the cells against these fixed points leads to formation of isometric tension sufficient to promote the reorganisation of the seeded cells along the lines of principal strain. Consequentially, myotube formation is uniaxial, leading to the generation of bundles of aligned myotubes surrounded by extracellular collagen (Cheema *et al.*, 2003).

Evaluation of the contractile force generated by such constructs over several days in culture can be made in real time using the novel culture force monitor (CFM) system (Cheema *et al.*, 2003; Cheema *et al.*, 2005). Electrically stimulated contraction of cultured myotubes in 3D collagen models is also possible and has been used recently to highlight the positive effect that a programme of timed electrical stimulation has on the maturation of such constructs as measured by myogenic

regulatory factor expression and sarcomere assembly (Langelaan *et al.*, 2010). Although electrical stimulation and measurement of force generation are both possible using current collagen-based models, to date very little data pertaining to the level of contractile force elicited from constructs subjected to such stimulation has been published. Analysis has instead largely focused on the effects of mechanical stimulation (Vandenburgh *et al.*, 1993; Cheema *et al.*, 2005; Boonen *et al.*, 2010) and assessment of the levels of maturation occurring within the constructs (Cheema *et al.*, 2003; Mudera *et al.*, 2010; Langelaan *et al.*, 2010). Gene expression studies have demonstrated that aligned cells, seeded within a 3D collagen matrix, express insulin-like growth factor 1 (IGF-1) splice variants at specific time points in culture (Cheema *et al.*, 2003) and promote shifts in MYHC isoform expression towards a slow phenotype (Langelaan *et al.*, 2010; Mudera *et al.*, 2010). These data not only indicate the potential for differentiation that these cells possess, but also how the culture environment appears to have a strong effect on the construct's emerging phenotype.

3.1.3. Collagen as a matrix for 3D *in vitro* cell culture

As mentioned previously (see **Section 1.1.3.1.**), collagen is extremely abundant within mammalian bodies (Alberts *et al.*, 2002) and makes up the majority of the skeletal muscle ECM (Smith *et al.*, 2010). As such, its use as a scaffold for 3D *in vitro* culture of MDCs is entirely appropriate.

Collagen fibres are naturally remodelled by cells (Abou Neel *et al.*, 2006). Fibroblasts in particular are known to be highly adept at drawing strands of collagen together from their surroundings, generating organised structures of orientated collagen fibres (Alberts *et al.*, 2002). Cells *in vitro* bind to collagen via integrin mediated attachment, as they would *in vivo* (Bitar *et al.*, 2007), and hence allow

transmission of mechanical signals through the matrix to the seeded cells in a biologically relevant manner. Collagen is a highly biocompatible substrate with low immunogenicity and high levels of conservation across species (Abou Neel *et al.*, 2006), allowing for the use of MDCs from a wide variety of donor species in a single model.

Some studies (Khodabukus *et al.*, 2007; Khodabukus & Baar, 2009) have suggested that the relatively large volumes of matrix involved in generating the extant collagen models preclude their use as a relevant *in vitro* model of skeletal muscle since they limit the amount of specific force the contracting myotubes are able to generate. However, a recent study demonstrated no significant difference in the tetanic or peak-twitch responses from MDCs seeded in either fibrin or collagen constructs (Hinds *et al.*, 2011). Only when fibrin constructs were dosed with high levels of supplementary basement membrane proteins did their contractile ability become significantly greater than collagen constructs. Data regarding similar levels of basement membrane protein supplementation in collagen matrices were not included in the published data (Hinds *et al.*, 2011)

It is entirely possible, and even likely, that MDC contraction in 3D *in vitro* collagen constructs does not generate force equal to that seen *in vivo* but, in seeking to accurately model skeletal muscle tissue *in vitro*, one must consider whether or not this is actually critical. Certainly, the ability for *in vitro* models of skeletal muscle to generate significant levels of directed force from organised, timed contractions is vital and optimisation of this ability is important. It is equally important to remember however, that these models are not currently destined for *in vivo* transplantation and so will not suffer for possessing force generating abilities significantly less than that of nascent tissue. Once the ability to generate controlled contractions has been established (Langelaan *et al.*, 2010; Hinds *et al.*, 2011), it is of far greater

importance to investigate the construct's capacity to promote differentiation, and to develop methods for promoting further maturation towards a phenotype representative of the adult tissue. The initial priority therefore is not to optimise a model that generates maximal levels of force, but rather to establish correct physiological development *in vitro*.

Although the contractile ability of the fibrin model is now well documented (Dennis & Kosnik, 2000; Dennis *et al.*, 2001; Khodabukus *et al.*, 2007; Khodabukus & Baar, 2009), there is little supporting data regarding the development and maturation of the seeded cells. Analysis of the collagen model (Cheema *et al.*, 2003; Cheema *et al.*, 2005; Mudera *et al.*, 2010; Boonen *et al.*, 2010; Langelaan *et al.*, 2010), while by no means complete, represents a more in depth study of the ability of the seeded MDCs to promote differentiation. Furthermore, considering the overall goals of this project, the predictable surface topography of the collagen model and a greater control over construct shape will be advantageous in generating a reproducible interface between the established muscle construct and the infiltrating motoneurons.

In fact, arguably the best solution for generating maximum levels of both contractile ability and construct maturation is to use a mixture of biopolymers which provide elasticity for force generation and biologically correct ECM proteins for MDC attachment and development. Matrigel (BD Biosciences, Oxford, UK) is a commercially available basement membrane extract containing a variety of ECM components including laminin, type IV collagen and perlecan as well as a number of growth factors and proteases (Kleinman & Martin, 2005). It is therefore well suited to promoting cell attachment and subsequent differentiation. A recent study presented convincing data for high levels of contractile force and organised sarcomere assembly in MDC seeded constructs utilising a fibrin-matrigel composite matrix (Hinds *et al.*, 2011). Products such as matrigel do however represent something of a

"black box" in their ability to promote cellular differentiation. With so many factors present, it can be problematic to ascertain exactly which factor is having the positive effect on the seeded cells. In a purely collagen matrix, a complete understanding of all the factors present in culture allows for greater clarity when investigating the cellular events taking place *in vitro* and the requirements for promoting maturation of the culture model.

3.1.4. Aims of this Chapter

In most relevant publications, the supposed improvements over conventional 2D culture methods that 3D models represent are constantly referred to. Attention is continually focused on optimising contractile force output (Dennis & Kosnik, 2000; Khodabukus *et al.*, 2007) and demonstrating the ability of these cultures to promote differentiation (Cheema *et al.*, 2003; Cheema *et al.*, 2005; Mudera *et al.*, 2010; Boonen *et al.*, 2010; Langelaan *et al.*, 2010). However, there is very little data in the public domain that actually compares and contrasts MDC differentiation ability in 2D and 3D culture. Furthermore, in the collagen model, most analysis is carried out between 0 and 7 days *in vitro,* with no supporting evidence to suggest this is time frame is at all appropriate. This group has helped develop the CFM system as a means to examine MDC development in 3D (Brady *et al.*, 2008; Mudera *et al.*, 2010). However, the "semi-open" culture environment precludes the use of this model in the study of long-term 3D culture development, since cultures typically become infected after 72 hours *in vitro*.

To that end, the experiments described in this Chapter aim to establish optimal culture conditions for primary rat MDCs in both conventional 2D culture and in a 3D collagen culture model adapted from the published CFM protocol ((Mudera *et al.*, 2010). Once completed, comparisons of the differentiation ability of the cells seeded

into each system will be made in order to fully evaluate the suitability of 3D collagen constructs for the *in vitro* modelling of skeletal muscle development.

1. Is it possible to adapt the current CFM protocol to generate a simple, reproducible, long-term 3D culture model that closely mimics the cellular architecture of *in vivo* skeletal muscle tissue?
2. To what degree does this model represent an improvement over conventional tissue culture techniques?

3.2. Materials and Methods

3.2.1. Cell culture

3.2.1.1. Establishment of 2D primary MDC cultures

Primary MDCs, isolated from the hind limbs of P1 neonatal rat pups, were seeded onto gelatin treated, 13 mm glass coverslips at varying seeding densities and maintained *in vitro* according to the protocol described in Chapter 2 (see **Section 2.1.4.**).

3.2.1.2. Passage of cultured MDCs

Isolated MDCs were seeded onto gelatin coated T75 tissue culture flasks (BD Biosciences) at 1000 cells/ cm^2. MDC cultures were passaged when they reached roughly 80% confluency to prevent differentiation of the seeded myogenic cells. Once the cells reached 80% confluency, the GM was removed and the cells washed twice with PBS. Each flask was then treated with 1.5 ml trypsin-EDTA (Sigma-Aldrich) and the solution agitated until it covered the entire cell colony. The flasks were incubated for 5 minutes or until all the cells had detached from the plastic. The cell suspension was then treated with 1.5 ml GM and the resulting solution transferred to a 15 ml centrifuge tube. The cells were spun at 450 g for 5 minutes; the supernatant was removed and the cells resuspended in GM. The cells were counted using a haemocytometer (see **Section 2.1.3.**) and plated onto fresh 0.2% gelatin coated T75 flasks at a density of 1000 cells/ cm^2. Flasks were returned to the incubator and the media changed subsequently every 2-3 days.

3.2.1.3. Establishment and maintenance of 3D primary MDC cultures

Primary rat MDCs were seeded within 3D collagen constructs as described previously (see **Section 2.1.7.2.**). MDC seeding density varied depending on specific experimental parameters but was always within the range of 1 and 6 million cells/ ml. MDC seeded constructs were maintained in GM until 2D control cultures (see **Section 2.1.4.**) reached confluency, at this point the GM was replaced with DM+IGF1. Media was replaced daily throughout the culture period.

3.2.2. Immunocytochemistry

MDCs seeded onto glass cover slips (2D) or within un-sectioned tissue fragments of collagen constructs (3D) were immunostained using a desmin antibody (see Table 2.1.) as a marker of commitment to the myogenic lineage, and DAPI (Sigma-Aldrich) counter-stained to visualise nuclei, in order to assess their purity and level of fusion. Fixation and staining was carried out using the protocol described in Chapter 2 (see **Section 2.2.**).

3.2.3. Image analysis

Image analysis was carried out using the guidelines described in Chapter 2 (see **Section 2.2.3.**). Cultured MDCs were stained for desmin and nuclei were visualised using the DNA binding probe DAPI. The level of co-localisation between these 2 markers was then used to calculate the number of myoblasts in culture as a percentage of the total MDC population. The fusion efficiency (the number of myogenic nuclei incorporated into myotubes, calculated as a percentage of the total number of myogenic nuclei present) of cultured MDCs was also estimated using desmin stained cultures. Myoblasts were identified as any mononuclear, desmin

positive cell and a myotube was defined as a desmin positive cell with at least 3 nuclei (Figure 3.1).

3.2.4. PCR analysis of 2D and 3D MDC cultures

Cultures designated for PCR analysis were homogenised in TRIzol reagent and the RNA purified using the protocol described previously (see **Section 2.3.1.**). RNA was then converted to cDNA using the protocol described previously (see **Section 2.3.2.**).

3.2.4.1. Conventional PCR analysis

cDNA samples were amplified by PCR and run on 2% polyacrylamide gels using the protocol previously described (see **Section 2.3.3.**). PCR was used to test cultures for expression of a number of genes indicative of muscle maturation: myogenin, troponin and acetylcholine receptor ε-subunit (AChRε). β-actin was used as an endogenous control in all cultures examined. A list of the primer sequences used in these experiments is provided in Table 2.2.

3.2.4.2. Quantitative PCR analysis

Quantitative PCR (qPCR) was carried out using the Applied Biosystems 7300 Real-Time PCR System (Applied Biosystems, CA USA). The PCR reaction mixture (12.5 µl TaqMan universal PCR Master Mix, 2.5 µl cDNA, 1.25 µl probe and 8.75 µl nuclease-free water) was made up for each gene to be analysed in quadruplicate wells over a 96 well plate (Applied Biosystems, CA USA). The plate was incubated at 50^{o}C for 2 minutes and 95^{o}C for 10 minutes before being cycled 40 times at 95^{o}C for 15 seconds and then 60^{o}C for 60 seconds. This protocol was specifically designed by Applied Biosystems for use with any assays designed according to Applied Biosystems assay design guidelines, therefore no optimisation of the

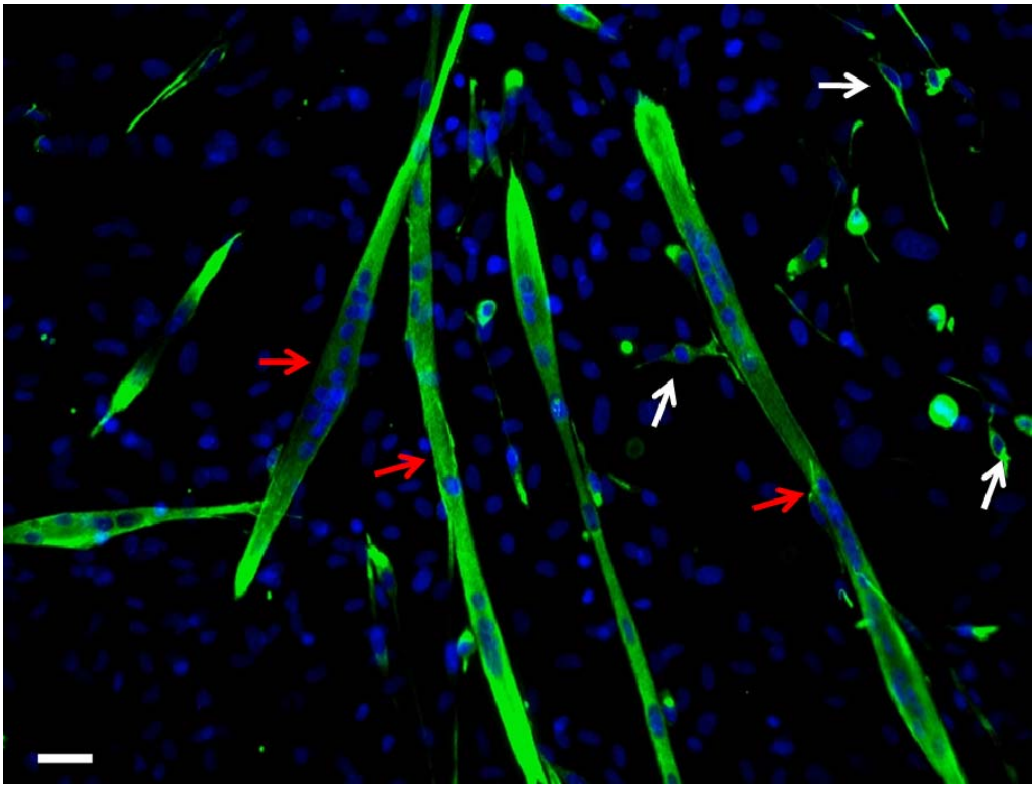

Figure 3.1: 2D culture of primary rat MDCs. Cultures were immunostained for desmin (green) and nuclei visualised using the DNA binding probe DAPI (blue). Myoblasts were identified as desmin positive mononuclear cells (white arrows) while myotubes were defined as desmin positive cells with at least 3 nuclei (red arrows). Scale bar = 20 μm.

thermal cycling parameters was necessary for the probes used; myogenin (assay ID, Rn00567418_m1) and β-actin (assay ID, Rn00667869_m1).

The threshold cycle (C_T) was defined as the fractional cycle number at which the fluorescence generated by cleavage of the probe exceeded a fixed threshold above the baseline. To quantitate the amount of each target gene present, the comparative C_T method was used, as outlined in Applied Biosystems *User Bulletin No. 2: ABI PRISM 7700 Sequence Detection System* (Applied Biosystems, CA USA). The mean C_T value from quadruplicate wells for each sample was determined and normalised to that of the endogenous housekeeping gene (β-actin). The amount of target amplification relative to the experimental control was calculated by the formula $2^{-\Delta\Delta C_T}$.

3.2.5. Statistical Analysis

All experiments were repeated at least 3 times using cultures prepared on different days from pups of different litters. Statistical significance between 2D and 3D cultures for myogenin expression, as well as for fusion efficiency, were assessed using separate t-tests in Sigma Stat (version 2.03, Erkrath, Germany). Significant differences in myogenin expression between time-points in either 2D or 3D systems were separately assessed using one-way analysis of variance (ANOVA) in Sigma Stat, as were differences in fusion efficiency at multiple 3D seeding densities. Differences in numbers of myotubes formed in 2D culture, due to changes in media type and seeding density, were assessed using two-way ANOVA, again using Sigma Stat. Values are expressed as mean ± standard error of the mean. Significance was set at $p<0.05$.

3.3. Results

MDCs derived from the hind limbs of P1 rat pups were assessed for their survival and maturation in 2D culture conditions. Evaluation of the cells in culture was carried out by microscopy in conjunction with several immunocytochemical (ICC) markers. Once the culture conditions were optimised in 2D, MDCs were seeded into 3D collagen constructs and compared to 2D culture controls. Assessment of the 2 culture models was achieved using ICC microscopy and qPCR analysis.

3.3.1. Myogenicity of cultured primary rat MDCs in 2D

In order to assess the myogenic potential of MDCs derived from P1 rat pups, isolated cells were seeded at 1,500 cells/ cm^2 on 0.2% gelatin treated coverslips and cultured for 3 days. They were then fixed, stained for desmin and the percentage of cells committed to the myogenic lineage established. Figure 3.2 shows examples of MDCs cultured and immunostained for determining myogenicity.

The myogenic fraction of cells from separate dissections, as determined by desmin positivity, was found to vary substantially in 2D cultures. Under these conditions, the cultures were found to be between 20% and 40% myogenic, with a mean value of 26.46% ± 3.31 (n=5).

3.3.2. Passage ability of cultured primary rat MDCs in 2D

To determine whether this myogenic fraction was stable over a series of trypsinisation and replating procedures, MDCs were put through multiple passages and the myogenicity calculated at various points throughout the culture period. The myogenic fraction of cultures put through such stress (n=4) was shown to rapidly deteriorate (Table 3.1). Within 2 trypsin treatments the desmin positivity dropped

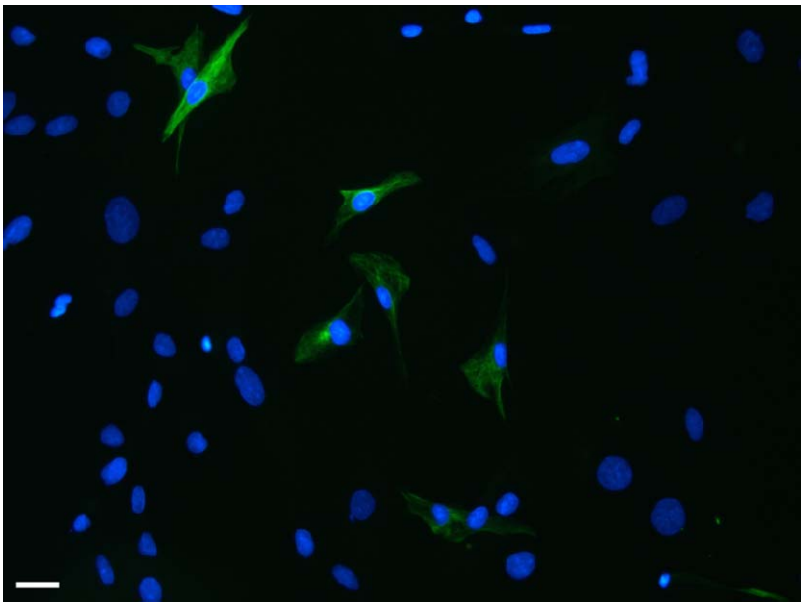

Figure 3.2: Example image from 2D culture of primary rat MDCs used for estimating desmin positivity. Cells were immunostained for desmin (green) with nuclei visualised using the DNA binding probe DAPI (blue). Such images were used to estimate the myogenic fraction within any given MDC culture. Scale bar = 20 μm.

Digest	Passage 1	Passage 2	Passage 3	Passage 4	Passage 5
1	30.52		5.92		0.00
2	37.29			0.00	0.00
3	19.76		0.00		0.00
4	20.55	0.17	0.00	0.00	0.00

Table 3.1: Percentage of desmin positive cells within primary rat MDC populations in 2D *in vitro* culture over multiple passages. Blank fields indicate no counts performed.

almost to zero, indicating the inability of these cultures to maintain their myogenic population over multiple passages.

3.3.3. Effect of seeding density and feeding media on cultured primary rat MDC differentiation in 2D

The seeding density of cells and the feeding media used can have profound impacts on the level of differentiation of myoblasts in culture. In order to assess the effect of these variables on the differentiation ability of primary rat MDCs, cells were plated at densities of 10,000, 25,000 and 50,000 cells/ cm^2. At each density, cells were grown to confluency in standard GM before being switched to DM with different supplements; DM + 0.5% CEE, DM + IGF-1 (10ng/ ml) or DM without supplements. The cultures were maintained for a further 3 days before being fixed and immunostained for desmin expression.

Density was found to have a significant impact on the number of myotubes formed in culture, regardless of the medium used (Figure 3.3). In all DM types, a significant difference between the number of myotubes formed at 25,000 cells/ cm^2 and 50,000 cells/ cm^2 was observed. A significant difference was likewise found between the number of myotubes formed at 10,000 cells/ cm^2 and 25,000 cells/ cm^2 in all DM types with the exception of DM without supplementation.

There was also a significant difference in the number of myotubes formed when cultures seeded at 50,000 cells/ cm^2 were fed with different media (Figure 3.4). Cultures exposed to IGF-1 supplemented media developed the greatest number of myotubes of all media tested. Roughly 25% fewer myotubes developed in cultures supplemented with CEE while cultures given no supplementation demonstrated a drop in myotube number of over 60%. At 10,000 cells/ cm^2 and 25,000 cells/ cm^2, no significant difference was found between any media types ($p>0.05$).

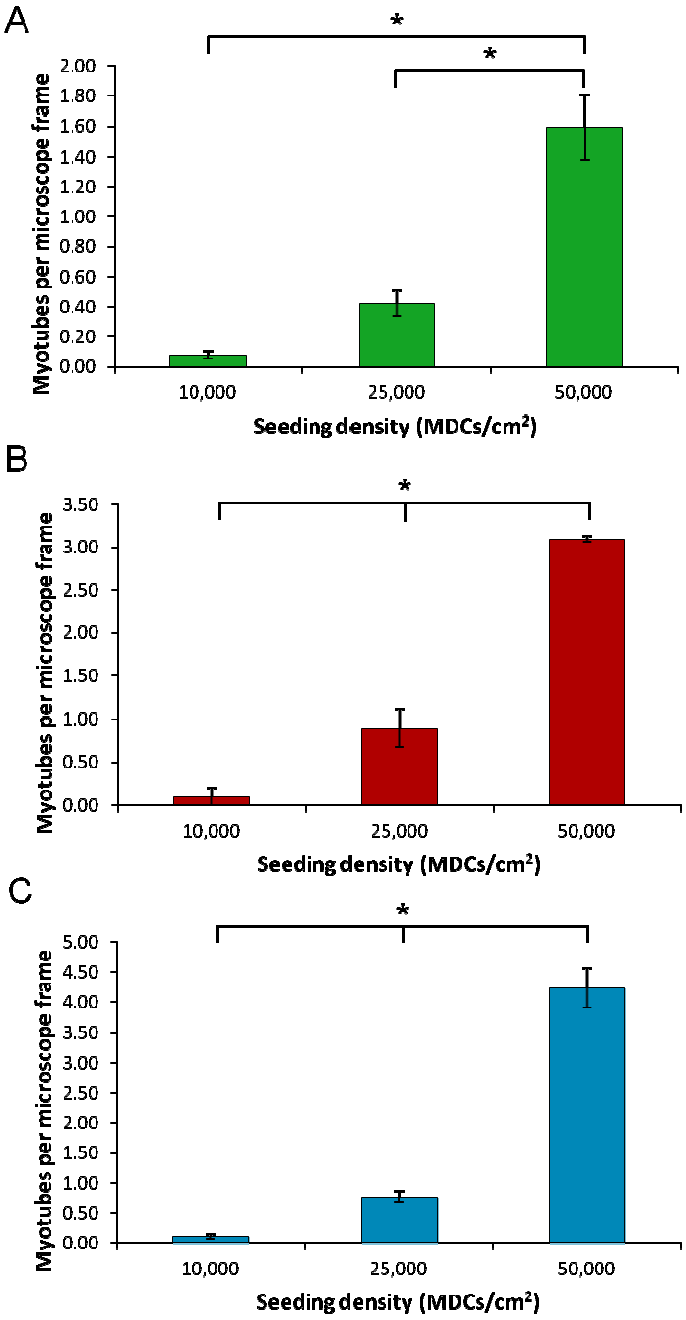

Figure 3.3: The effect of altered cell seeding density on the mean number of myotubes formed in 2D cultures of primary MDCs maintained in different differentiation media. Numbers of myotubes were counted from cultures fed with (A) DM without supplementation, (B) DM+CEE and (C) DM+IGF-1. n = 3 across all cultures. Error bars = standard error of the mean, *p<0.01.

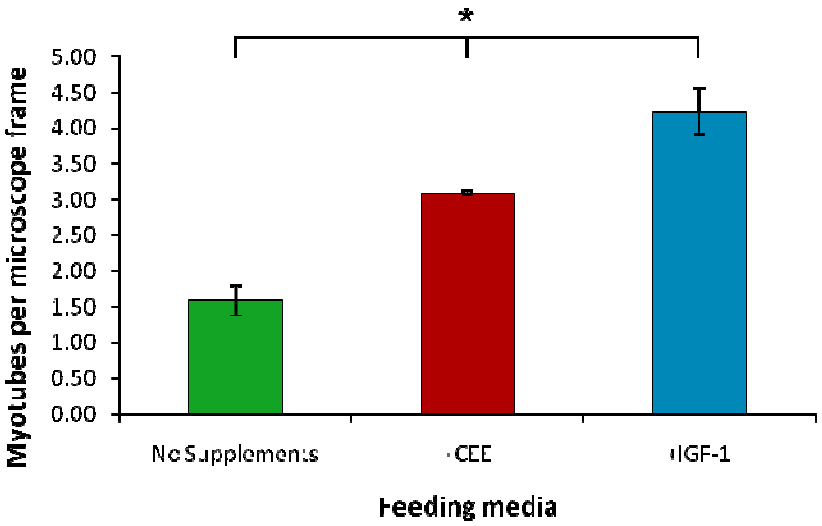

Figure 3.4: The effect of different feeding media on the mean number of myotubes formed in 2D cultures of primary MDCs seeded at 50,000 MDCs/ cm^2. n = 3 across all cultures. Error bars = standard error of the mean, *p<0.01.

Preliminary investigations revealed that cultures seeded more densely than 50,000 MDCs/ cm^2 were too crowded to promote reliable cell attachment, leading to large numbers of floating, dead cells after 24 hours. Given this observation and the data collected here, 50,000 MDCs/ cm^2 fed with DM + IGF-1 was established as optimum conditions for promoting the greatest level of MDC differentiation in 2D.

3.3.4. Adaptation of the CFM system for generation of simple long-term 3D cultures

Established 3D cultures utilising collagen matrices often rely on the novel CFM system (Cheema *et al.*, 2005; Mudera *et al.*, 2010). In order to adapt this established protocol for successful long-term culture of primary rat MDCs in 3D, a number of methods were analysed. The protocol described in Chapter 2 for generating 3D MDC cultures therefore represents the culmination of a number of preliminary investigations into various techniques and assessment of their suitability for use in this model. The modifications and alterations made to the culture model during this assessment are summarised in Table 3.2.

3.3.5. Comparison of primary rat MDC differentiation in 2D and 3D culture models

The viability of MDCs cultured in 3D collagen constructs has been verified previously, as has their ability to express a number of markers indicative of skeletal muscle differentiation (Cheema *et al.*, 2005; Mudera *et al.*, 2010). In conjunction with published data, PCR analysis of collagen constructs seeded with 1 million primary rat MDCs/ ml demonstrates the expression of mRNA transcripts for markers of muscle maturation myogenin, troponin and AChRε (Figure 3.5A).

Technique used	Used because?	Problems	Replaced with?
Adult rat hind limb muscle as source of *in vitro* MDCs.	Large cell population. Better for mimicking adult skeletal muscle *in vitro.*	Enzymatic digestion yielded few cells. Explant culture yielded cells of very low myogenicity.	**P1 neonatal rat muscle:** Sufficient cell number and substantial myogenic fraction (see **Section 3.3.1.**)
Custom built PTFE moulds	Easily sterilised. Comparison to CFM data more directly relevant.	Flotation bar attachment problematic. Insufficient numbers for large scale investigation.	**Chamber slides:** Easily available in large numbers. Reduces the bespoke nature of the system – more repeatable/ reliable results.
Stainless steel mesh flotation bars	Easily sterilised	Issues with attachment to collagen gel.	**Polyethelyne meshwork:** Construct attachment greatly improved.

Table 3.2: Summary of the alterations made to the CFM system in order to establish a simplified culture model for the long-term maintenance of MDCs in 3D.

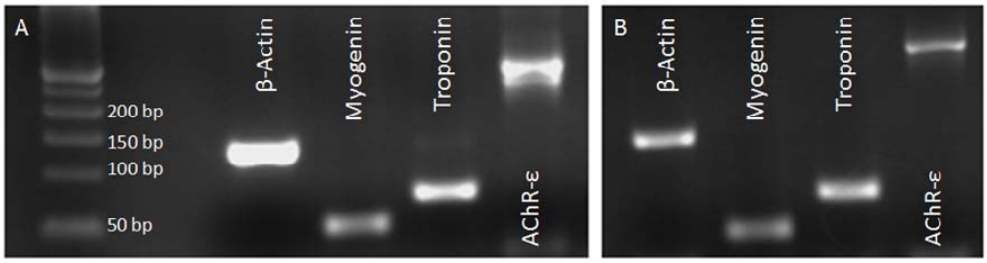

Figure 3.5: Examples of conventional PCR results for markers of muscle maturation from *in vitro* cultures of primary rat MDCs. Results are shown from both 3D (A) and 2D (B) cultures. 2D tissue culture plastic was seeded with 50,000 MDCs/ cm^2 and 3D collagen constructs seeded with 1 million MDCs/ ml. Identical results were achieved over 3 separate cultures.

Expression of these genes in culture suggests an ability for MDCs to differentiate when cultured in 3D. These genes are also expressed in 2D culture however (Figure 3.5B), and the ability for cells cultured in this 3D environment to differentiate to similar levels as those seen in conventional 2D culture has not been previously demonstrated. Comparison of differentiation ability in 2D and 3D was achieved in this study using qPCR analysis. Purified RNA from specific time points over a 3 week period was collected from both 2D and 3D cultures and myogenin expression levels used as an indicator of the level of fusion that had occurred. MDCs were seeded at 25,000 cells/ cm^2 in 2D, despite data suggesting higher densities yield greater levels of fusion, in order to ensure the 2D cultures survived the entire 3 week culture period without detaching from the substrate. 3D cultures were established at 1 million MDCs/ ml. Previous work using fibroblasts (Eastwood *et al.*, 1996; Eastwood *et al.*, 1998) supported the use of this density as an optimum for generating predictable lines of tension within the construct, thereby ensuring the correct mechanical signals were delivered to the seeded cells. 2D and 3D cultures were also fixed at equivalent time points and immunostained for desmin to provide visual support to the qPCR data.

Analysis of the myogenin qPCR data (Figure 3.6) indicated a substantial decrease in myogenin expression over time as a general trend in both 2D and 3D. In 2D culture, there was a significant drop in myogenin expression levels between days 3 and 9 ($p=0.003$) and between days 6 and 13 ($p=0.006$). From day 13 until the end of the culture period myogenin expression remained at a constant low level, with no further significant differences seen at any subsequent time point.

By comparison, myogenin expression in the 3D model appeared to be considerably more variable and remained at a consistently high level over the first 9 days in culture. By day 13, myogenin expression patterns more closely resembled those in

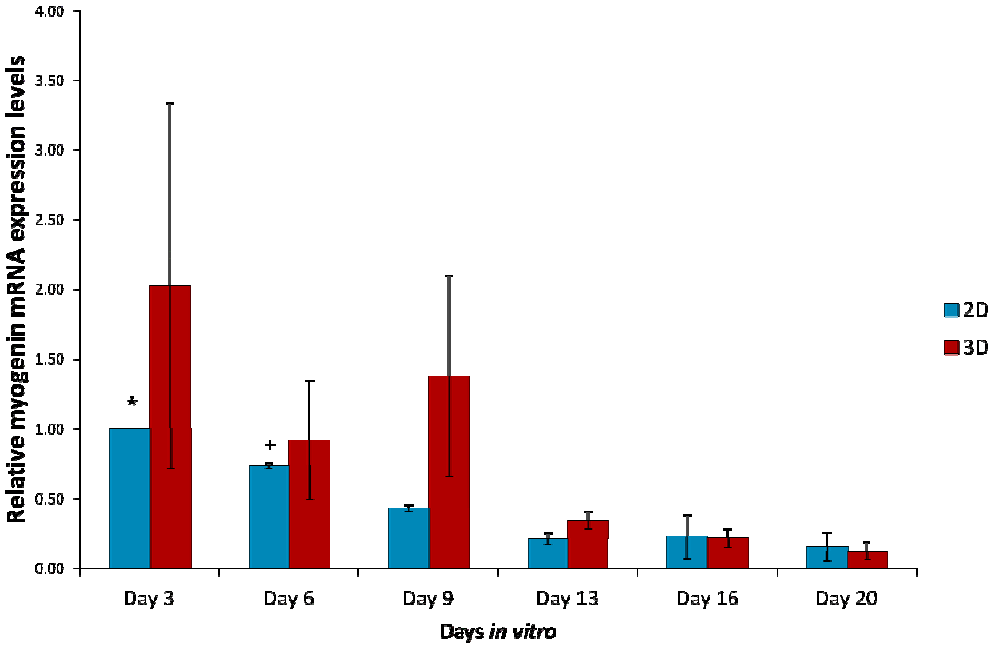

Figure 3.6: Myogenin expression in MDCs from 2D and 3D cultures, over 3 weeks *in vitro*, as determined by qPCR. C_T values were normalised to an internal housekeeping gene (β-actin) and expressed relative to levels recorded for 2D culture at day 3. n = 3, error bars = standard error of the mean. In 2D, myogenin expression at day 3 was found to be significantly greater than expression at days 9, 13, 16 and 20 (*$p<0.005$). Expression at day 6 was also found to be significantly greater than expression at days 13, 16 and 20 ($^{+}p<0.01$). No significant differences were observed between 2D and 3D cultures at equivalent time points ($p>0.05$).

2D culture, with a substantial drop both in expression and in variance between cultures. While the mean myogenin expression at day 3 was twice that seen in 2D culture, the substantial variability between cultures removed any significance from this difference ($p=0.478$). Likewise, there was no significant difference in expression between the 3D cultures and their 2D counterparts at days 6 ($p=0.696$) and 9 ($p=0.258$), despite substantially greater mean expression levels in 3D at the latter time point. From day 13 onwards, expression levels were broadly equal between 2D and 3D cultures, with no significant differences found at any time point ($p>0.05$).

A lack of significant difference between the 2 culture models indicates that the level of differentiation seen in conventional 2D culture, while not improved, is preserved in 3D. Cells were seeded in 2D at a low density to prevent their detachment from the plastic and ensuring their survival over the entire 3 week culture period. This low seeding density led to low levels of myotube formation in these cultures, as indicated by immunostaining of identical cultures at equivalent time points (Figure 3.7A). Similarly, immunostaining of frozen sections from the 3D constructs revealed very low levels of myotube formation (Figure 3.7B).

3.3.6. Effect of seeding density on myotube formation in 3D culture

Since differentiation of muscle precursor cells is known to be highly dependent on density and cell-cell contact (Lindon *et al.*, 2001; Dee *et al.*, 2002) and had already been shown to be a strong determining factor on the level of myotube formation in 2D, the effect of seeding density on MDC ability to fuse in the 3D model was investigated next. Constructs were established at 3, 4, 5 and 6 million MDCs/ ml and cultured for 2 weeks. They were then fixed, immunostained and analysed by confocal microscopy for desmin positivity. The imaged cells were finally assessed for fusion efficiency as described previously (see **Section 3.2.3**).

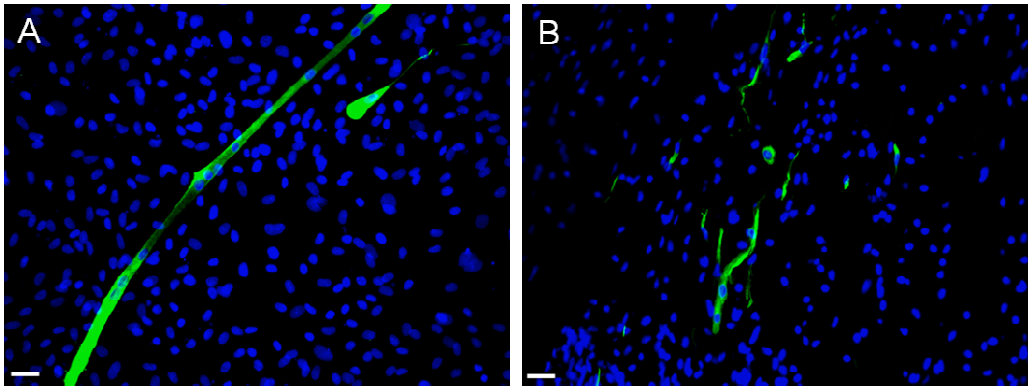

Figure 3.7: Comparison of MDC fusion in low density 2D and 3D cultures. Primary rat MDCs in culture were immunostained for desmin (green) and DAPI (blue). Note the low levels of fusion in (A) 2D culture at 25,000 MDCs/ cm^2 and (B) 3D culture at 1 million MDCs/ ml. Scale bars = 20 µm.

At 5 million MDCs/ ml the fusion efficiency was found to be 73.14% (± 3.45, n=4) of all myogenic nuclei present. At this density, only 30% of the desmin positive cells in culture failed to fuse into myotubes, indicating the strong potential for differentiation in MDCs seeded at this density. By comparison, at 3 million MDCs/ ml, the fusion efficiency was just 15.37% (± 5.66, n=3) demonstrating that the majority of myogenic cells at this density were unable to differentiate into multinuclear myotubes.

Significant increases in the fusion efficiency were found at each seeding density examined up to 5 million MDCs/ ml (Figure 3.8). At 6 million MDCs/ ml it was not possible to reliably culture the cells for the full 2 week period since the constructs generated sufficient tension to pull themselves off of the frames, thereby destroying the uniaxial tension developed.

As a comparison, seeding density in 2D culture was increased to 50,000 MDCs/ cm^2; in my hands, the highest density found to promote reliable cell attachment, survival and differentiation. At this density, the seeded MDCs demonstrated a fusion efficiency of 61.46% (± 1.16, n=3) after 4 days in DM + IGF-1. This value is significantly lower than its equivalent in 3D culture ($p=0.039$). Furthermore, attempts to maintain 2D cultures for the 2 weeks used in 3D were not successful. Cultured MDCs did not survive more than 5 days in DM before the cells detached from the plastic. Hence the level of differentiation of high density primary MDCs using conventional tissue culture methods is not only significantly lower than in 3D culture, but the maintenance of such cultures for any substantial length of time is problematic due to the cell's spontaneous contractions pulling them off of the substrate. Conversely, differentiated cells at high density in 3D were maintained for 2 weeks in this study and if necessary could be maintained for significantly longer periods of up to 8 weeks.

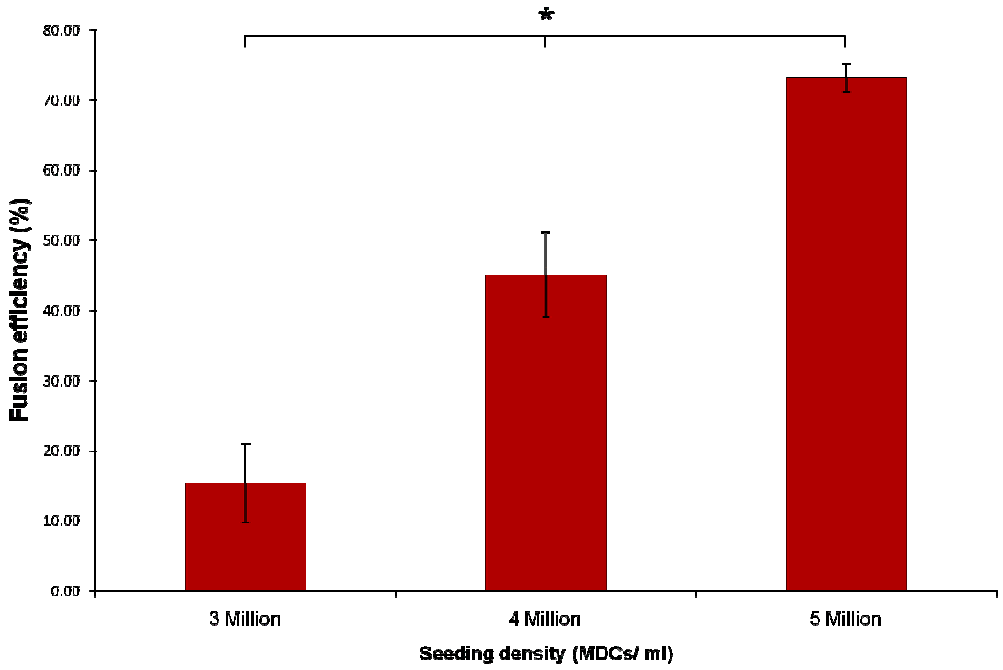

Figure 3.8: The effect of increasing cell seeding density on the fusion efficiency of primary rat MDCs seeded within 3D collagen constructs. n=3 except for cultures seeded at 5 million MDCs/ ml where n=4, error bars = standard error of the mean, *p<0.001.

3.3.7. Improved cellular architecture of MDCs seeded in 3D culture

Phase contrast microscopy of the cells seeded within collagen gel constructs revealed that the MDCs showed alignment along the lines of principle strain in a longitudinal direction between the anchor points at each end of the construct as early as 48 hours post-seeding. This behaviour has been described previously in collagen constructs using the established CFM system (Cheema *et al.*, 2003), and is not observed in collagen constructs in the absence of the uniaxial tension provided by fixed floatation bars (Vandenburgh *et al.*, 1988).

ICC analysis of frozen sections from the constructs demonstrated the alignment of differentiated myotubes in parallel with the long plane of the gel (Figure 3.9A). When compared with 2D control cultures (Figure 3.9B), the improved cellular architecture of the 3D model is clear. Further comparison of 2D and 3D culture images to sections of *in vivo* skeletal muscle tissue (Figure 3.9C) demonstrates the improvement that uniaxial tension in culture provides to developing MDCs. In 3D culture, differentiated myotubes were found densely packed and lying in a parallel conformation, mirroring that seen *in vivo,* while 2D cultures demonstrated no organised structure or notable orientation. Furthermore, and again similar to *in vivo* muscle, the myotubes in 3D constructs were entirely unbranched in all cultures examined (n=9). In 2D culture however, branching was seen in 8.59% (±1.38, n=3) of the myotubes present.

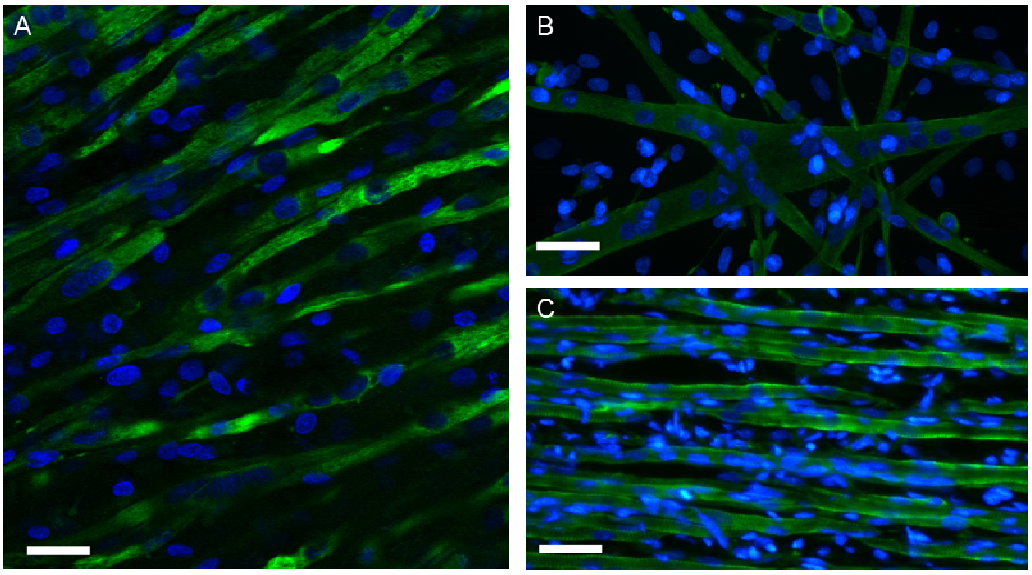

Figure 3.9: Comparison of 2D and 3D cultures of primary rat MDCs with rat skeletal muscle tissue. (A) A 30 µm thick longitudinal section from a 3D collagen construct seeded with primary rat MDCs at 5 million cells/ ml and immunostained for desmin (green) and the nuclear marker DAPI (blue). (B) Primary rat MDCs seeded on 2D tissue culture plastic at 50,000 cells/ cm^2 and again stained for desmin (green) and DAPI (blue). (C) A 30 µm thick, longitudinal section of *in vivo* skeletal muscle from the hind limb of a P1 rat pup stained for desmin (green) and DAPI (blue). Scale bars = 20 µm.

3.4. Discussion

Previous work using the culture force monitor (CFM) system has focused on the use of either human derived muscle cells (Mudera *et al.*, 2010) or the C2C12 mouse muscle cell line (Cheema *et al.*, 2003). In order to expand the application of the collagen model as a whole, optimum conditions for promoting the development and maturation of primary rat muscle cells within this model have been investigated in this Chapter. Successful generation of 3D cultures using primary animal cells will pave the way for the use of cells from established animal disease models in this system, providing a more biomimetic *in vitro* environment in which to investigate the behaviour of these aberrant cell types.

In order to effectively utilise specific primary cells in any new culture system, it is important to first understand how these cells behave in standard *in vitro* environments. Knowledge of optimal seeding densities, feeding media and culture periods is essential to ensure generation of the best *in vitro* cultures possible. Only by comparing optimised results for 2D and 3D cultures can there be any certainty that the improvements seen are a result of the differences in the culture model and not due to a lack of optimisation in one or other system.

3.4.1. Optimisation of 2D culture conditions for primary rat MDCs

3.4.1.1. MDC myogenicity

Desmin is a cytoskeletal intermediate filament protein expressed in both proliferating myoblasts and terminally differentiated myotubes (Allen *et al.*, 1991). *In vivo*, desmin is known to be expressed as early as 8.25 days post coitus in the neuroectoderm of developing embryos and by day 9 in the myotome (Li & Capetanaki, 1993). It is one of the earliest known muscle specific proteins to be expressed *in vivo* and, given its

continued expression in differentiated fibres, is an excellent marker of a cell's commitment to the myogenic lineage (Allen *et al.*, 1991).

Cultures established using the methods described in this Chapter were consistently shown to possess a significant population of desmin positive cells, although their numbers as a proportion of the total number of cells present varied considerably. Desmin positive cells were found to constitute between 20% and 40% of the total cells in culture. This variation is likely due to differing levels of contaminating connective tissue included with the dissected muscle in the collagenase digest solution. While every effort was made in this study to reduce connective tissue contamination, it is not possible to remove it completely and the amount of contamination will always vary between cultures. This degree of variance mirrors figures published previously regarding the myogenicity in MDCs derived from human muscle tissue, which ranges between 5 and 45% (Lewis *et al.*, 2000; Singh *et al.*, 2000; Sinanan *et al.*, 2004; Brady *et al.*, 2008), as well as previous work with rat primary muscle cultures (Kaufman *et al.*, 1991), indicating the suitability of the described protocol for obtaining primary myoblasts for use in this study.

The capacity of these cells to maintain their myogenic population in culture over multiple passages would prove incredibly useful. Particularly in human cultures, the use of cells from a single sample in multiple experiments reduces the chance of any observed differences being attributable to alterations in genotype. This benefit is somewhat diminished in laboratory animal models since all individuals are genetically similar. Never-the-less, the use of cells from a single digest ensures a constant population (i.e. no fluctuations in myoblast: fibroblast ratios) and allows for repeats to be built in to the experimental model. Furthermore, passaged cells reduce the total number of animals used in experiments, thus representing a more ethically sound protocol.

Unfortunately, the ability of primary MDCs isolated from P1 neonatal rat pups to maintain their myogenic fraction over multiple passages appears to be negligible. In this study, by the third passage, in all but one of the repeats, no discernable myogenic cells remained and by passage 5, the myogenic fraction had completely disappeared in all cultures examined. This finding is supported by a previous study from Machida *et al.* (2004), who demonstrated that purified rat muscle precursor cells exhibit a significant drop in the expression of myogenic, satellite cell and haemopoietic stem cell markers over 3 passages. The percentage of desmin positive cells in these purified cultures dropped from over 90% to just 55% in this short period.

Populations of cells pushed down the myogenic lineage are likely to become progressively quiescent as they move towards terminal differentiation and fusion into myotubes. To that end, prolonged time in culture should lead to a progressive decrease in cell divisions within this population. Concurrently, the relatively stable population doubling rate of fibroblasts makes it likely that myogenic cells in these cultures are rapidly out competed, dictating the necessity for freshly isolated MDCs to be used in all future experimental cultures.

3.4.1.2. Media optimisation in relation to promoting MDC differentiation

Once a stable myogenic fraction has been established, it is essential for these cells to demonstrate an ability to fuse and form myotubes in culture. Furthermore, the development of an optimal media composition for promoting the highest level of differentiation possible is also necessary. There is no universally accepted feeding media for primary rat MDCs. Although most protocols conform to a general standard, considerable variation exists in the volume of certain constituents used. Favoured media commonly consists of horse serum in high glucose DMEM in order

to induce differentiation. Concentrations of serum vary between 2% (Machida *et al.*, 2004) and 10% (Allen *et al.*, 1991; Kaufman *et al.*, 1991) however and there is some disparity in the use of chick embryo extract (CEE) (Allen *et al.*, 1991; Kaufman *et al.*, 1991). CEE is a cocktail of growth factors, enzymes and co-factors isolated from chicken eggs and has long been used as a potent inducer of cellular differentiation in *in vitro* cultures (Slater, 1976; Nicolas-Bolnet & Dieterlen-Lievre, 1995). The wide range of agents present likely ensures that any and all factors a cell requires to survive and mature will be present. Unfortunately, as discussed previously in relation to Matrigel (see **Section 3.1.3.**), lack of knowledge as to the specific constituents of the extract does introduce a level of ambiguity into what components are acting on the cells to promote differentiation.

The use of 2% serum conforms to the serum concentration of CNB media in which the MDC-motoneuron co-cultures will eventually be maintained. Hence it was decided that a 2% serum concentration would be used in the DM throughout this study, in order to eliminate the possibility that continued alterations in serum concentrations would impact negatively on the maturation of the 3D co-culture model. Investigations were instead focused on the ability of CEE supplements to promote myogenic differentiation in primary rat MDC cultures. The importance of IGF-1 in promoting the proliferation and differentiation of myoblasts is well established (Florini *et al.*, 1996). It was therefore decided that, in this study, this growth factor would also be investigated as an alternative supplement to CEE without the ambiguity of activity that inclusion of embryo extract entails.

As can be seen from the results (Figure 3.4), there is a clear step up in the levels of fusion seen in cultures treated with CEE when compared to unsupplemented controls, and between cultures given CEE and those treated with IGF-1. The low fusion level in unsupplemented cultures demonstrates that media supplementation

is necessary to promote high levels of MDC differentiation *in vitro* and indicates that cells in culture are poorly equipped to promote their own differentiation. Previous studies *in vivo* have demonstrated that autocrine or paracrine IGF-1, rather than circulating IGF-1, is important for skeletal muscle regeneration (Duan *et al.*, 2010). Since muscle cells *in vivo* are capable of producing sufficient IGF-1 to promote their own differentiation, significant increases in the number of myotubes formed in culture when media was supplemented with IGF-1 demonstrates that MDCs in culture may lack this ability.

The difference observed between CEE and IGF-1 treated cultures is particularly interesting. IGF-1 treatment led to the development of significantly more myotubes in culture after 3 days in DM. This suggests either that the CEE possesses some antagonistic factors to myogenic differentiation, that act to inhibit fusion in treated cultures, or that the IGF-1 presence in the CEE is lower than the 10 ng/ ml present in the IGF-1 supplemented cultures. A third possibility is that, instead of IGF-1, CEE possesses some other factor that is a less potent inducer of MDC differentiation and so elicits lower levels of fusion. Regardless of the reason, these results indicate that IGF-1 treated cultures promote the greatest levels of fusion in primary rat MDCs and should therefore be used in all subsequent experiments.

3.4.1.3. The effect of increased cell seeding density on MDC differentiation

Even without media optimisation, the number of myotubes able to form in culture is clearly density dependent. The higher the initial seeding density, the greater the number of myotubes formed, regardless of DM supplementation (Figure 3.3). This finding is consistent with previous publications (Lindon *et al.*, 2001; Dee *et al.*, 2002) and its interpretation is straightforward. Cells capable of fusing to form myotubes need to be in close contact so that the membranes of the two cells are able to

interact with each other. Denser cultures will have a greater number of myogenic cells present and so a greater chance of cell-cell contact between them. Myogenic cells in more sparsely seeded cultures will have less chance of adhering within close proximity of a compatible cell and therefore less chance of being able to fuse. The progressive drop in doubling rates of myogenic cells in culture (Machida *et al.*, 2004) and the consistent rate of growth of fibroblasts means that once the population reaches confluency, the percentage of myoblasts is likely to be lower than it was at the time of isolation; thus there is an even greater reduction in the fusion potential of such cultures.

3.4.2. Development of a 3D collagen based culture model using primary rat MDCs

Optimisation of culture conditions for primary rat MDCs in 2D allowed for progression into 3D culture analysis. Assessment of cultured muscle cell's functional output is not possible in standard 2D systems and essential to quantifying the phenotypic effect that disease or drug treatment has on the affected tissue. Direct measurements of the contractile force generated by 3D collagen constructs can be made in real time using the novel CFM system (Cheema *et al.*, 2003). However, the open nature of the system makes the maintenance of cultures difficult in the long term. By moving the collagen based 3D model into standardised chamber slides, the establishment of reproducible, long term cultures was possible. Although this decision prevented direct measurements of contraction being made in the present study, it allowed for the formation of 3D cultures better suited to the study of cellular maturation and physiology over extended periods and so was judged to be more appropriate for the particular aims of this investigation.

3.4.2.1. Comparison of MDC differentiation in 2D and 3D culture systems

Expression of mRNA for the myogenic regulatory factor myogenin by MDCs suggests an ability for these cells to promote differentiation in 3D culture (Figure 3.5A). Furthermore, expression of mRNA for cellular contractile machinery proteins (troponin) and post synaptic structures specific to neuromuscular junctions (AChRε) implies a significant level of maturation within the seeded cells. The importance of this data is reduced substantially however when one considers that PCR results for 2D cultures are identical (Figure 3.5B). Quantification of the level of differentiation possible in the 2 culture systems is therefore necessary, in order to evaluate the 3D construct's suitability as an *in vitro* culture system for MDCs.

Comparison of myogenin expression levels between 2D and 3D constructs as an indicator of muscle differentiation revealed no significant difference between the two systems at any time point (Figure 3.6). This implies that the substantial capacity of cultured primary MDCs to fuse *in vitro,* as observed in 2D control cultures (Figure 3.3), is neither improved nor inhibited by transferring them to the 3D model.

3.4.2.2. The effect of increased seeding density on MDC differentiation in 3D culture

While this analysis seems logical based on the myogenin expression data alone, conclusions regarding equal levels of differentiation in 2D and 3D are not upheld when the seeding density is increased. Analysis of ICC data from high density cultures demonstrated significantly higher fusion efficiencies in 3D cultures seeded at 5 million MDCs/ ml when compared with 2D controls seeded at 50,000 MDCs/ cm^2. The ability for the 3D model to promote greater levels of fusion is difficult to confirm however, since it cannot be stated for certain that the seeding densities examined in 2D and 3D are in any way equivalent or comparable. For each culture

model the highest density to produce usable cultures was used, but it seems likely that the flexible nature of the 3D model permits the successful culture of more densely packed cells than is possible in 2D. If this is the case then the significant increase in fusion efficiency observed would rather be a result of a higher density in 3D rather than any inherent differences in the culture environment. Never-the-less, this observation does illustrate the improvement to MDC culture that the 3D model generates.

Analysis of myogenin expression was undertaken in 3D constructs seeded at 1 million MDCs/ ml since this density was previously optimised using primary human fibroblasts for the generation of predictable lines of tension within the CFM system (Eastwood *et al.*, 1996; Eastwood *et al.*, 1998). Fusion efficiency studies demonstrated that this cell seeding density is inappropriate for MDC culture however, and the ability of MDCs to differentiate into multinuclear myotubes in 3D is far greater when the seeding density is increased (Figure 3.8). The explanation of this phenomenon is likely to follow the same logic employed when analysing seeding density in 2D culture; the greater the seeding density, the greater the number of myoblasts present and hence the greater the probability that they will be seeded at a proximity sufficiently close to fuse. In theory, by continuing to increase the seeding density of MDCs, it should be possible to achieve greater and greater levels of myotube formation, as well as the increased density of the resulting fibres into a more fascicle like arrangement. However, this ability is limited by the inherent strength of the model tissue. A seeding density of 6 million MDCs/ ml led to the formation of an unreliable construct that sometimes survived and sometimes pulled itself off of the frames. The tendency for densely seeded MDCs to detach themselves from their substrate (Vandenburgh *et al.*, 1988) is not completely removed when using the 3D model, but the flexibility of the matrix permits highly

differentiated, contractile cultures to be maintained for weeks in culture rather than days.

The data obtained in this study suggests that the optimum seeding density for primary rat MDCs in this model is 5 million cells/ ml. In comparison, similar work using the C2C12 mouse cell line (Cheema *et al.*, 2003) suggested that 4 million MDCs/ ml was an optimum seeding density. Conversely, work with primary human cells in this model suggests an optimum of 8 million MDCs/ ml for generating the most physiologically relevant model tissue possible (Mudera *et al.*, 2010). This disparity is likely to be the result of significant differences in the size of the myogenic fraction in MDC populations from different sources. The C2C12 cell line is a homogeneous population of myogenic cells and as such requires lower seeding densities than primary MDCs, which possess a significant number of fibroblasts and other non-myogenic cell types. The reduced presence of myogenic cells in primary culture, when compared to the C2C12 cell line, suggests that a larger seeding density would be required in primary cells in order to illicit similar levels of fusion and construct maturation. The human cells in the published study (Mudera *et al.*, 2010) were from adult donors while the rats used in the present study were P1 pups. Since the fraction of myogenic precursors from tissue of increasing age is known to drop off substantially (Kaufman *et al.*, 1991) it seems likely that this higher optimum seeding density is attributable to a smaller myogenic fraction in the human cultures.

3.4.2.3. Rate of MDC differentiation in 3D culture

While the overall differentiation ability of MDCs appears to be significantly improved in 3D culture, the substantial variance in myogenin levels at early time points (Figure 3.6) suggests a delayed and variable rate at which this differentiation takes place when compared with 2D controls. In 2D, the level of myogenin expression

significantly dropped during the first 2 weeks *in vitro,* suggesting most fusion events took place early during culture. By comparison, 3D cultures displayed no significant decreases in myogenin levels throughout the culture period and maintained high mean expression levels up to day 9. This variability in rate of differentiation within the collagen model is likely to be attributable to more complex cellular interactions in 3D. While cells in 2D culture need only align themselves on 2 axes, cells in 3D must align in 3 planes before fusion is possible. This is likely to lead to greater variation in the levels of myoblast fusion occurring at any one moment within this system. Furthermore, the contraction of the construct as it develops will bring a greater number of myogenic nuclei into contact with one another over time, which will in turn lead to new opportunities for fusion events to take place. These data suggest that 2D cultures promote early fusion events, hence a significant drop in myogenin expression at later time points, while the 3D model exhibits a more variable rate of fusion due to complex cellular interactions and the contraction of the gel over time.

The varied rate of differentiation over the first two weeks in 3D culture holds strong implications for the future use of this model. Between days 9 and 13 there is a substantial drop in myogenin expression in 3D culture and the variance between cultures is greatly diminished. Myogenin is known to be constitutively expressed at low levels in differentiated muscle tissue *in vivo* (Sinanan *et al.*, 2006; de Almeida *et al.*, 2010). The shift in expression pattern between these 2 time points implies that by day 13, myogenin expression has dropped to the low levels seen in differentiated fibres and, consequentially, that no further fusion events are occurring. This in turn suggests that any future analysis of these constructs should occur after 13 days *in vitro*, once differentiation of MDCs has subsided and the construct enters a more stable state. While this model represents a reliable method for culturing aligned myotubes *in vitro*, one must be careful to ensure that time points for analysis are appropriate and likely to generate repeatable results.

3.4.2.4. The development of tension in 3D culture

The bowing of these collagen constructs as they develop (Figure 2.1C) is characteristic of the culture model. As already discussed (see **Section 3.1.2.2**.), recent work involving electrical stimulation of similar collagen constructs (Langelaan *et al.*, 2010) demonstrated that a twitch response is elicited from the model in response to electrical impulses. The rapid twitch observed is believed to be the direct result of contraction of the differentiated myotubes in culture. By comparison, measurement of continued construct contraction over time as measured previously using the CFM system (Cheema *et al.*, 2003; Cheema *et al.*, 2005), is unlikely to generate data pertaining to the specific force generated by spontaneous contractions of individual myotubes since such activity would be far too rapid to register over such a large time frame. Instead the contraction measured in these studies is more likely to reflect incremental increases in tension within the system due to a combination of matrix contraction by myoblasts and non-myogenic cell types (in the case of primary cell cultures) and spontaneous contraction from myotubes. The slow and incremental bowing seen in these un-stimulated constructs appears to correlate with the contractile force measured on the CFM system previously (Brady *et al.*, 2008). From this assumption, it can be deduced that the level of bowing (i.e. the reduction in construct area) provides a strong indication as to the level of matrix contraction carried out by the cells as they mature and is therefore indicative of the strength of the mechanical signal fed back to the seeded cells.

3.4.2.5. Myotube orientation and morphology in 3D culture

In this study, the directional cue provided by increasing cell mediated tension was sufficient to promote cellular reorganisation after several days *in vitro* and alignment of differentiated myotubes was found in all cultures examined (n=9) (Figure 3.9A). This uniformity provides an indication of the reliability of this culture method for generating organised *in vitro* muscle cultures. Furthermore, it demonstrates that the cellular alignment seen in constructs utilising both primary human cells and C2C12 cells in the CFM system (Cheema *et al.*, 2003; Cheema *et al.*, 2005; Mudera *et al.*, 2010), is conserved when using primary animal cells in the chamber slide model.

The unbranched conformation of the cultured myotubes indicates the added benefit to MDC differentiation that provision of a directional signal affords. In conventional 2D culture (Figure 3.9B), adherence of the cells to a flat, rigid surface provides multiple attachment points and directional cues which prevent the differentiation of the cells in an organised manner. The fusion of randomly aligned myoblasts leads to the formation of branching myotubes when cultured in 2D, a feature wholly uncharacteristic of *in vivo* muscle fibres (Figure 3.9C). The uniaxial directional signal inherent within the 3D culture model therefore promotes the orientation of cultured fibres and the formation of a far more physiologically relevant model for *in vitro* study.

3.5. Conclusions

From the data presented in this Chapter, optimal feeding media, seeding densities and culture time frames have been established for primary rat MDCs in both conventional 2D and novel 3D culture systems. The ability for MDCs to differentiate into primary myotubes within this 3D model has been confirmed using both immunocytochemistry and PCR analysis. Levels of differentiation in 3D were found

to be at least equal to, and possibly greater than, those achievable in conventional cultures as indicated by myogenin expression data and immunocytochemical analysis. Conservation of the cellular differentiation possible in 2D, the ability to maintain densely seeded cultures over many weeks and the improved cellular architecture afforded the seeded cells, all act to highlight the significant improvement to standard culture techniques that the model developed in this study represents.

4. Analysis of myotube-motoneuron interaction within a 3D collagen based model of skeletal muscle

4.1. Introduction

In seeking to develop 3D *in vitro* culture models that more closely recapitulate the physiology and function of tissues *in vivo*, there is a need to develop systems in which the principal cell types can interact. In order to effectively model skeletal muscle, the engineered tissue should therefore be able to generate biologically accurate representations of the vascular interface as well as the myotendinous and neuromuscular junctions (Larkin *et al.*, 2006a).

In vitro, culture of mouse myoblasts with human umbilical vein endothelial cells within a porous polymer scaffold leads to the development of partially aligned myotubes interwoven with tubular vessel networks (Levenberg *et al.*, 2005). Furthermore, both collagen and fibrin based constructs have independently been shown to promote the infiltration of new blood vessels throughout their matrices when implanted *in vivo* (Borschel *et al.*, 2006; Hadjipanayi *et al.*, 2011).

Similarly, interaction of fibrin based skeletal muscle constructs with sections of tendon tissue leads to the formation of robust junctions capable of withstanding tensile loading beyond the physiological strain range (Larkin *et al.*, 2006b). These constructs are not only functionally viable, but possess structural features and protein expression patterns similar to those seen in neonatal myotendinous junctions *in vivo* (Larkin *et al.*, 2006b; Kostrominova *et al.*, 2009).

Current *in vitro* models of skeletal muscle clearly possess the ability to interact correctly with certain supporting tissues, thereby greatly increasing their biomimicity and hence their value as a tool for studying muscle physiology and pathology. The

interaction of cultured myotubes with elements of the peripheral nervous system, specifically with ventral horn α-motoneurons, within a 3D culture environment has been less well characterised however. Myoblasts are capable of differentiating into myotubes and maturing to a certain degree without a neural input (Vrbova *et al.*, 1995). Maturation of a fibre's contractile and metabolic properties to an adult phenotype however, is largely dependent on the control of electrical activity by the nerve (Hughes & Salinas, 1999). Integration of a physiologically correct neural input with an existing skeletal muscle model would therefore likely promote the maturation of the *in vitro* construct towards a more adult phenotype, leading to the development of a model more closely representative of adult tissue. Furthermore, formation of functional neuromuscular junctions in organised 3D skeletal muscle cultures would allow for the study of novel neuromuscular agents in a controlled environment as well as reducing dependence on animal models for such research.

4.1.1. 3D MDC-nerve co-cultures

As already discussed (see **Section 1.4.3.**), the ability to successfully co-culture primary embryonic motoneurons with MDCs in standard 2D *in vitro* culture has been well documented (Daniels *et al.*, 2000; Lanuza *et al.*, 2006; Das *et al.*, 2010). Despite advances in conventional co-culture systems, to date there have been very few investigations into what effect introducing a neural input has on the physiology and function of 3D muscle culture models.

In 2003, Bach *et al.* constructed a 3D MDC-nerve co-culture system by embedding primary rat MDCs in a fibrinogen-thrombin gel mixture. Organotypic neuronal slices were laid on top of this construct before a second MDC containing fibrinogen-thrombin gel was placed on top. These constructs exhibited spontaneous contractions that were blocked by treatment with depolarising and non-depolarising

muscle relaxants. They also demonstrated an upregulation of the acetylcholine receptor ε-subunit (AChRε), as well as the important synaptogenic factor agrin and the dihydropyridine receptor trisk-51. Since AChRε is thought to be expressed at mature NMJs and trisk-51 is an important component of the Ca^{2+} release mechanism in correctly functioning muscle fibres, the expression of these genes suggests a significant level of neuromuscular interaction and muscle cell maturation in this 3D *in vitro* culture system (Bach *et al.*, 2003).

Interaction of cultured MDCs and neuronal slices within a 3D matrix was further developed by Larkin *et al.* (2006a). The authors plated primary rat MDCs on to a Petri dish prepared with Sylgard and laminin, using a technique similar to those discussed previously (see **Section 3.1.2.1.**), and attached two spinal cord explants to this monolayer using pins placed 12 mm apart. Contraction of the MDCs as they matured led to the generation of tension between the spinal cord explants which in turn promoted the alignment of the seeded cells along the lines of strain within the culture. Use of this model introduced a directional signal lacking from the previous study (Bach *et al.*, 2003), and so allowed for the co-culture of aligned myotubes with neuronal slices *in vitro*. By detaching one of the pins from the Sylgard and fixing it to a force transducer it was then possible to evaluate the contractile ability of the aligned cells in culture. The authors suggested that neuronal cells migrating from the explant were able to fuse with the myotubes underneath, exhibiting clustering of AChRs surrounded by neurofilament stained neural extensions. They also demonstrated a shift from neonatal myosin heavy chain (MYHC) expression in the myotubes towards a more developmental phenotype, indicating the effect of the nerve cells on the maturation of the construct. This was coupled with a significant increase in the maximum twitch and tetanus responses of the muscle-nerve construct when compared with MDC only controls.

More recently, Dhawan *et al.* (2007) implanted fibrin based constructs seeded with MDCs in close proximity to the transected femoral nerve of adult rats. After 4 weeks *in situ*, functional analysis of the retrieved constructs demonstrated far greater contractile function compared with control cultures. Such cultures exhibited “rare” AChR clustering which was not observed in the control cultures.

Such studies demonstrate the improvement to MDC maturation that can be brought about by the inclusion of neuronal tissue within a 3D culture system, and highlight the corresponding improvement in contractile function that this generates. However, the work to date falls short of characterising the formation of mature neuromuscular synaptic contacts *in vitro*. As previously discussed (see **Sections 1.3.2.** and **1.4.3.**), initial contact of the developing growth cone of a nerve with the muscle membrane *in vivo* leads to substantial upregulation of neurotransmitter release, resulting in muscle membrane depolarisation similar to the miniature endplate potentials (MEPPs) seen in mature NMJs (Vrbova *et al.*, 1995). The amplitude of such depolarisations can be very large and have been shown to trigger muscle contractions, irrespective of whether or not action potentials are produced in either the nerve or the underlying muscle fibre (Vrbova *et al.*, 1995). It seems plausible that the spontaneous contractions witnessed in these 3D co-cultures could be due to the occurrence of such events rather than the activation of mature NMJs. Given this possibility, more definitive histochemical and electrophysiological data is required in order to confirm the capacity for 3D *in vitro* co-culture models to promote the development of robust NMJs.

4.1.2. Aims of this Chapter

All published work to date on neuron-myotube interaction in 3D co-culture has focused on the fibrin system. Furthermore, no study has yet been published in this field in which isolated motoneurons, rather than organotypic slices, have been used as a neural input. Consequentially, there remains some ambiguity as to whether or not motoneurons are capable of surviving and interacting correctly with MDCs in such a culture model.

The experiments described in this Chapter aim to establish a physiologically relevant neural input, in the form of primary rat motoneurons, for the collagen model developed in Chapter 3. Characterisation of the interaction of motoneurons and myotubes in this environment will be carried out in order to determine whether or not generation of synaptic contacts is possible in this model and, if possible, what effect this has on the maturation of the co-cultured MDCs.

1. Can the model developed in Chapter 3 be adapted to promote primary motoneuron survival in co-culture with primary MDCs?
2. To what degree does the presence of the motoneuron population have an effect on the development and maturation of the cultured MDCs?

4.2. Materials and Methods

4.2.1. Cell culture

4.2.1.1. Establishment of 2D primary MDC cultures

MDCs were isolated from the hind limbs of P1 neonatal rat pups, as described in Chapter 2 (see **Section 2.1.1.**), and were then seeded on to gelatin coated 13 mm sterile glass coverslips at a density of 50,000 cells/ cm^2. Cultures were maintained in growth media (GM) until they reached confluency. At this point the media was replaced with CNB+IGF-1 in order to promote fusion of the myogenic cells. Data demonstrating the ability to successfully culture primary rat MDCs using this media composition is presented later in this Chapter (see **Section 4.3.2.**).

Such cultures were maintained in this media for 3 days before being fixed in a methanol/ acetone solution for staining. For certain cultures, CNB+IGF-1 was further supplemented with agrin recombinant protein (R&D Systems, Abingdon, UK), at a 200 pM concentration, and Wnt3 recombinant protein (R&D systems) at 20 ng/ µl.

4.2.1.2. Establishment of 2D primary mixed ventral horn cultures

Isolated mixed ventral horn cells were plated onto poly-ornithine and laminin treated, 13 mm glass cover slips at a density of 25,000 cells/ cm^2 as described previously (see **Section 2.1.5.**). Cultures were maintained *in vitro* in CNB+IGF1 media for 7 days before being fixed in a methanol/ acetone solution for staining. As for MDC cultures, data demonstrating the ability for cultured ventral horn cells to survive in this media composition is presented later in this Chapter (see **Section 4.3.1.**). During this culture period, the feeding media was changed every 2-3 days.

4.2.1.3. Establishment of 2D primary MDC-motoneuron co-cultures

2D MDC cultures were established as described above (see **Section 4.2.1.1.**), and maintained in GM until they reached confluency. At this point, GM was replaced with CNB+IGF-1 and 50,000 mixed ventral horn cells (see **Section 2.1.2.**) were pipetted directly on top of the seeded MDCs. The co-cultures were returned to the incubator and maintained for a further 4 days before being prepared for analysis. In certain cases, as with MDC only 2D cultures, CNB+IGF1 was further supplemented with agrin recombinant protein, at a 200 pM concentration, and Wnt3 recombinant protein at 20 ng/ µl.

4.2.1.4. Establishment and maintenance of 3D primary MDC cultures

MDCs were isolated from the hind limbs of P1 neonatal rat pups and seeded within 3D collagen constructs at a density of 5 million MDCs/ ml as described previously (see **Section 2.1.7.2.**). After 4-7 days *in vitro*, GM was replaced with CNB+IGF-1. For certain cultures, CNB+IGF-1 was further supplemented with agrin recombinant protein, at a 200 pM concentration, and Wnt3 recombinant protein at 20ng/ µl. Media was replaced daily throughout the culture period.

4.2.1.5. Establishment and maintenance of 3D primary MDC-motoneuron co-cultures

3D muscle constructs were established as described above and maintained in GM for 4-7 days. At this point GM was replaced with CNB+IGF-1 and the desired number of motoneurons (see **Section 2.1.2.**) were pipetted directly onto the upper surface of the collagen gel. Constructs were returned to the incubator and maintained for a further 7-14 days before being prepared for analysis; media was changed daily during this period. For certain cultures, as with MDC only constructs,

CNB+IGF-1 was further supplemented with agrin recombinant protein, at a 200 pM concentration, and Wnt3 recombinant protein at 20ng/ µl.

4.2.2. Immunocytochemistry

MDC and motoneuron 2D and 3D cultures were immunostained for a variety of immunocytochemical (ICC) markers (Table 2.1) in order to assess both their levels of maturation and to observe the interaction of the motoneurons with myotubes. Fixation and staining was carried out using the protocol described in Chapter 2 (see **Section 2.2.**).

4.2.3. Image analysis

Image analysis was carried out using the guidelines described in Chapter 2 (see **Section 2.2.3.**). MDCs and mixed ventral horn cells were stained for desmin and microtubule-associated protein 2 (MAP-2) respectively. Nuclei were visualised by staining with the DNA binding probe DAPI, and the number of nuclei present was used to calculate the percentage positivity of myoblasts and motoneurons in their respective cultures.

As in Chapter 3 (see **Section 3.2.3.**), myoblasts were identified as any mononuclear desmin positive cell while a myotube was defined as a desmin positive cell with at least 3 nuclei. Motoneurons were defined as MAP-2 positive cells with a cell body greater than 15 µm in diameter and at least 3 neuritic processes (Figure 4.1).

Cultures stained using Texas Red conjugated α-bungarotoxin were analysed for clusters of AChR. An AChR cluster was classified as any foci of red staining

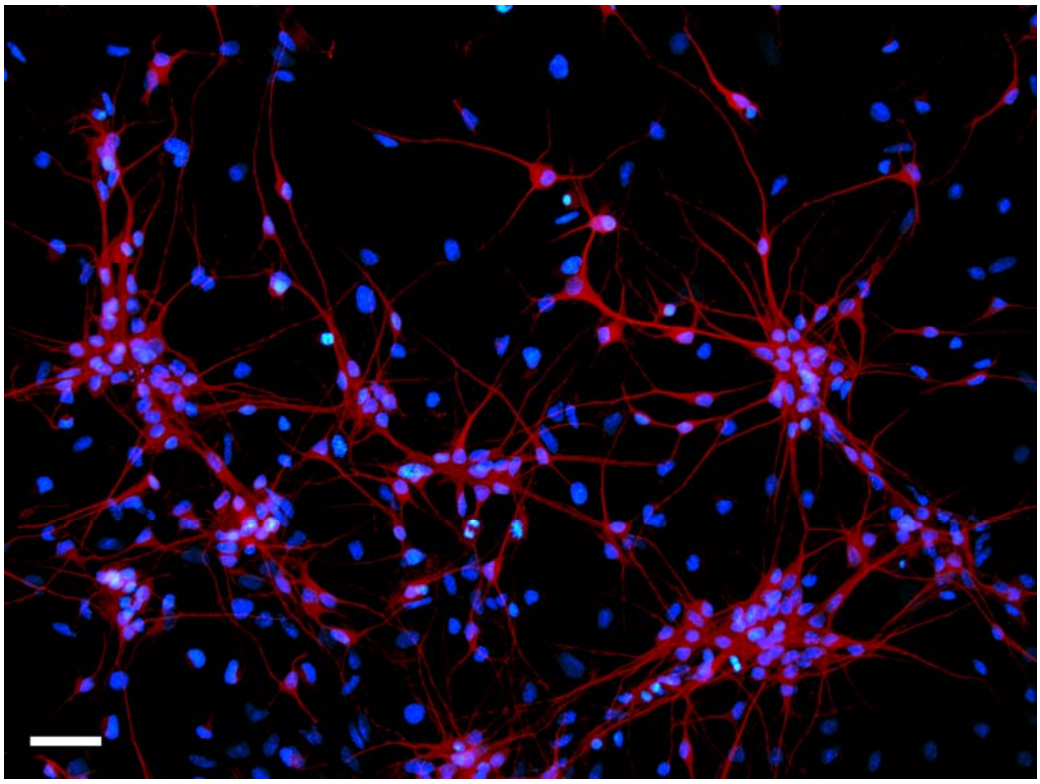

Figure 4.1: Primary cells from a mixed ventral horn population derived from E14 rat embryos in standard 2D culture. Cultures were immunostained for MAP-2 (red) and DAPI (blue). Motoneurons were defined as cells with a cell body diameter greater than 15 μm with at least 3 neuritic processes. Scale bar = 50 μm.

separate and distinct from others nearby and clearly distinguishable above background staining levels.

As well as staining for desmin and MAP-2, 3D cultures were also stained for AChR and synaptic vesicle protein-2 (SV-2) co-localisation and 2H3 neurofilament presence as a marker of synaptic contact and neurite outgrowth respectively.

Macroscopic images of constructs were taken using a Canon PowerShot A460 5.0MP digital camera and processed using Image J software (National Institute of Health, USA).

4.2.4. PCR analysis of 3D MDC-motoneuron co-cultures

Cultures designated for PCR analysis were homogenised in TRIzol reagent and the RNA isolated according to the protocol described previously (see **Section 2.3.1.**). RNA was then converted to cDNA using the protocol described previously (see **Section 2.3.2.**).

4.2.4.1. Conventional PCR analysis

cDNA samples were amplified by PCR and run on 2% polyacrylamide gels using the protocol described previously (see **Section 2.3.3.**). PCR was used to test cultures for expression of a number of genes indicative of muscle maturation: MYH1, MYH3, MYH7, MYH8, troponin, AChRε and choline-acetyl transferase (ChAT). RNA polymerase II (RPII) was used as an endogenous control across all cultures examined. A list of the primer sequences used is provided in Table 2.2.

4.2.4.2. Quantitative PCR analysis

Quantitative PCR was carried out using the Rotor-Gene Q real-time PCR cycler (Qiagen). The PCR reaction mixture (0.15 µl forward primer, 0.15 µl reverse primer,

0.2 µl QuantiFast RT mix (Qiagen), 10 µl SYBR green (Qiagen) and 9.5 µl sample RNA at 7.3 ng/ µl) was prepared for each gene to be analysed in duplicate micro-centrifuge tubes using the QIAgility automated PCR setup machine and accompanying software (Qiagen). Tubes were transferred to the Rotor-Gene Q and incubated at 50^{o}C for 10 minutes and 95^{o}C for 5 minutes before being cycled 40 times at 95^{o}C for 10 seconds and then 60^{o}C for 30 seconds. This protocol was designed by Qiagen for use with the QuantiFast Probe PCR kit and so no optimisation of the thermal cycling parameters was necessary. The primers utilised in this analysis were the same as those used for conventional PCR analysis (see **Section 4.2.4.1.**) and are detailed in Table 2.2.

The threshold cycle (C_T) was defined as the fractional cycle number at which the fluorescence generated by binding of the SYBR green molecule to double stranded DNA exceeded a fixed threshold above the baseline. To quantitate the amount of each target gene present, the comparative C_T method was used, as outlined in the Qiagen "Analysis of real-time PCR" bulletin (Qiagen). The mean C_T value from duplicate reactions for each sample was determined and normalised to that of the endogenous housekeeping gene (RPII). The amount of target amplification relative to the endogenous control was calculated using the formula $2^{-\Delta\Delta C_T}$.

4.2.5. Western blot analysis of 3D MDC-motoneuron co-cultures

Sample preparation, gel electrophoresis, membrane transfer and immunoblotting were carried out on 3D co-cultures and 3D MDC only cultures, as well as positive and negative controls, according to the protocols described previously (see **Section 2.4.**).

4.2.6. Statistical Analysis

All experiments were repeated at least 3 times using cultures prepared on different days from pups of different litters. For most experiments, statistical significance between 2 groups (e.g. 3D cultures +/- motoneurons) was assessed using t-tests in Sigma Stat (version 2.03, Erkrath, Germany). The effect of agrin and Wnt treatment as well as motoneuron presence on AChR clustering in 2D myotubes was assessed using two-way ANOVA, again using Sigma Stat. QPCR data from MDC-motoneuron co-cultures was expressed relative to MDC only controls. As such, control values were always 1. In this case a one sample t-test was used to calculate whether or not the mean expression levels were statistically different from 1. Values are expressed as mean ± standard error of the mean. Significance was set at $p<0.05$.

4.3. Results

In this Chapter, the ability for the model developed in Chapter 3 to support the survival and growth of E14 primary rat motoneurons was assessed and the effect of the motoneuron presence on construct maturation was analysed. Evaluation of motoneuron-MDC interaction within this *in vitro* co-culture model was carried out using microscopy in conjunction with immunostaining for a number of markers. Measurement of construct maturation was achieved using ICC microscopy as well as macroscopic imaging, western blot and quantitative PCR analysis.

4.3.1. Motoneuron survival in 2D using standard media and standard media supplemented with IGF-1

Standard motoneuron feeding media (CNB – detailed in **Section 2.1.2.**) consists of a high glucose (4.5 g/ L) media supplemented with L-glutamine and 2% horse serum amongst other factors required for motoneuron survival. These constituents mirror those in the MDC differentiation media used in previous publications (Machida *et al.*, 2004) and optimised in Chapter 3. As such, addition of IGF-1 should produce a media capable of promoting motoneuron survival and MDC differentiation.

In order to assess whether or not addition of IGF-1 to CNB media had a negative effect on motoneuron survival *in vitro*, isolated ventral horn cells from E14 rat embryos were seeded at 25,000 cells/ cm^2 on to poly-ornithine and laminin treated glass coverslips. These cells were then cultured for 7 days in CNB media with and without IGF-1 supplementation at 10 ng/ ml. The cultured cells were fixed, stained for MAP-2 and the number of motoneurons calculated as a percentage of the total number of cells *in vitro*.

Motoneurons from mixed ventral horn populations, maintained in CNB, were found to constitute 30.47% (± 3.20) of all cells in culture following 7 days *in vitro*. This result is in line with data published previously regarding the size of the motoneuron fraction from unsorted ventral horn populations (Bloch-Gallego *et al.*, 1991), indicating the suitability of the described protocol for obtaining primary motoneurons for *in vitro* culture.

Motoneuron survival in culture did not differ significantly in IGF-1 treated cultures compared with untreated controls (p=0.319) (Figure 4.2). In IGF-1 treated cultures, motoneurons were found to constitute 34.85% (± 2.15) of the population compared with 30.47% (± 3.20) in untreated cultures, suggesting IGF-1 had no ill effects on ventral horn motoneuron survival *in vitro*.

4.3.2. MDC differentiation in 2D using standard motoneuron media supplemented with IGF-1

CNB media supplemented with IGF-1 should contain the all the necessary factors to facilitate MDC differentiation. However, this media also contains a number of other constituents, such as B27 supplement and 2-mercaptoethanol as well as a number of growth factors, not normally provided to MDCs *in vitro.* To verify the ability for this media to promote MDC differentiation to a similar level as that achieved using DM+IGF-1, isolated MDCs were seeded at 50,000 cells/ cm^2 on 0.2% gelatin treated coverslips and cultured in GM until confluent. They were then switched to CNB with IGF-1 and maintained for a further 3 days. The cultured cells were then fixed, stained for desmin and assessed for fusion efficiency (the number of myogenic nuclei incorporated into myotubes, calculated as a percentage of the total number of myogenic nuclei present in culture) as well as the number of myotubes formed per

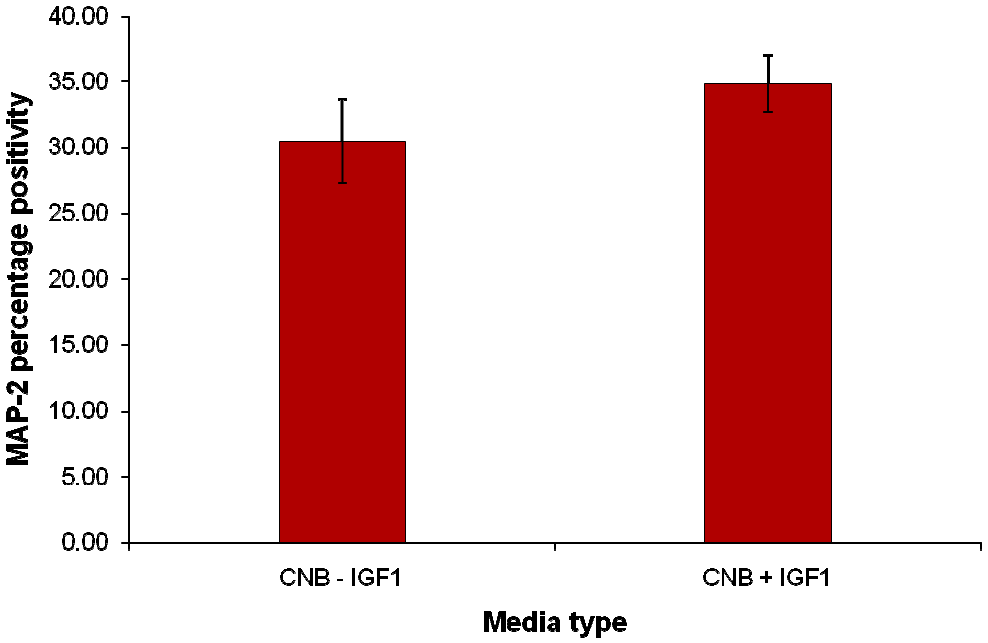

Figure 4.2: The effect of IGF-1 on motoneuron survival *in vitro*. The percentage of motoneurons in mixed ventral horn populations cultured in media with and without IGF-1 supplementation. No significant difference was found between the culture conditions (p=0.319). n=3, error bars = standard error of the mean.

x20 field of view. The values obtained were then compared to those achieved in Chapter 3 for MDCs cultured in DM+IGF-1 (see **Sections 3.3.3.** and **3.3.5.**).

Comparison of the two media types (Figure 4.3) illustrates that culture of MDCs in CNB+IGF-1 results in a significant increase in fusion efficiency of cultured myoblasts. MDCs cultured in DM+IGF-1 possessed 4.23 (± 1.19, n=3) myotubes per x20 field of view, with a fusion efficiency of 61.46% (± 1.16). In comparison, treatment with CNB+IGF-1 led to an average of 5.67 (± 0.27, n=3) myotubes per frame, with a fusion efficiency of 71.22% (± 2.76, n=3). No significant difference was observed in the total number of myotubes observed in culture ($p=0.183$) suggesting that IGF-1 presence had a positive effect on the recruitment of myogenic nuclei to existing myotubes, rather than to the development of new myotubes. Regardless, these data indicate a significant increase in the differentiation ability of MDCs fed with this adapted media ($p<0.03$).

This data, as well as that from **Section 4.3.1.**, indicates the suitability of CNB media supplemented with IGF-1 for the maintenance of MDC-motoneuron co-cultures.

4.3.3. Preliminary immunocytochemical characterisation of 3D MDC-motoneuron co-culture

As a preliminary experimental setup, 3D constructs were established using 5 million MDCs/ ml and maintained in GM for 7 days. The media was then switched to CNB+IGF-1 and primary mixed ventral horn cells pipetted directly on to the top surface of the collagen gel at a density of 500,000 cells/ construct; these co-cultures were maintained for 7 days before being prepared for ICC analysis.

MAP-2 positive cell bodies found on immunostained frozen sections from co-cultured 3D constructs indicate the ability for primary rat motoneurons from mixed

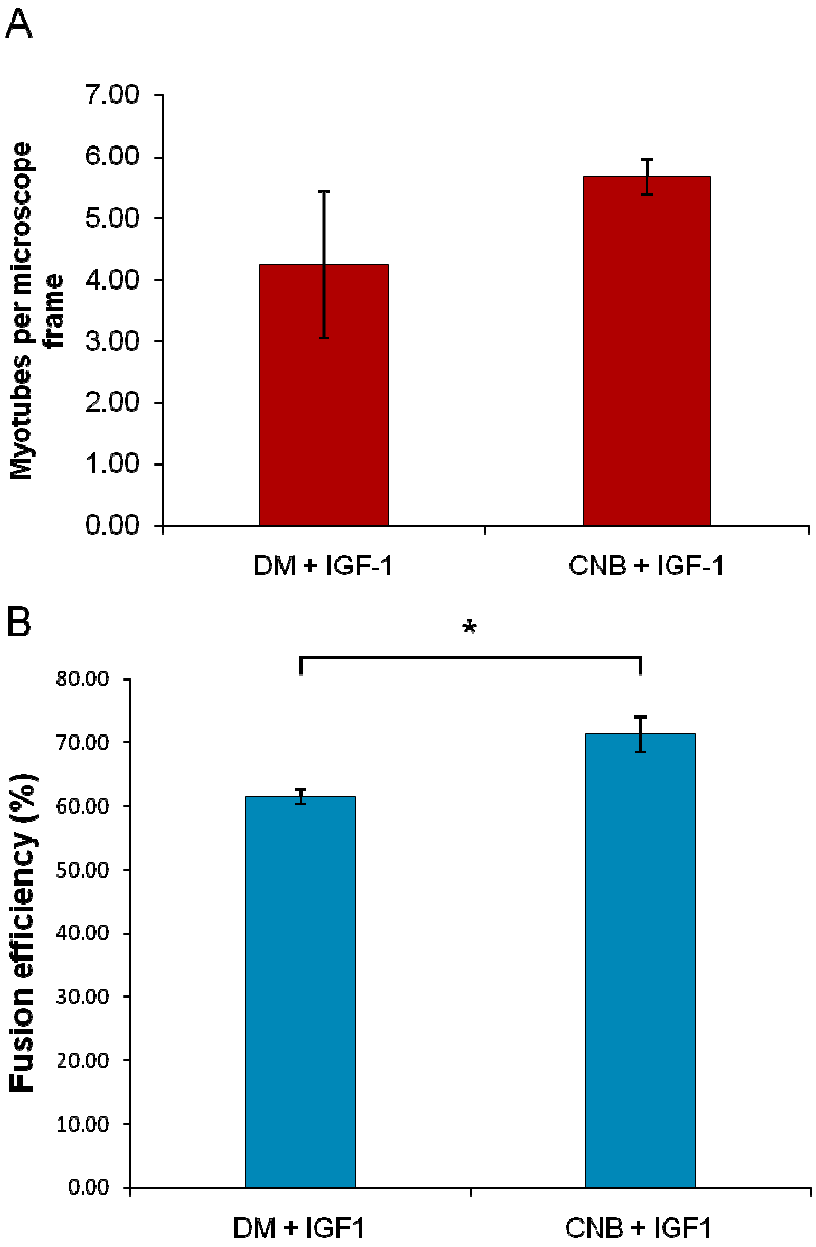

Figure 4.3: The effect of motoneuron media on primary rat MDC differentiation *in vitro*. (A) The number of myotubes per field of view at x20 magnification in primary rat MDC populations cultured with DM+IGF-1 or CNB+IGF-1. No significant difference was observed between the 2 conditions (p=0.183). (B) The fusion efficiencies of primary rat MDC populations cultured with DM+IGF-1 or CNB+IGF-1 (*p=0.011). In both figures, n=3, error bars = standard error of the mean.

ventral horn cultures to survive in this *in vitro* system. Since it was impossible to distinguish non-neuronal nuclei, derived from mixed ventral horn cultures, from non-myogenic nuclei derived from MDC cultures, the number of surviving neurons as a percentage of the total number of ventral horn cells plated could not be calculated. MAP-2 positive cells tended to aggregate into large clusters which also made absolute neuron counts difficult. Staining did indicate however that the number of neurons surviving on the construct surface was substantial (Figure 4.4). No such positive staining was observed on MDC only controls, indicating that the positive staining observed was not due to non-specific or background fluorescence.

ICC analysis revealed that the majority of MAP-2 positive neurites extended across the surface of the collagen gels (Figure 4.4). Exploratory neural extensions were also seen within the body of the constructs however, indicating the ability for surviving motoneurons to infiltrate the collagen matrix; an important capability for facilitating myotube-motoneuron contact (Figure 4.5). Neurites were typically seen running parallel, and in close proximity to, the underlying myotubes (Figure 4.5A) but were also occasionally observed wrapping themselves around these multinuclear structures (Figure 4.5B).

Co-localisation of AChRs, stained for α-bungarotoxin, and synaptic vesicle protein 2 (SV-2) suggests the close association of pre- and post-synaptic terminals in this model (Figure 4.6A). This data is similar to structures observed at the functional NMJ *in vivo* (Figure 4.6B) and provides evidence for the formation of putative neuromuscular junction-like structures in 3D collagen based co-culture constructs. The incidence of formation of such structures was extremely low however; across 6 cultures, 2 such structures were observed from 9 mm^2 sections of tissue, equating to 0.04 co-localisations/ mm^2. MDC only control cultures had no positive SV-2 staining and so no co-localisation with AChRs was observed (n=6).

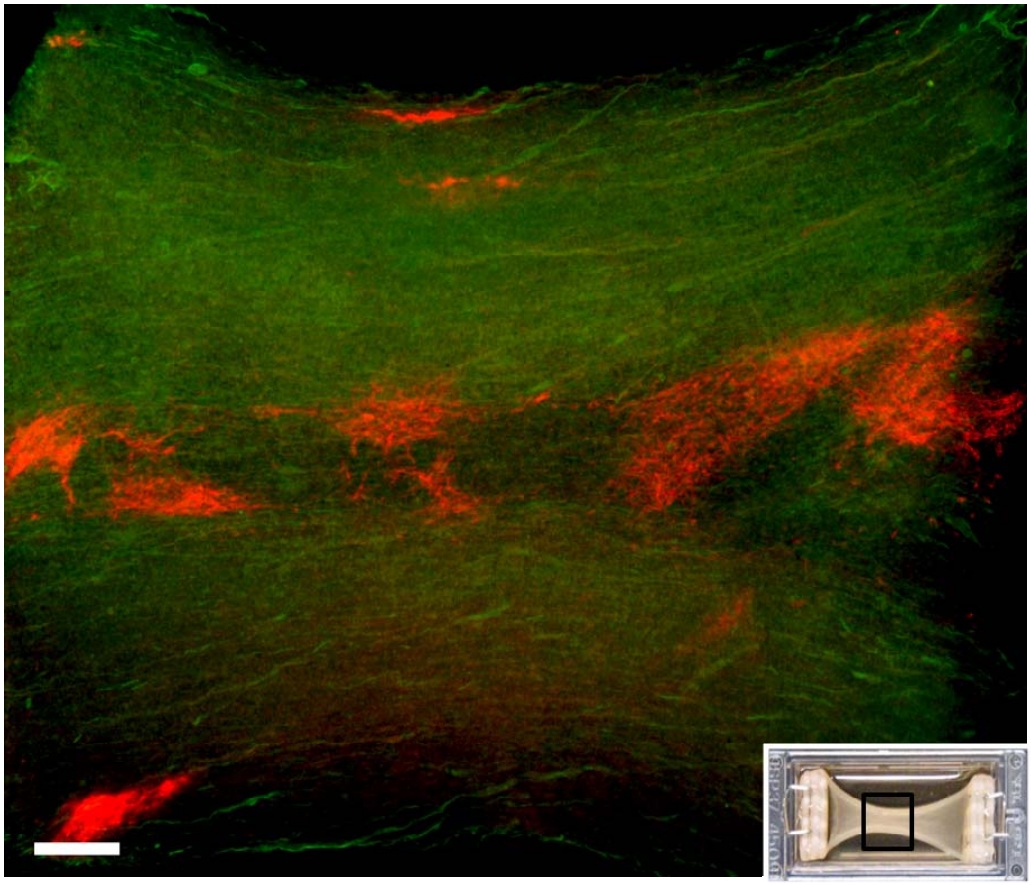

Figure 4.4: Primary rat motoneuron survival in 3D co-culture with primary rat MDCs. The co-culture construct was established using 5 million MDCs/ ml and 500,000 motoneurons . It was immunostained for MAP-2 (red) and desmin (green) following 7 days in co-culture. The area displayed is taken from the central region of the collagen gel (insert). Scale bar = 100 µm.

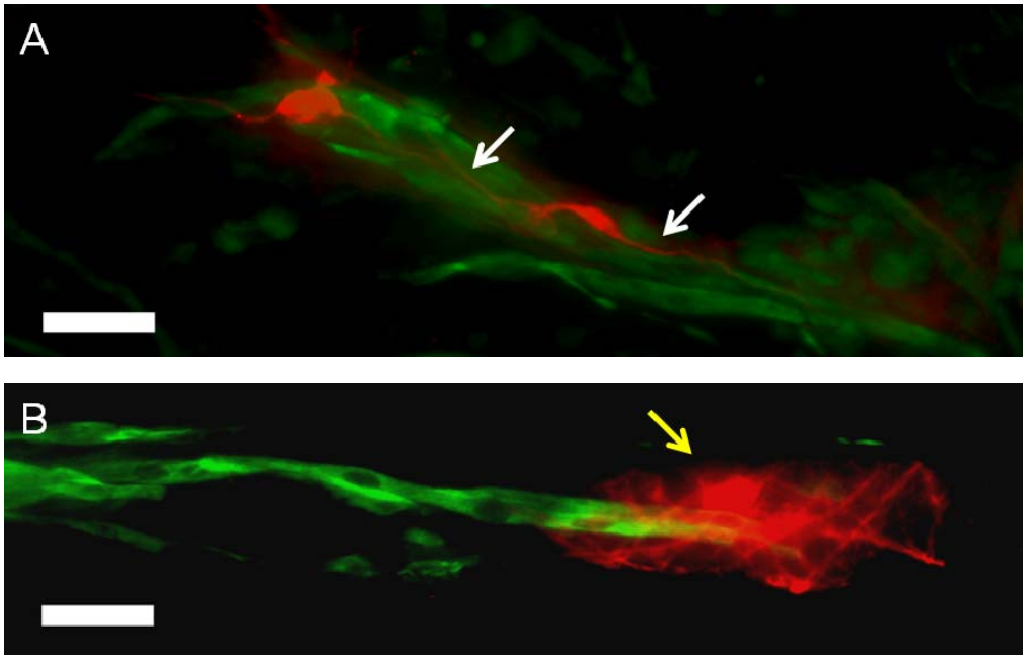

Figure 4.5: Neurite development within 3D collagen based co-culture constructs. Longitudinal sections (30 μm) were immunostained for desmin (green) and MAP-2 (red). Neurites were typically seen tracking along parallel and in close proximity to underlying myotubes (A – white arrows). Occasionally, neurites were also found wrapped around cultured myotubes (B – yellow arrow). Scale bars = 20 μm.

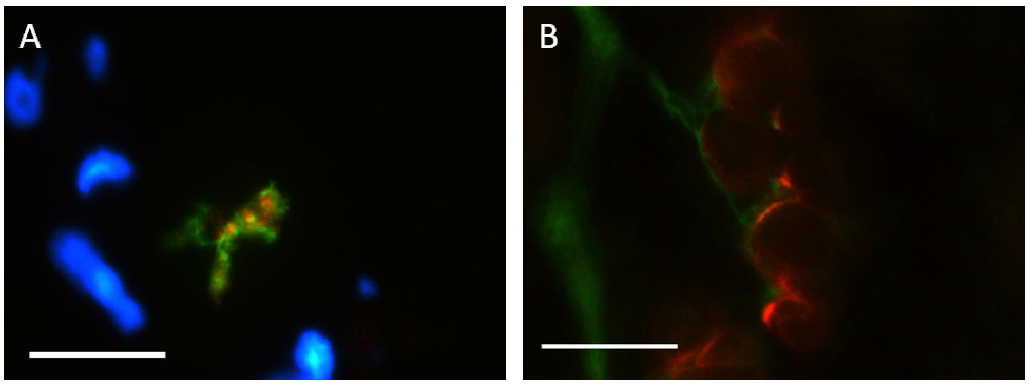

Figure 4.6: Co-localisation of pre- and post-synaptic structures *in vitro* and *in vivo.* (A) A 30 µm thick longitudinal section from a 3D collagen based construct seeded with 5 million MDCs/ ml, co-cultured with 500,000 motoneurons and stained for SV-2 (green), AChRs (red) and DAPI (blue). (B) A 30 µm thick cross section of *in vivo* skeletal muscle from the hind limb of a P1 rat pup stained for 2H3 neurofilament and SV-2 (both green) as well as AChRs (red). Scale bars = 20 µm.

4.3.4. Improvements to the 3D co-culture model

In an attempt to improve the occurrence of AChR-SV-2 co-localisation within the co-culture model, the ventral horn cell seeding density was increased to 1 million cells/ construct. Recently published work, focusing on NMJ formation in 2D culture, has shown that between 12 and 15 days are required before interaction between motoneuron axons and skeletal muscle myotubes are seen *in vitro* (Das *et al.*, 2010). Given this data, it was therefore also decided to extend the time frame of the 3D co-cultures to 14 days.

4.3.4.1. Agrin and Wnt3 treatment

To further improve culture conditions for promoting NMJ formation, the effect of additional media supplements were also investigated. Treatment of MDC cultures with agrin and Wnt3 has been shown previously to improve levels of postsynaptic patterning, characterised by a significant increase in clusters of AChRs on myotube membranes (Henriquez *et al.*, 2008). Since aneural AChR clustering is believed to play a role in axon guidance (Wu *et al.*, 2010), an ability to increase the appearance of such structures may well improve chances for NMJ formation in culture.

To see if the published results (Henriquez *et al.*, 2008) could be repeated, 2D cultures of primary rat MDCs were established at 50,000 cells/ cm^2 and cultured to confluency in GM. They were then switched to CNB+IGF1 with and without agrin and Wnt3 supplementation and cultured for a further 4 days before being fixed and stained with Texas-Red conjugated α-bungarotoxin to visualise AChR clustering. MDC-motoneuron co-cultures were also set up, using 50,000 MDCs/ cm^2 and 25,000 ventral horn cells/ cm^2, and again cultured with and without additional supplementation for 4 days before being fixed and stained. Figure 4.7 shows examples of cells stained in such a manner for analysis.

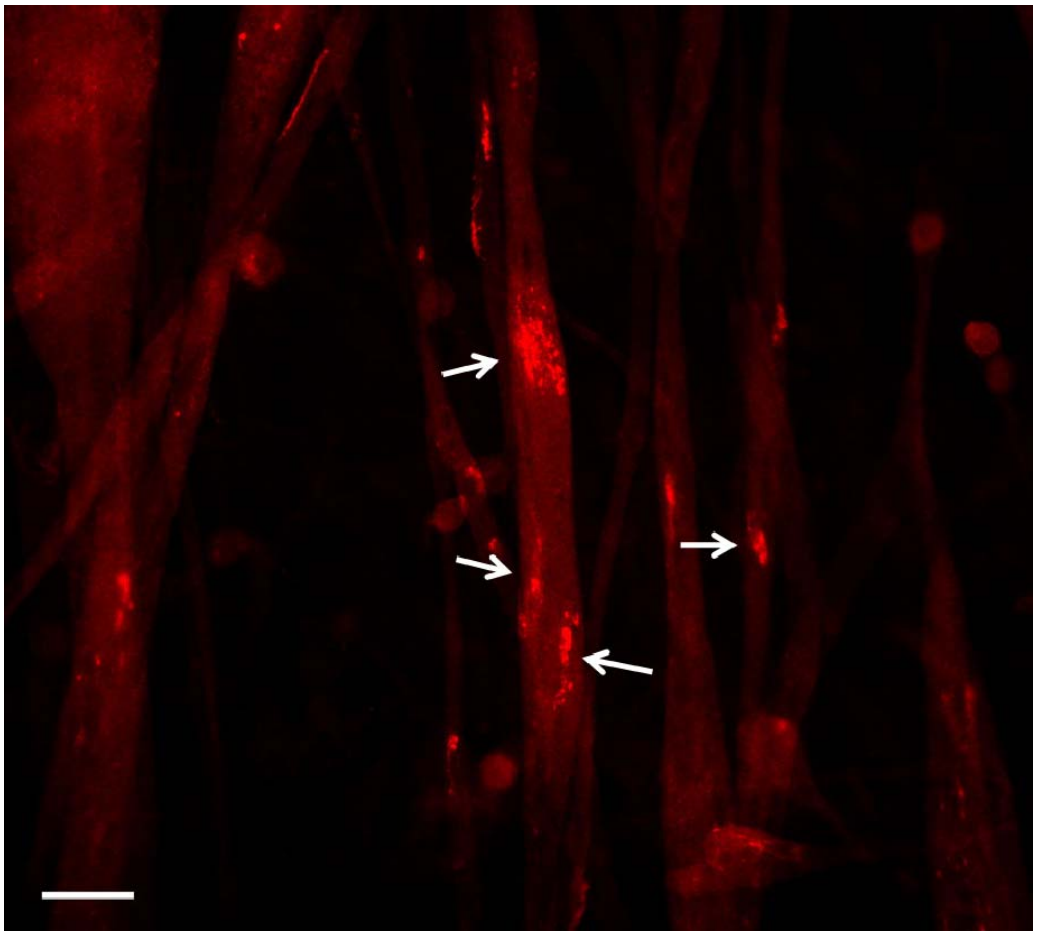

Figure 4.7: Acetylcholine receptor clustering in cultured primary myotubes. Primary rat myotubes in 2D culture with AChR clusters (white arrows) were stained using Texas-Red conjugated α-bungarotoxin. AChR clusters were classified as any foci of red fluorescence separate and distinct from nearby areas of staining and clearly distinguishable above background levels. Scale bar = 20 μm.

AChR clusters were only found on 5% (± 0.77, n=4) of myotubes cultured without motoneurons and without agrin and Wnt3 supplementation (Figure 4.8). AChR clustering was significantly increased in myotube cultures when co-cultured with motoneurons (12.34% ± 1.88, n=4, $p<0.002$). Agrin and Wnt3 media supplementation however, led to significantly higher numbers of myotubes displaying AChR clustering compared with untreated muscle only and co-culture controls (20.09 % ± 1.34, n=4, $p<0.002$). This finding indicates that the ability for cultured neurons to promote post-synaptic differentiation in the myotube membrane is weaker than if induced through media supplementation. MDC cultures supplemented with agrin and Wnt3 and co-cultured with primary motoneurons displayed significantly greater numbers of myotubes possessing AChR clusters than any other culture condition examined (27.55 % ± 1.21, n=4, $p<0.002$), indicating the additive effect of media supplementation and motoneuron presence on AChR clustering. This data suggests that the greatest levels of post-synaptic differentiation can be achieved through addition of motoneurons and media supplementation with agrin and Wnt3. All subsequent cultures were therefore maintained in CNB + IGF-1, agrin and Wnt3 (CNB+).

4.3.5. Characterisation of the improved 3D MDC-motoneuron co-culture model

Following the changes to the established culture protocol described above (namely an increased ventral horn cell seeding density, an increased length of time in co-culture to 14 days and further media supplementation with agrin and Wnt3), a series of experiments were carried out to investigate the effect of motoneuron presence on the development and maturation of the seeded MDCs in 3D. MDC constructs were established with a seeding density of 5 million cells/ ml and maintained in GM for 7 days. They were then switched to CNB+ and 1 million ventral horn cells were

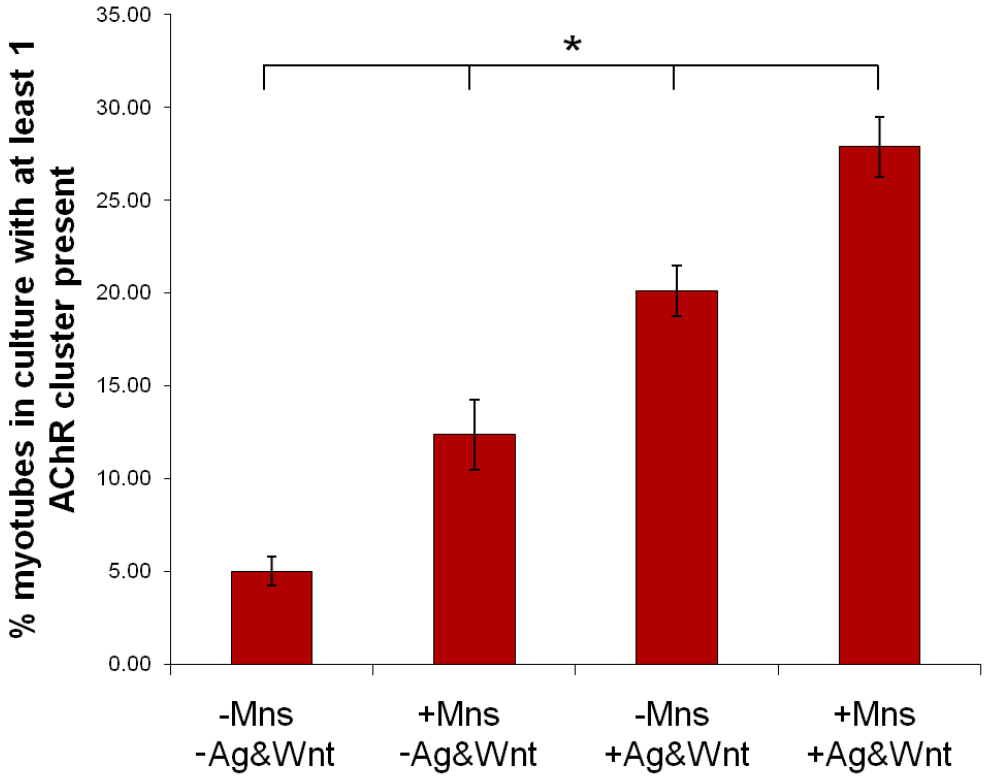

Figure 4.8: The effect of motoneuron presence and agrin and Wnt3 supplementation on AChR cluster formation in cultured primary rat myotubes. The percentage of myotubes in 2D culture possessing distinct AChR clusters. n=4, error bars = standard error of the mean, *p<0.002.

pipetted on top. The co-cultures were subsequently cultured for 14 days before being prepared for analysis. Comparative analysis of 3D co-cultures and MDC only controls was performed using macroscopic observations, ICC staining, western blotting and quantitative PCR.

4.3.5.1. MDC differentiation in 3D constructs cultured with and without motoneurons

Fusion efficiencies of MDCs in 3D co-culture and MDC only controls were examined at 21 days *in vitro*, in order to determine whether or not co-culture with primary motoneurons had any effect on the ability of primary MDCs to differentiate into multinuclear myotubes.

Analysis showed that the fusion efficiency of MDCs in co-culture was 47.85% (± 6.94, n=5) compared with 31.24% (± 11.12, n=5) when MDCs were maintained alone (Figure 4.9). There was therefore no significant difference between these 2 culture conditions (p=0.241, n=5), which suggested that co-culture of MDCs with motoneurons has no significant effect on the myoblast's ability to fuse in this 3D model.

Data analysed in Chapter 3 (see **Section 3.3.6.**) shows that the fusion efficiency in 3D MDC only constructs maintained in DM+IGF-1 was 73.14% (±3.45, n=4). Comparison of this result to results achieved in this Chapter highlights that cultures maintained in CNB+ promote significantly lower levels of fusion than those maintained in DM+IGF-1, regardless of motoneuron presence ($p<0.02$). This is surprising since previous analysis (see **Section 4.3.2.**) suggested that CNB+IGF-1 promoted significantly greater levels of fusion in conventional 2D culture when compared with DM+IGF-1.

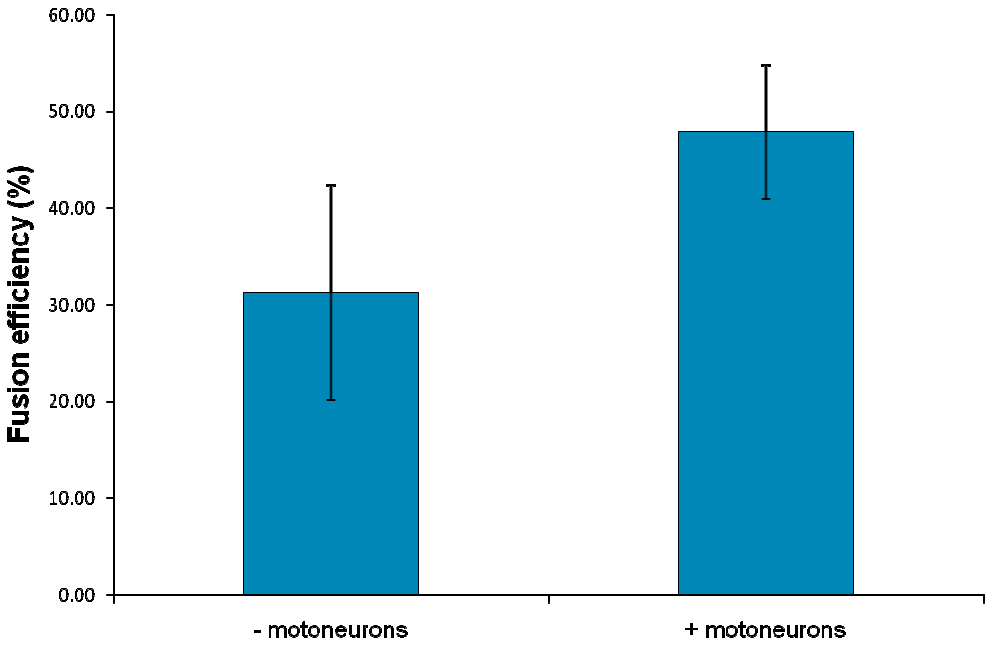

Figure 4.9: The effect of motoneuron presence on the fusion efficiency of co-cultured MDCs in 3D. The fusion efficiency of primary rat MDCs seeded within 3D collagen constructs at a density of 5 million cells/ ml and either with or without 1 million motoneurons added after 7 days in culture was measured. No significant difference was observed between the 2 culture conditions ($p=0.241$). n=5, error bars = standard error of the mean.

For logistical reasons, MDC constructs analysed so far in this Chapter were maintained for 7 days in GM before being switched to CNB+. Constructs analysed in Chapter 3 however, were switched to DM+IGF-1 when 2D controls reached confluency, which typically took 3-4 days. Therefore, the effect of switching constructs to CNB+ at an earlier time point on MDC fusion efficiencies was examined next and compared to those constructs switched after 7 days *in vitro*.

3D constructs seeded with 5 million MDCs/ ml were established as described previously (see **Section 4.3.5.**) but maintained in GM for just 4 days. At this point cultures were switched to CNB+ and either maintained as MDC only controls or had 1 million mixed ventral horn cells plated on top. Co-cultures and MDC only controls were cultured for a further 14 days before being prepared for ICC staining.

MDC-motoneuron co-cultures and MDC only controls switched to CNB+ after 4 days *in vitro* displayed fusion efficiencies of 61.64% (± 6.04, n=3) and 63.17% (± 5.52, n=3) respectively. This increase in fusion levels removes any significance from the difference between cultures switched to CNB+ and cultures switched to DM+IGF-1 ($p>0.05$) (Figure 4.10).

As was the case for constructs switched to CNB+ at day 7, no significant difference in fusion efficiencies between MDC only controls and MDC-motoneuron co-cultures were observed in constructs switched to CNB+ and co-cultured with motoneurons from day 4. This data suggests that motoneuron presence has no significant effect on the ability of MDCs to fuse in 3D culture. It does, however, highlight the importance of switching 3D constructs to differentiation media at the correct time point in order to promote maximal levels of construct maturation. Unless otherwise stated, all further experiments were carried out on cultures switched to CNB+ and given motoneurons after 4 days *in vitro*.

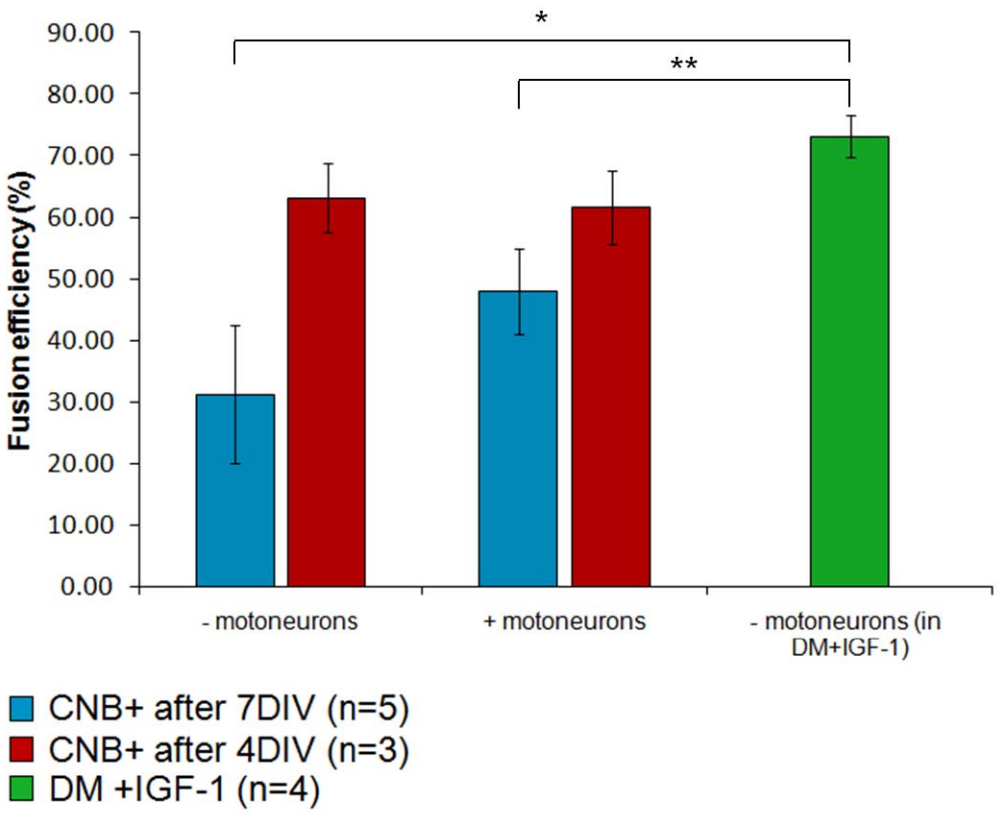

Figure 4.10: The effect of motoneuron co-culture and different time frames for addition of differentiation media (CNB+) on the fusion efficiency of primary rat MDCs cultured in 3D. Constructs were seeded with 5 million MDCs/ ml and with 1 million motoneurons where applicable. In all cultures, motoneurons were added to the culture model at the same time point as addition of CNB+. Data from Chapter 3 also shown: Fusion efficiency of 3D constructs seeded with 5 million MDCs/ ml but instead switched to DM+IGF-1, rather than CNB+, after 3-4 days in culture. Error bars = standard error of the mean, *p=0.014, **p=0.02.

4.3.5.2. Neurite outgrowth and neuromuscular junction formation in 3D co-culture

Frozen 30 μm sections were collected from MDC constructs following 14 days in co-culture with motoneurons. These sections were immunostained for MAP-2 as well as pre- and post-synaptic markers in order to gauge both neuron survival and the level of neuromuscular interaction within the constructs.

As was the case previously (see **Section 4.3.3.**), motoneuron survival was shown to be substantial, as indicated by positive MAP-2 staining, although absolute neuron numbers could not be calculated due to the density of the cells in culture and the characteristic clustering of the seeded neurons (Figure 4.11). Neurite development was again found to be predominantly focused on the surface of the collagen constructs but infiltration into the matrix appeared more extensive than was observed previously.

Co-localisations of SV-2 and AChR clusters were still low in number but showed a significant improvement over constructs examined during preliminary investigations (see **Section 4.3.3.**). In cultures produced using the improved protocol, 4.24 (± 2.69, n=3) distinct AChR/ SV-2 co-localisations were recorded per mm^2, a significantly greater number than the 0.04 co-localisations/ mm^2 observed in preliminary cultures ($p=0.024$). Low levels of SV-2 positive staining (in comparison to those seen in neuronal cell bodies) were also consistently observed running in close proximity to underlying myotubes (Figure 4.12), indicating the path of developing neurites through the collagen construct. No positive SV-2 staining, and therefore no AChR/ SV-2 co-localisation, was observed in MDC only constructs (n=3).

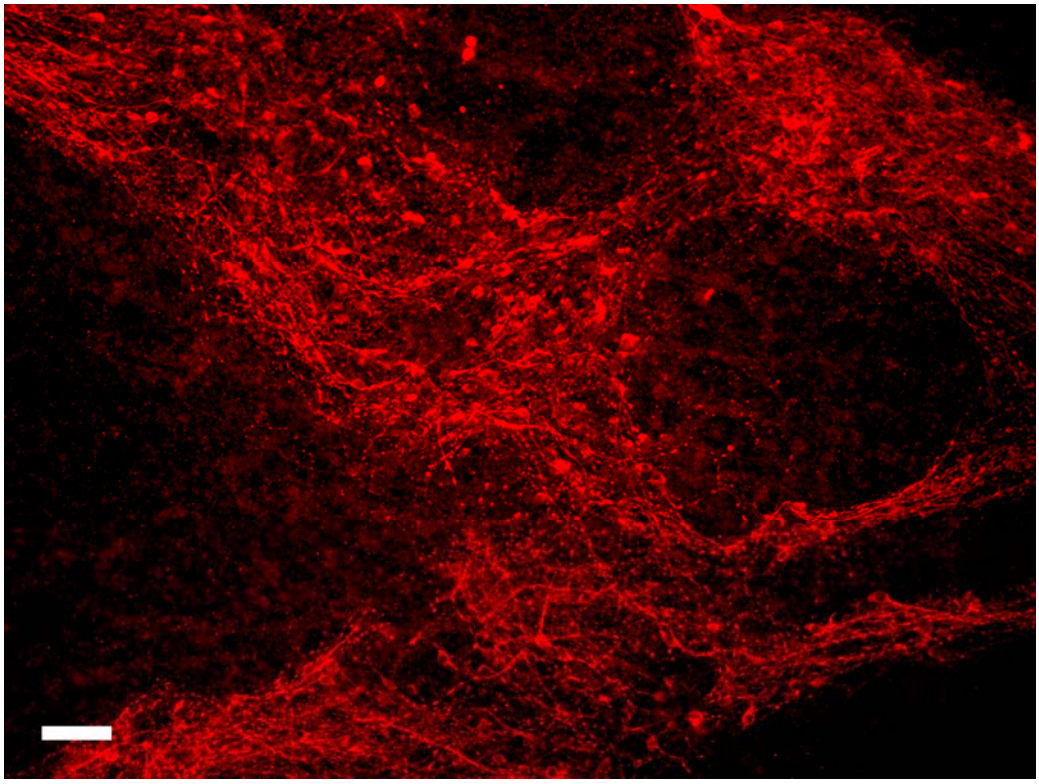

Figure 4.11: Motoneurons from mixed ventral horn cultures attached to the surface of a 3D collagen construct. Fixed constructs were immunostained for MAP-2 (red). Scale bar = 50 μm.

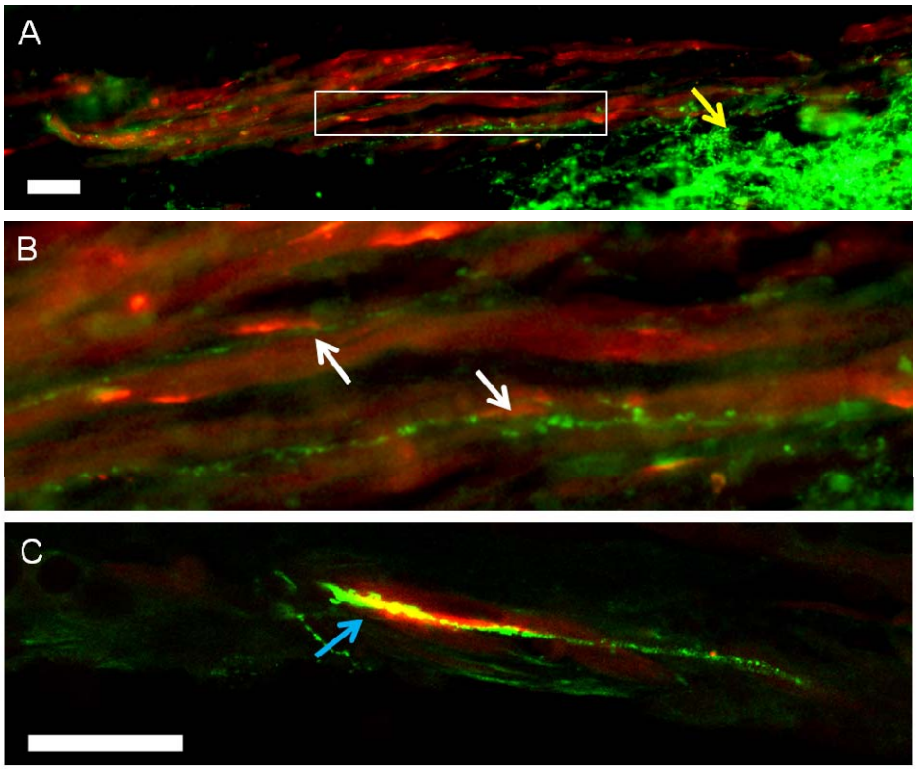

Figure 4.12: Neuromuscular interaction in 3D co-culture. (A) x20 magnification of a 30 µm thick longitudinal section from a 3D collagen based construct, seeded with 5 million MDCs/ ml, co-cultured with 1 million motoneurons, and immunostained for SV-2 (green) and AChRs (red). Intense foci of green staining (yellow arrow) correlated to neuron cell body positions when immunostained for MAP-2 or neurofilament (2H3) (B) Magnification of the highlighted area from A. Note the thin network of SV-2 positive projections (white arrows) running in close proximity to the underlying myotubes. (C) x63 magnification of a 30 µm thick longitudinal section from a 3D collagen based construct cultured and stained as above. Distinct co-localisations of AChR and SV-2 (blue arrow) were observed at a frequency of 4.24/ mm^2 (± 2.69). Scale bars = 20 µm.

4.3.5.3. Macroscopic gel contraction in 3D constructs cultured with and without motoneurons

In order to characterise any macroscopic differences in levels of matrix contraction between co-cultures and MDC only controls, constructs were established as described previously (see **Section 4.3.5.**) and switched to CNB+ and given motoneurons after 4 days *in vitro*. Macroscopic images were taken every 7 days and processed using ImageJ software to determine the surface area of the construct as a measure of matrix remodelling (Figure 4.13), where a decrease in area correlates to an increase in matrix contraction. No difference was observed between co-cultures and muscle only controls after 7 days *in vitro*. A divergence was observed between the two cultures after 14 days *in vitro*, and the average construct area in co-culture was 222.35 mm^2 (± 25.33, n=5), compared with 307.54 mm^2 (± 42.24, n=5) in muscle only controls. This difference was not significant however (p=0.159) and only after 21 days *in vitro* did the difference between the two cultures reach significance (p=0.03). At this time point, average construct surface area was 162.00 mm^2 (± 10.74, n=5) in co-culture, compared with 273.08 mm^2 (± 34.44, n=5) in muscle only controls, indicating increased levels of matrix contraction in co-culture compared with MDC only constructs.

Comparison of co-culture constructs with MDC only controls suggested increased whitening along the outside edges of the collagen matrix (Figure 4.13B). It is possible such whitening was a result of increased collagen fibril density due to greater matrix contraction by MDCs. However, it may also be due to cells within the mixed ventral horn population remodelling the collagen fibrils close to the construct surface and drawing them together.

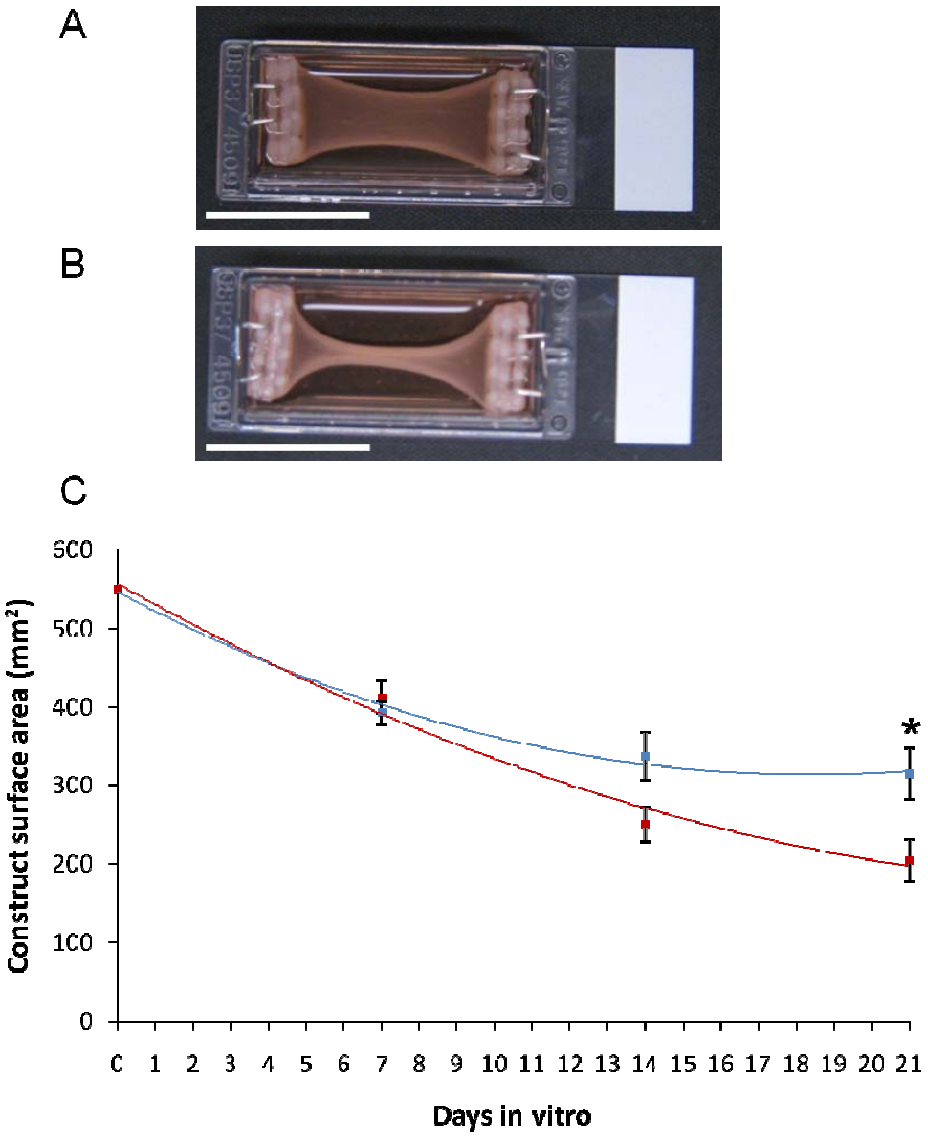

Figure 4.13: The effect of motoneuron presence on the level of matrix contraction observed in 3D culture. (A) Macroscopic image of a collagen construct seeded with 5 million MDCs/ ml following 21 days *in vitro*. Scale bar = 25 mm. (B) Macroscopic image of a collagen construct seeded with 5 million MDCs/ ml and 1 million motoneurons following 21 days *in vitro*. Motoneurons were added to the culture model after 4 days *in vitro.* Note the increased whitening of the collagen gel along the outer edges. Scale bar = 25 mm. (C) The reduction in surface area of collagen constructs seeded with 5 million MDCs/ ml either in co-culture with motoneurons (red) or in monoculture (blue). n=5, error bars = standard error of the mean, *p=0.03.

In order to investigate levels of matrix surface contraction by ventral horn cells in co-culture, frozen cross sections were obtained from both co-culture and muscle only controls and immunostained for MAP-2 and desmin (Figure 4.14). Analysis showed that MDC only cultures displayed elongated cross sectional structures with widths far greater than their heights, while MDC-motoneuron co-cultures, by comparison, possessed a cross section far closer to circular. While the captured images provide some evidence for surface contraction of the collagen gels by mixed ventral horn cells, the rounded morphology of the co-culture cross sections, compared with the elongated shape of the MDC only controls, also suggests an increased level of contraction from within the construct. This data therefore implies that the increased contraction levels observed in 3D co-culture are due both to the contractile activity of fibroblasts within the mixed ventral horn population, and to increased contraction from cultured MDCs. However, the precise mechanism behind this increased contraction could not be determined from the available data.

4.3.5.4. QPCR gene expression analysis in 3D constructs cultured with and without motoneurons

QPCR was used to evaluate the expression levels of a number of markers of muscle maturation and NMJ formation in MDC constructs maintained in co-culture with mixed ventral horn cells for 14 days. Constructs which had been switched to CNB+ and had motoneurons added at both day 4 and day 7 were analysed, in order to gain further insight into the effect switching media at different time points had on the subsequent maturation of the seeded cells. Expression of genes to be analysed from 3D cultures was first verified by conventional PCR analysis and all PCR products sequenced to ensure correct amplification had occurred (Figure 4.15).

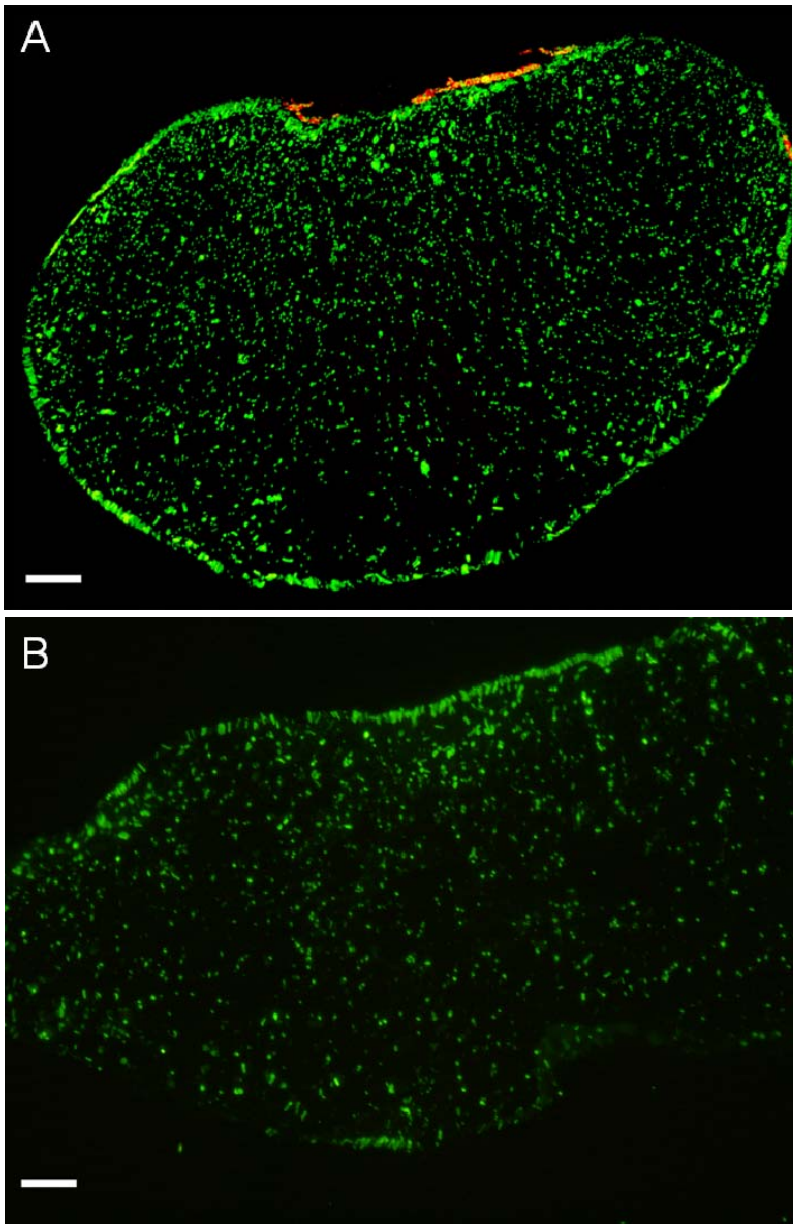

Figure 4.14: The effect of motoneuron presence on the cross sectional conformation of 3D constructs co-cultured with primary rat MDCs. 30 µm thick cross sections were taken from 3D collagen based constructs seeded with 5 million MDCs/ ml and stained for desmin (green) and MAP-2 (red). Note the difference in shape between the rounded construct co-cultured with 1 million motoneurons (A) and the elongated MDC only control (B). N.B. The image in B represents half the total width of the construct since the entire gel was too large to reliably section. Scale bars = 100 µm

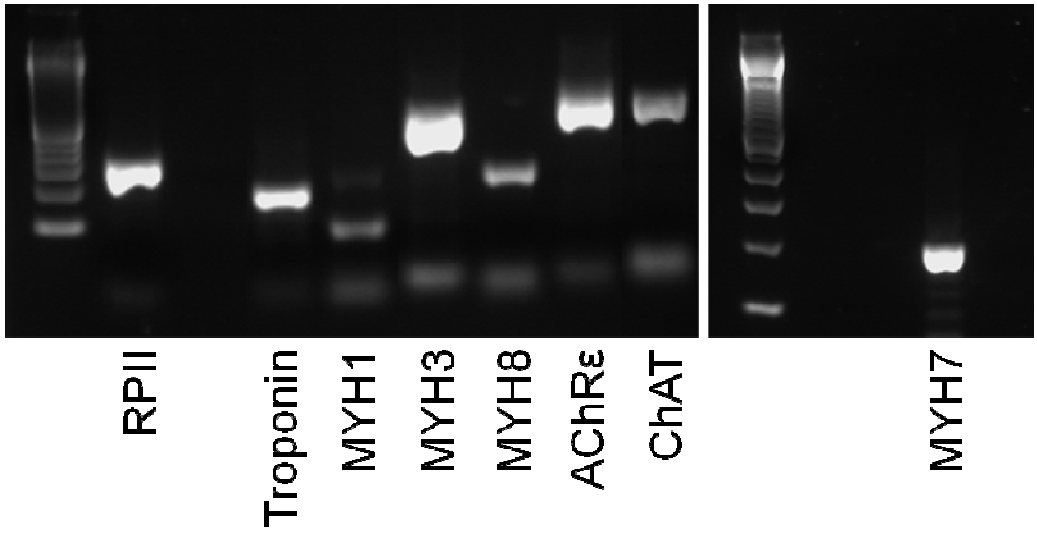

Figure 4.15: Conventional PCR products for markers of muscle maturation from purified 3D co-culture RNA. All PCR products were sequenced (see **Section 2.3.5.** and **Appendix C**) in order to confirm the validity of the designed primers.

Pooled qPCR data for cultures switched to CNB+ and co-cultured with motoneurons from day 4 and day 7 showed no significant difference in the expression levels of any myosin heavy chain genes or troponin T1. A small, but significant increase was recorded for mRNA transcripts of AChRε in co-culture compared with MDC only controls ($p<0.05$). As expected, a highly significant increase ($p<0.0025$) was seen in expression levels of *ChAT* transcripts in co-culture compared with MDC only controls (Figure 4.16).

Although no changes in expression for markers of muscle maturation were observed between co-cultures and MDC only cultures when all data was pooled, significant differences were found when cultures were divided based on when they were switched to CNB+ and were co-cultured with motoneurons. Constructs switched to CNB+ and co-cultured with motoneurons after 7 days *in vitro,* showed a significant decrease in expression of *MYH1*, the fast adult myosin isoform ($p<0.025$) (Figure 4.17A). All other genes examined in this sample group, including AChRε, were found to be statistically similar to values achieved in MDC only controls. This culture model therefore appears to discourage NMJ formation since the upregulation of AChRε subunit (specific to NMJs) seen in the pooled data is lost within this subset. Addition of neurons to this culture model seems to have little effect on expression of troponin T1 and most MYHC genes and in fact promotes a down regulation in the fast *MYH1* gene. When CNB+ and motoneurons are added at day 7 it seems the motoneurons are unable to promote maturation of the seeded MDCs above levels achievable in MDC only cultures. The down regulation of *MYH1* could perhaps be attributed to increased matrix stiffness in co-cultures due to the greater level of matrix contraction as observed in **Section 4.3.5.3.**

When constructs were switched to CNB+ and co-cultured with motoneurons on day 4, the significant increase in AChRε subunit expression in co-cultures over MDC

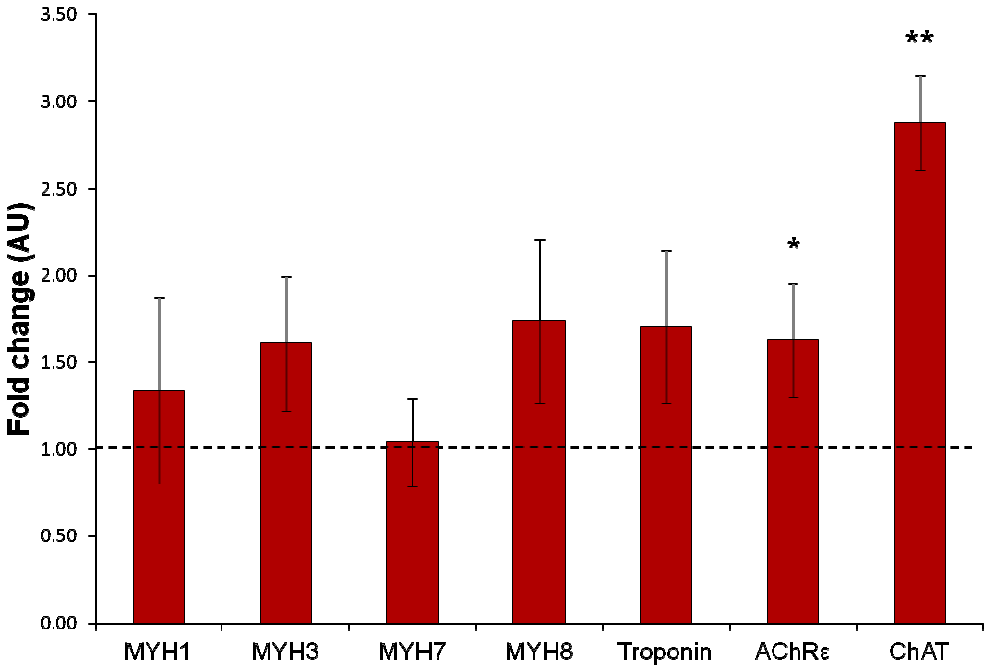

Figure 4.16: Fold change in mRNA expression levels for markers of muscle maturation and NMJ formation in 3D co-cultures of MDCs and motoneurons. Constructs seeded with 5 million MDCs/ ml and co-cultured with 1 million primary rat ventral horn cells for 14 days. Cultures were switched to CNB+ and co-cultured with motoneurons following 4-7 days *in vitro* with GM. C_T values were normalised to an internal house-keeping gene (RPII) and expressed relative to levels recorded for 3D constructs without motoneurons at equivalent time points. n=8, error bars = standard error of the mean, * $p<0.05$, ** $p<0.0025$.

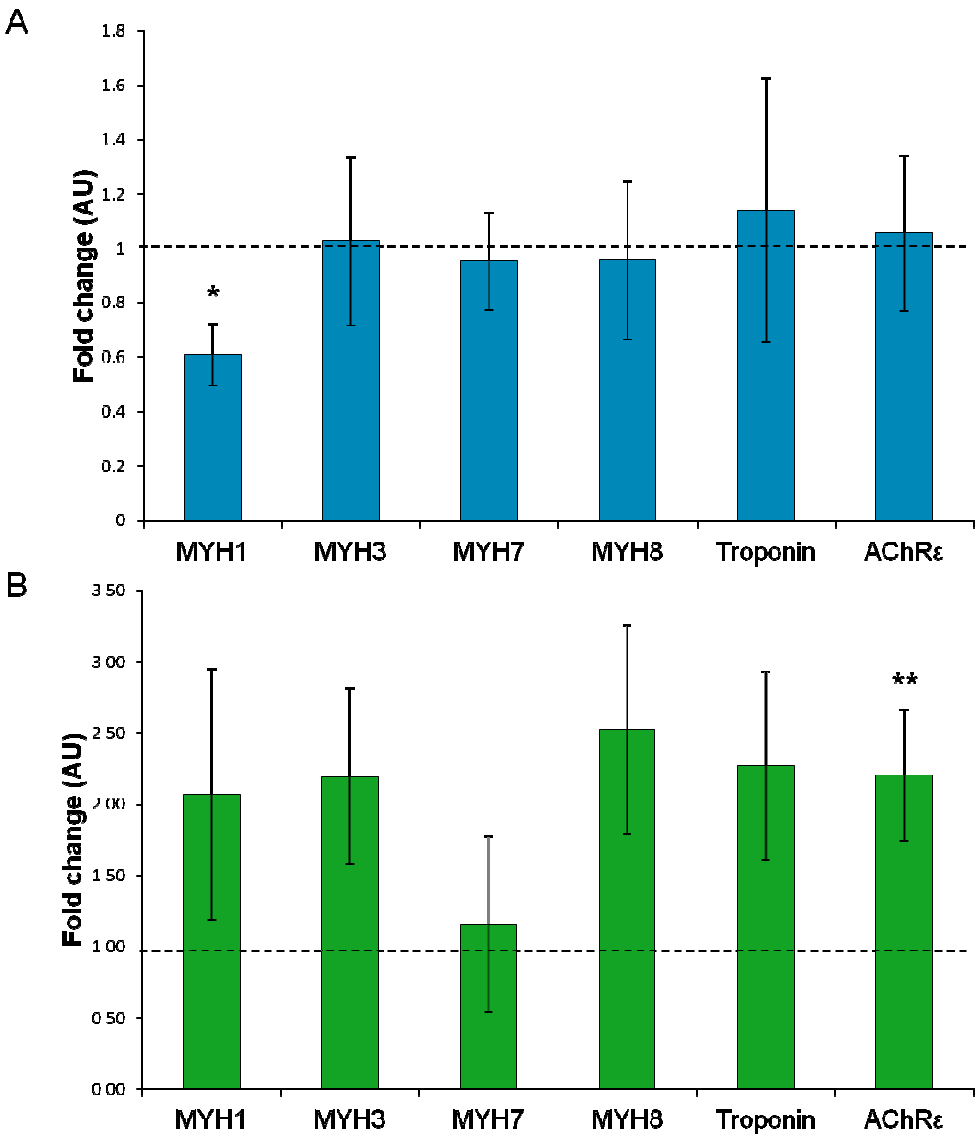

Figure 4.17: The effect of changing the motoneuron seeding time point on fold changes in mRNA expression levels for markers of muscle maturation and NMJ formation. (A) A subset of the data described in Figure 4.16, all constructs were switched to CNB+ and co-cultured with motoneurons after 7 days in culture with GM. n=4. (B) A subset of the data described in Figure 4.16, all constructs were switched to CNB+ and co-cultured with motoneurons after 4 days in culture with GM. n=4. For both graphs, error bars = standard error of the mean, *p<0.025, ** p<0.05.

only controls was restored ($p<0.05$, n=4) (Figure 4.17B). No significant increases were observed in any other genes examined across the entire data set (n=4). However, it should be noted that this is largely attributable to a single culture in which expression of these genes dropped. Excluding this culture as an outlier, there was a significant upregulation in the expression of *MYH3, MYH8* and troponin T1 across the remaining cultures ($p<0.05$, n=3). Since no significant increase in the level of fusion between MDC only constructs and MDC-motoneuron constructs was observed in these cultures (see **Section 4.3.5.1.**), this data suggests an increase in myotube maturation and transcription of contractile machinery is not due to increases in myotube formation, but rather to the upregulation of these genes within the existing myotubes.

4.3.5.5. Protein expression in 3D constructs cultured with and without motoneurons

To determine whether changes observed in transcription profiles between co-cultures and MDC only cultures were mirrored at the protein level, constructs were established as described previously (see **Section 4.3.5.**) and maintained in co-culture for 14 days before being prepared for western blot analysis using antibodies specific for MYHC isoforms, AChRε and β-actin.

Although positive bands were detected for MYHC and the β-actin endogenous control, no consistent upregulation in MYHC expression was observed (Figure 4.18). Across the 3 cultures examined, MYHC expression appeared to increase once, decrease once and remain constant once, when comparing co-culture to MDC only controls. Since β-actin expression remained relatively constant across all cultures, this would suggest that motoneuron presence had no significant effect on the level of MYHC protein detectable in 3D culture.

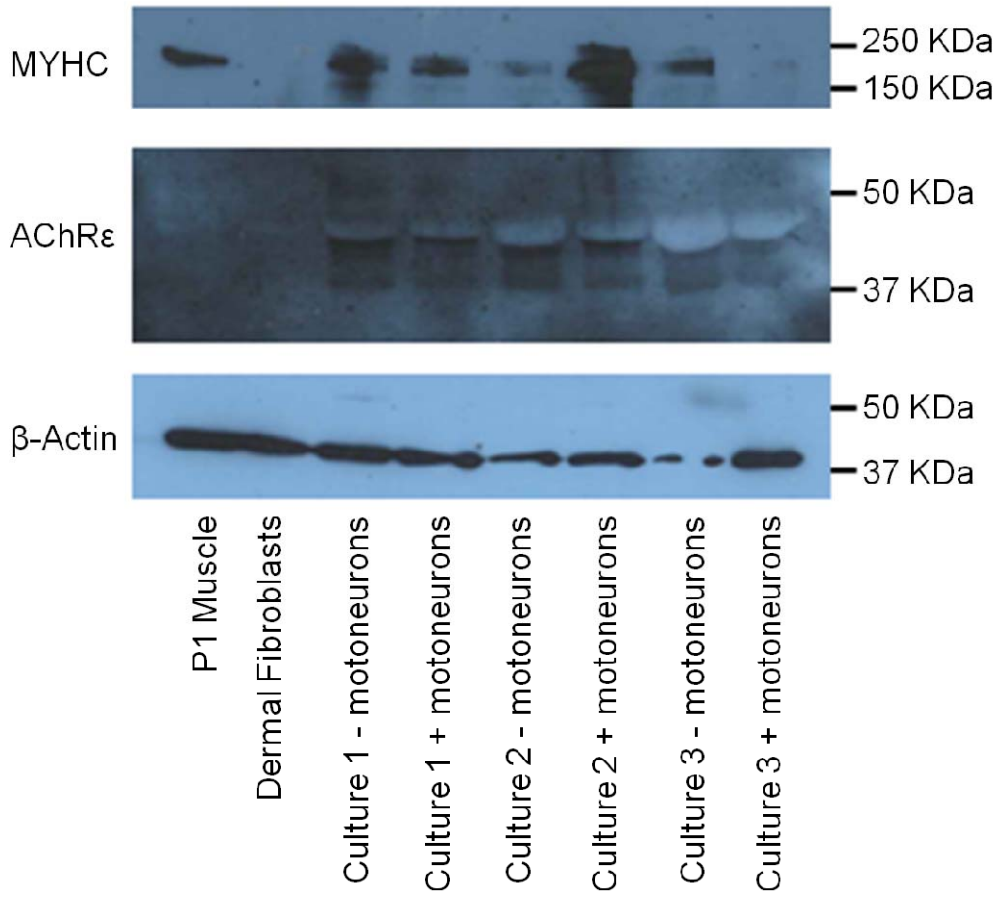

Figure 4.18: Immunoblots for myosin heavy chain (MYHC), acetylcholine receptor epsilon subunit (AChRε) and β-actin proteins for 3 separate sets of 3D co-cultures. A P1 muscle sample and cultured dermal fibroblasts were used as positive and negative controls respectively.

No detectable protein was recorded for AChRε (Figure 4.18), which may be due to there being very low levels of this protein in culture. However, a lack of signal from positive control P1 muscle tissue suggests further optimisation of the protocol is required before any conclusions regarding the presence or absence of this protein in culture can be made.

4.4. Discussion

An *in vitro* model of skeletal muscle capable of promoting the formation of robust and functionally mature NMJs between co-cultured myotubes and motoneurons would be of enormous benefit for the future study of neuromuscular physiology and pathology. The first step in achieving this goal is to characterise the behaviour of motoneurons within such a system so as to optimise the culture conditions for promoting maximal levels of myotube maturation and nerve-muscle interaction.

4.4.1. Adaptation of culture media for co-culture of motoneurons and MDCs

Primary mixed ventral horn cultures are a heterogeneous population of cells including motoneurons and interneurons as well as astrocytes and other glial cells. In seeking to purify motoneurons from this mixed population, a number of protocols have been developed involving density centrifugation and immunopanning (Camu *et al.*, 1993). However, such methods typically result in the isolation of far smaller populations of cells for use in subsequent culture (roughly 30-40 thousand cells per cord). Furthermore, the long term survival of these cells *in vitro* is known to be problematic, with survival past 7-10 days extremely difficult to maintain (Henderson *et al.*, 1995). Given the large number of cells required for 3D culture and the desire to maintain such cultures for several weeks, it was decided to utilise unsorted ventral horn cells as a means to achieving greater cell numbers capable of surviving for longer periods *in vitro*.

Given the mixed nature of the cultures, identification of the motoneuron subpopulation became important. Microtubule-associated protein 2 (MAP-2) is expressed predominantly in the cell body and dendrites of central nervous system

neurons and is critical in controlling microtubule polymerisation (Shafit-Zagardo & Kalcheva, 1998). In this manner it plays a major role in controlling dendritic polarity, outgrowth, branching and stability during neuronal development (Shafit-Zagardo & Kalcheva, 1998). While MAP-2 is neuron specific, it is not motoneuron specific and as such, further exclusion criteria must be instituted when estimating motoneuron survival from cultures immunostained for MAP-2, in order to discount the presence of interneurons from mixed ventral horn cultures. Since motoneurons are multi-polar and among the largest neurons in the developing spinal cord (Camu *et al.*, 1993), discounting smaller MAP-2 positive cells (<15 μm), as well as bipolar neurons likely to be interneurons, provides criteria to ensure reasonably accurate estimations of motoneuron number are achieved when analysing populations of mixed ventral horn cells.

Primary mixed ventral horn cultures were seeded in 2D at a density of 25,000 cells/ cm^2 for 7 days before being prepared for ICC analysis. This seeding density and culture time frame have been previously established as appropriate for generating motoneurons with distinct axonal and dendritic processes and appropriate electrophysiological profiles (Alessandri-Haber *et al.*, 1999; Kalmar & Greensmith, 2009). Motoneurons maintained under these conditions, in a complete neurobasal medium (CNB) (Kalmar & Greensmith, 2009), were consistently found to make up roughly 30% of the total cells in culture. This result is supported by previously published data (Bloch-Gallego *et al.*, 1991), highlighting the suitability of the described protocol (see **Section 2.1.2.**) for the dissection and *in vitro* culture of primary embryonic motoneurons.

In order to adapt this media to encourage myoblast differentiation however, the addition of IGF-1 was necessary. Investigation was therefore required to ensure this addition had no negative impact on the survival of motoneurons *in vitro*.

Inclusion of IGF-1 in culture was found to increase motoneuron positivity to almost 35% of the total population although this increase was not statistically significant (p=0.319) (Figure 4.2). This result is in line with previously published data regarding motoneuron survival in culture with and without IGF-1 supplementation (Ang *et al.*, 1992).

In vivo, IGF-1 knock-out or antibody neutralisation leads to a significant reduction in neuron numbers (Arsenijevic & Weiss, 1998). The presence of IGF-1 and its receptor throughout the central nervous system during development therefore suggests a role for this factor in neurogenesis (Arsenijevic & Weiss, 1998). Furthermore, IGF-1 has demonstrated a neuro-protective ability in chick and mouse motoneurons following axotomy (Arsenijevic & Weiss, 1998). Given these data, it seems logical to assume that IGF-1 *in vitro* should have no negative impact on motoneuron survival, and this assumption is borne out by the data recorded here. Furthermore, the neuro-protective capacity which IGF-1 possesses *in vivo*, may also be beneficial when seeking to maintain motoneurons for longer periods *in vitro*.

Assessment of MDC fusion ability using CNB+IGF-1 demonstrated improvements to levels of myoblast differentiation. 2D cultures differentiated using muscle differentiation media demonstrated a fusion efficiency of 61.46% which increased to 71.22% when cultures were given CNB+IGF-1 (Figure 4.3). CNB media contains BDNF which is known to be expressed in satellite cells and is believed to play a role in satellite cell mediated regeneration (Clow & Jasmin, 2010). BDNF knock-outs exhibit abnormal differentiation of primary myotubes which can be rectified through treatment with exogenous BDNF (Clow & Jasmin, 2010). It seems likely therefore that the addition of neurotrophic factors to cultured MDCs had a positive effect on the activity of the satellite cell population, leading to increased levels of differentiation and fusion in culture.

The increase in fusion efficiency in 2D MDCs to 71.22% removes significance from the difference between 2D and 3D cultures with regards to the levels of fusion possible *in vitro*. As documented in Chapter 3 (see **Section 3.3.6.**), fusion efficiency was found to be 73.14% in 3D culture, which is not significantly different from the 71.22% recorded from 2D MDC cultures differentiated using CNB+IGF-1 ($p=0.699$). Contrary to the conclusions of Chapter 3, this finding suggests that equal rates of fusion are possible in 2D and 3D, provided 2D cultures are given additional media supplementation. This provides further evidence for the improvement of the 3D model over conventional culture systems since the culture environment appears capable of promoting levels of MDC differentiation which would alternatively require the addition of further media supplements to achieve. However, since, as mentioned previously, it is not possible to determine whether the seeding densities of cells in 2D and 3D are in any way comparable, the possibility that differences in fusion levels are due to differing seeding densities cannot be excluded.

Overall, these data indicate the suitability of CNB+IGF-1 for use as a media for the co-culture of primary motoneurons and primary MDCs. This verification allowed for the progression into preliminary analysis of motoneuron-MDC interaction within a 3D collagen matrix.

4.4.2. Establishment and characterisation of preliminary 3D co-culture conditions

Initial parameters for 3D co-culture of primary MDCs and motoneurons were extrapolated from previous findings and published work. An MDC seeding density of 5 million cells/ ml was established in Chapter 3 as optimal for promoting the greatest levels of myoblast fusion, whilst simultaneously ensuring stability of the culture in the face of increasing mechanical strain due to matrix contraction by the seeded cells

(see **Section 3.4.2.4.**). Previous experience has shown that constructs often take several days to begin to contract and, if likely to detach from the flotation bars, typically did not do so until 5-6 days after establishment of the culture. Procurement of primary motoneurons is both costly and requires the sacrifice of a large number of animals. It was therefore decided to maintain the constructs for 7 days prior to the addition of CNB+IGF-1 media and primary motoneurons, in order to ensure the viability of the 3D MDC construct before motoneurons were added to the culture model. A 7 day co-culture period was selected since this would equate to a 2 week culture of the MDCs. qPCR data for myogenin, obtained in Chapter 3 (see **Section 3.3.5.**), indicated that 2 weeks in culture was sufficient to allow all fusion events likely occur in 3D culture to have taken place. Culturing ventral horn neurons for 7 days has been used previously as a time frame to allow development of correct electrophysiological profiles as well as axon and dendritic outgrowth (Alessandri-Haber *et al.*, 1999; Kalmar & Greensmith, 2009).

In 2D culture, 25,000 cells/ cm^2 has previously been shown to be optimal for promoting *in vitro* development of primary motoneurons (Kalmar & Greensmith, 2009). The surface area of the chamber slides used for culturing the 3D collagen construct is 9.4 cm^2, suggesting an appropriate seeding density of 235,000 cells per construct. However, since the surface area of the 3D construct was considerably larger than the 2D chamber slide culture surface area, and the mixed ventral horn cell's affinity for attaching to the collagen gel uncertain, it was initially decided to double this seeding density in order to ensure a significant number of cells were attaching to the matrix.

Cultures established using 5 million MDCs/ ml and co-cultured with 500,000 motoneurons for 7 days were investigated for signs of neuromuscular interaction using ICC staining and confocal microscopy. MAP-2 immunostaining demonstrated

substantial levels of neuron survival in 3D co-culture with primary MDCs. A 3 ml collagen gel meant 15 million MDCs and 500,000 ventral horn cells were present in each culture. The intense concentration of cells made realistic cell counts impossible, thereby rendering any attempt to quantify motoneuron survival in 3D culture very difficult. While motoneuron survival appeared substantial as determined by MAP-2 immunostaining, the characteristic clustering of cells made cell body diameter and neurite outgrowth difficult to estimate. It was therefore not possible to determine the size of the motoneuron population in these 3D cultures. Every attempt was made to limit the infiltration of other neural cell types during the dissection and preparation of ventral horn cultures. Cell counts in 2D also demonstrated a consistent 30% of the population to be made up of motoneurons while interneuron presence appeared to be minimal. Given these provisos, the assumption that strong levels of MAP-2 positivity was indicative of substantial motoneuron survival within this culture model could be made. It should be noted however, that an inability to verify for certain the size of the motoneuron population in this culture model is a limitation that must be considered when analysing data from this system.

Infiltration of exploratory neurites was observed within this co-culture model and the development of these neural extensions typically ran in parallel and close proximity to underlying myotubes (Figure 4.5). To what extent this observation is indicative of MDC-motoneuron communication is difficult to determine. It may be that the developing neurites, growing in parallel to cultured myotubes, were simply following the path of least resistance through the collagen gel and were therefore adhering to the mechanical cues within the construct brought about by MDC contraction against isometric anchor points. However, the wrapping of neurites around myotubes, and the localisation of developing neurites to areas with substantial myotube development, suggests a level of cross talk between the two cell types encouraging neurite growth toward the developing muscle fibres.

As described previously (see **Section 1.3.**), NMJ synaptic transmission involves the release of acetylcholine and the binding of this neurotransmitter to receptors within the muscle fibre membrane. Synaptic vesicle protein 2 (SV-2) is a synaptic vesicle membrane glycoprotein expressed in all neural cells as well as endocrine secretory granules (Janz *et al.*, 1999). A component of synaptic vesicles in all presynaptic nerve terminals, SV-2 plays a crucial role in regulating cytoplasmic Ca^{2+} levels in the nerve terminal during repetitive stimulation (Janz *et al.*, 1999). The specific localisation of SV-2 and AChR proteins to the pre- and post-synaptic motor end plates respectively suggests that areas of co-localisation in culture are indicative of direct apposition between nerves and myotubes *in vitro* and therefore suggestive of neuromuscular contact between the co-cultured cells.

Extremely low levels of AChR/ SV-2 co-localisation were observed in these preliminary cultures (Figure 4.6). Just 2 distinct co-localisations were found from 9 mm^2 sections taken from 6 independent cultures. While an incidence rate of 0.04 co-localisations/ mm^2 clearly indicates the difficulty in promoting the development of neuromuscular contact within this *in vitro* model, it does indicate that it is possible. Close association of pre- and post-synaptic markers do occur within this system therefore but methods for improving the incidences of such structures should be investigated.

4.4.3. Improvements to the preliminary co-culture model

Seeding densities were increased in order to improve chances of neuromuscular contact in 3D co-culture. Typically, 2-3 million cells were recovered from dissections of rat primary ventral horns. Since multiple 3D constructs were cultured from any one P1 muscle digest, 1 million cells per construct was selected as a maximum seeding density for mixed ventral horn cells which would still allow sufficient

numbers of constructs to be completed for analysis. Furthermore constructs now contained up to 16 million cells and the size of the chamber slides being used limited feeding media to 5-6 mls per construct. Constructs were therefore already overpopulated with regards to the amount of media provided. Further increases in cell numbers ran the risk of leading to cell death through starvation or exposure to acidic, nutrient-depleted media.

It was decided a 2 week co-culture period should be attempted in order to allow more time *in vitro* for the developing neurites to form synaptic contacts with the underlying myotubes. This decision was based on recent work with 2D co-cultures which affirmed that 12-15 days in culture was required before evidence of NMJ formation was observed (Das *et al.*, 2010).

Further media supplementation was also examined in order to provide more favourable conditions for NMJ formation in culture. As discussed previously (see **Section 1.3.1.**), neural cell derived agrin and Wnt3 proteins are believed to play crucial roles in NMJ formation *in vitro* through interaction with the MuSK protein complex (see Wu *et al.* (2010) for review). These proteins are believed to be involved in the pre-patterning of muscle fibre membranes, axon guidance towards underlying fibres and stabilisation of the newly formed NMJ (Wu *et al.*, 2010).

Previously published work has demonstrated that treatment with agrin and Wnt3 recombinant proteins combined leads to a significant upregulation of AChR cluster formation compared with untreated controls and cultures treated with each protein individually (Henriquez *et al.*, 2008). Since the patterning of the post-synaptic membrane is believed to be important for axon guidance and correct NMJ assembly, it seems logical to assume that treatment of co-cultures with exogenous agrin and Wnt3 proteins may stimulate the interaction of cultured motoneurons with myotubes.

Analysis of 2D cultures demonstrated that addition of agrin and Wnt3 to the culture media, at concentrations described in the previously published study (Henriquez *et al.*, 2008), had a significantly greater effect on AChR clustering than did the presence of neurons in co-culture (Figure 4.8). This implies that the signal released from the cultured neurons was perhaps too weak to illicit significant levels of synaptic assembly in the developing myotubes. The fact that a further significant increase was found in co-cultures treated with agrin and Wnt3 suggests an additive effect of these proteins in culture with neurons. Whether the release of other factors from the neurites or higher concentrations of agrin and Wnt3 in treated co-cultures were responsible for the greater incidences of AChR cluster formation cannot be inferred from this data. It should be also noted that, in order to prevent myotube detachment from the substrate, cells were fixed and analysed following just 4 days in co-culture. As already discussed, cultured primary motoneurons require 7 days *in vitro* in order to develop characteristic electrophysiological profiles (Alessandri-Haber *et al.*, 1999; Kalmar & Greensmith, 2009). It is possible therefore that analysis of these cells after 4 days *in vitro* did not allow them time to mature fully and so likely inhibited their ability to initiate post-synaptic differentiation in the cultured myotubes. Consequentially, one cannot conclude from this data set that treatment with agrin and Wnt3 protein *in vitro* provides a stronger AChR clustering influence on myotubes than does co-culture with primary motoneurons. The apparent additive effect of agrin and Wnt3 treatment and motoneuron co-culture over either condition individually however, does imply that addition of these proteins into the culture media is likely to lead to increased levels of post-synaptic differentiation over that achievable with co-culture of motoneurons alone.

Since aneural post-synaptic differentiation is believed to be involved in axon guidance and subsequent assembly of the NMJ (Wu *et al.*, 2010), it was decided to include these proteins in the CNB+IGF-1 media, as a means to improve the

probability of successful synaptic contact being made in this *in vitro* co-culture system.

4.4.4. Characterising the effect of co-cultured motoneurons on the improved MDC-motoneuron 3D culture model

4.4.4.1. The effect of motoneuron presence and culture timeframe on the fusion efficiency of MDCs in 3D culture

Fusion efficiency was not found to increase substantially in MDC constructs co-cultured with motoneurons. During development *in vivo*, myoblasts are known to differentiate and even display fibre type diversity prior to innervation (Navarrette & Vrbová, 1993). Given the data presented here, coupled with the fact that motoneurons *in vivo* interact with already differentiated muscle fibres, it seems logical to assume that introduction of motoneurons to developing MDCs in culture would have little influence on their capacity to differentiate.

Of far greater importance to the development of this model however, is the observation that, regardless of motoneuron presence, the cultures developed in this Chapter have far lower levels of fusion than cultures developed previously. From Chapter 3, a fusion efficiency of 73.14% was established for MDC constructs maintained in a basic muscle differentiation media (DM). Since analysis of 2D cells demonstrated that CNB+IGF-1 media produced greater levels of fusion than DM+IGF-1, the fact that, in 3D, significantly lower fusion efficiencies were observed when using CNB+IGF-1 media suggests some other factor had significant bearing on the ability of MDCs to fuse in 3D.

The only alterations to culture conditions from the previous Chapter and 2D experiments using CNB+IGF-1 was the time point at which 3D cultures were switched to CNB and the addition of agrin and Wnt3 proteins to the media. Since no

evidence in the literature could be found for agrin or Wnt3 mediated inhibition of myoblast differentiation, the culture time frame seemed far more likely to play a significant role in regulating MDC maturation. In Chapter 3, 3D constructs were switched to DM once 2D controls reached confluency. This was to ensure the greatest levels of comparability were maintained between 2D and 3D culture models. Having already established the superiority of 3D culture over 2D, in terms of cellular architecture and long term maintenance, this requirement was no longer necessary. Cultures were therefore maintained in growth media for 7 days as this presented a logistical benefit in terms of experiment cost (see **Section 4.4.2.**) and, at the time, was not determined to be detrimental to the seeded MDCs.

Switching 3D MDC cultures and MDC-motoneuron co-cultures to CNB+ after 4 days *in vitro*, to correlate with cultures switched to DM from Chapter 3, restored the fusion efficiency of the seeded MDCs. Maintenance of MDCs in GM for too long therefore, clearly has an adverse effect on the cultured myoblasts' ability to fuse in 3D. This may be due to increased proliferation of fibroblasts in culture during this time. If fibroblast number increased substantially during the 3 extra days in GM, then it could conceivably have a negative impact on the levels of cell-cell contact between myoblasts, which would in turn hamper these cells' ability to fuse. Human dermal fibroblast proliferation rates have been shown to increase substantially in collagen gels of increasing stiffness (Hadjipanayi *et al.*, 2009). The matrix contraction brought about by MDC interaction with the exogenous collagen in these cultures leads to a gradual increase in both tension and stiffness within the system. It seems plausible therefore that increased time in GM may well lead to rapid and substantial increase in fibroblast population doubling within this model, which would in turn inhibit levels of myoblast cell-cell contact.

An alternative hypothesis is that the matrix contractile ability of cultured fibroblasts for 3 extra days significantly increased the compression of the seeded myoblasts and collagen fibril density surrounding these cells. Plastic compression has been used as a means to increase the density of seeded cells within collagen matrices as well as increasing construct stiffness through expulsion of water (Mudera *et al.*, 2010). Studies using plastic compression on MDC seeded collagen constructs demonstrated a negative effect on the seeded cells' ability to mature with regards to MYHC gene expression levels (Mudera *et al.*, 2010). Unpublished electron microscopy data from this group, examining plastic compressed collagen constructs seeded with MDCs, demonstrates that myoblasts in this environment exhibit a rounded and greatly compressed morphology with little development of membrane projections into the surrounding matrix. Such data suggest that cultured myoblasts exposed to dense extracellular matrices are less able to differentiate, possibly due to a reduced ability to migrate through the matrix in order to make essential cell-cell contacts. It seems possible therefore that greater levels of matrix contraction by fibroblasts when constructs are maintained in GM for 7 days could lead to an inhibition of myoblast fusion through greater collagen fibril density surrounding these cells.

These data indicate the importance of adopting appropriate culture timeframes when seeking to promote the greatest levels of myotube development in 3D culture. Comparison of MDC only controls to MDC-motoneuron co-cultures, both switched to CNB+ and given motoneurons (where applicable) after 4 days *in vitro*, again showed no significant difference in fusion efficiency. This observation provides further support for the earlier conclusion regarding the lack of influence cultured motoneurons have on the fusion of MDCs in 3D culture.

4.4.4.2. Neuromuscular contact in optimised 3D co-culture

The improvements made to the 3D culture system appeared to have a strong positive effect on the co-localisation of pre- and post-synaptic markers. Given the number of cells per mm^2 in these constructs, 4.24. co-localisations/ mm^2 does not suggest a particularly substantial level of synaptic contact. However, it marks a significant increase from the 0.04 co-localisations/ mm^2 measured in the preliminary cultures.

This data provides evidence for the regular apposition of pre- and post-synaptic terminals in 3D culture. Thin SV-2 positive projections were seen running alongside cultured myotubes and are believed to indicate neurite growth into the construct. This in turn suggests that SV-2 in developing culture is not fully localised to the pre-synaptic terminal, likely being synthesised within the cell body and transported along the neurite to the developing growth cone. Brighter SV-2 staining was usually observed in close proximity to AChR clustering (Figure 4.12C), compared with levels along the rest of the developing neurites, perhaps indicating the development of the pre-synaptic terminal at these locations.

These co-localisations lack the clear definition of the *in vivo* NMJ. This is perhaps to be expected since maintenance of the mature NMJ *in vivo* is known to be activity dependent (Akaaboune *et al.*, 1999) and a lack of any co-ordinated stimulation protocols may well hinder development of these preliminary cell-cell contacts. In order to verify the functionality of these contacts one would, ideally, make intracellular electrophysiological recordings from individual myotubes (Miles *et al.*, 2004). Glutamate treatment has been shown previously to induce neuronal activity in muscle co-cultures (Miles *et al.*, 2004). Increased measurement of large endplate potentials in cultured myotubes following bath application of glutamate would

therefore provide conclusive proof of functional neurotransmission between these two cell types in culture. Unfortunately, the difficulty in effectively resolving individual myotubes embedded within a collagen matrix makes electrophysiological recordings problematic within this system.

While this ICC co-localisation data is a good indicator of neuromuscular contact within this co-culture system, and likely indicates a level of communication between the two cell types, further electrophysiological data would be required to verify their activity. It may simply be that the neurites, in growing alongside the cultured myotubes, release sufficient factors to encourage the development of post-synaptic structures underneath. Further data would be required to demonstrate that the relationship between the two cell types equates to more significant contact than this.

4.4.4.3. Effect of motoneurons on construct contraction

Given the current difficulty in making electrophysiological recordings from these 3D co-cultures, it was decided to use an alternative approach to investigate the functional capacity of the cultured cells, in order to ascertain whether or not motoneuron presence had a positive effect on construct development. Functional measurements of myotube contractile force could perhaps provide a suitable surrogate for direct electrophysiological recordings. Analysis of cultured myotubes' contractile ability in response to nerve stimulation from glutamate treatment would provide strong indication for functional NMJs if significant increases in force measurements were made post treatment. Work is currently ongoing in this lab to further develop the culture force monitor (CFM) system described previously (Mudera *et al.*, 2010), to be capable of measuring individual contractions rather than increases in overall strain. However, this system is not yet functional, and so recordings could not be made from the constructs prepared in this study.

Measurement of overall matrix contraction was instead used as a marker of increased contractile activity. As described previously (see **Section 3.4.2.4.**), the bowing observed in these constructs as they develop is believed to correlate to the level of cellular matrix remodelling occurring in culture. The greater the activity of the fibroblasts in culture, the larger the level of bowing observed in the construct. Myotubes in culture also spontaneously contract, and CFM recordings from mixed myoblast and fibroblast 3D constructs demonstrate a significantly greater level of overall strain developed compared with purified fibroblast or myoblast cultures (Brady *et al.*, 2008). It seems likely then that myotube activity would also contribute to the levels of matrix contraction occurring in these 3D constructs.

Measurement of construct surface area was made every 7 days during a 3 week culture period with constructs switched to CNB+ and given motoneurons after 4 days (Figure 4.13). After 3 weeks *in vitro*, co-culture construct surface area was significantly smaller than that of MDC only controls ($p=0.03$), suggesting the level of matrix contraction in co-culture was significantly up-regulated. Although contraction by cells within the mixed ventral horn population likely contributed to this result, the rounded morphology of the co-culture cross-section, compared with the elongated MDC only control morphology, also suggests greater levels of contraction from MDCs within the collagen matrix.

Assuming neuron presence did promote increased MDC contractile activity, this data still does not confirm active synaptic activity, since the increased contraction could be due to maturation of the cultured myotubes to a more adult phenotype. Assuming that interaction between muscle and nerve cells was promoting myotube maturation, then passive and spontaneous myotube contractions would be capable of generating greater levels of contractile force, leading to increased matrix contraction. There is also the possibility that release of certain factors from the

cultured neurons had a positive influence on the contraction of the non-myogenic cells in culture. Since motoneurons specifically interact with muscle fibres *in vivo* however, this hypothesis seems less likely.

Although direct synaptic neuromuscular activity cannot be inferred from the presented data, these observations provide evidence for increased matrix contraction in MDC constructs co-cultured with primary motoneurons, and suggest an overall positive neural influence on construct maturation in 3D.

4.4.4.4. Molecular maturation of MDCs in 3D co-culture with primary motoneurons

Given the positive indicators from the matrix contraction data, it was decided to investigate constructs for markers of MDC maturation and NMJ formation by quantitative PCR (qPCR) and western blotting. QPCR data was recorded both from cultures switched to CNB+ and given motoneurons at day 4 and at day 7. This was to explore whether the reduced fusion efficiency observed in cultures switched to CNB+ at the later time point correlated to altered gene expression in the myotubes that did form.

All cultures examined showed significant upregulation of *ChAT* in co-culture compared with MDC only controls. This was expected since *ChAT* is synthesised in the neuron. Only a 3 fold increase in *ChAT* expression over non-neuronal cultures however, indicates the low level of transcription of this gene in culture. This may be due to a lack of synaptic activity, reducing the need for acetylcholine synthesising agents, or in fact suggest the level of motoneuron survival in culture was lower than initially expected. While the level of positive MAP-2 staining achieved from these cultures was substantial, it was not possible to perform cell counts in order to quantify motoneuron survival over this time course. Survival of several thousand

motoneurons in culture would provide considerable levels of staining but still represent a very small percentage of the total number of cells in culture. This data appears to indicate that, while motoneuron survival over 2 weeks in this system is possible, the absolute neuron numbers as a percentage of the total number of cells in culture is very low, which may well have an impact on their ability to promote the maturation of the co-cultured myotubes.

AChRε mRNA expression was found to increase significantly, but this significance disappeared when only those cultures switched to CNB+ at day 7 were analysed. This observation indicates that this culture model is less able to promote NMJ formation since no upregulation of NMJ specific AChR subunit mRNAs was detected. It is possible this is due to lower levels of fusion, producing fewer myotubes than cultures switched to CNB+ at day 4, resulting in fewer multinuclear cells capable of promoting significant AChR upregulation. It may also be the case that increased matrix density in the 7 day model hindered neurite infiltration to the point where less contact was made with myotubes. Given the extremely low levels of AChR/ SV-2 co-localisation in preliminary cultures, this hypothesis certainly seems plausible. Increased matrix density may also explain the significant drop in *MYH1* expression in these cultures. Since *MYH1* encodes a fast myosin isoform, its expression would indicate the formation of fast fibres in culture. Previous work with human MDCs has demonstrated a switch towards a slow phenotype in un-stimulated collagen constructs, attributed to fixed physiological strains exerted on the seeded cells encouraging development towards a more postural phenotype (Mudera *et al.*, 2010). Increased matrix stiffness in this model could further add to this selection pressure, and may well instigate a down regulation of fast myosin isoforms since fast twitch contractions are undesirable in a “slow” muscle phenotype.

Constructs switched to CNB+ and co-cultured with motoneurons after 4 days showed a significant upregulation of AChRε mRNA. This, coupled with the increased incidences of AChR/ SV-2 co-localisation, provides strong evidence for improved conditions for NMJ development in this culture model. Unfortunately, western blots for AChRε protein were unsuccessful so this upregulation could not be confirmed at the protein level. The fact that no positive band was achieved from western blots for P1 muscle control samples however, suggests this was due to problems with protocol optimisation rather than a lack of protein expression.

Messenger RNA transcripts for troponin T1 and MYHC isoforms showed no upregulation in co-culture across all day 4 switched cultures examined. This negative result was largely attributable to a single culture in which expression went down. Excluding this data set as an outlier, the analysis showed that, in every other sample (n=3), expression of *MYH1, 3, 8* and troponin T1 all went up when MDCs were cultured with ventral horn cells. While the increase in *MYH1* was not found to be significant, increases in all other genes examined were. *MYH3* and *MYH8* encode embryonic and neonatal myosin isoforms respectively, while *MYH1* and *MYH7* are fast and slow adult isoforms. These increases do not therefore indicate increased levels of myotube maturation towards an adult phenotype in co-culture, since only developmental isoforms were significantly up-regulated. Increased transcription of elements of the sarcomeric contractile machinery however does indicate that MDCs co-cultured with ventral horn cells may well be capable of generating greater levels of contraction, thereby supporting the macroscopic matrix contractile analysis made earlier (see **Section 4.4.4.3.**). Since one data set did not correlate with these findings, it must be noted that while this upregulation occurs in the majority of cases using this system, it is not observed in every culture examined. This is perhaps due to variability in motoneuron survival levels or levels of matrix contraction affecting neurite infiltration.

Western blot data showed no significant upregulation of MYHC protein across 3 culture sets. However, the nature of the 3D matrix meant significant alterations had to be made to the western blot protocol in order to obtain positive results. The high level of extracellular collagen meant that cellular protein made up a very small percentage of the total protein within a sample. It was thus impossible to normalise the samples to ensure equal levels of cellular protein loading. As a result, it was not possible to determine whether equivalent levels of protein were loaded from co-culture and MDC only controls and hence no conclusions could be drawn regarding the up or down regulation of protein levels between these culture conditions. β-actin was used as an endogenous control in order to attempt to compensate for this discrepancy, but the ambiguity as to actual protein volumes loaded and the unknown effect excess collagen had on cellular protein isolation and antibody affinity still makes strong conclusions difficult to make. The data obtained demonstrates the presence of MYHC protein in culture and the ability to isolate proteins from such cultures by western blot. However, the difficulty in isolating the cellular component from such samples suggests alternative methods such as enzyme-linked immunosorbent assays (ELISA) should be explored in future.

4.5. Conclusions

From the data presented in this Chapter, survival and neurite outgrowth of neurons from mixed ventral horn populations was confirmed. Further amendments were made to the culture protocol in order to promote the greatest levels of maturation possible. Immunocytochemical staining provided evidence for close contact of pre- and post-synaptic terminals and at least superficial levels of communication between the co-cultured cells. Macroscopic contraction data and qPCR analysis provided some evidence for the improved maturation of seeded MDCs when cultured with ventral horn cells.

While the evidence presented here is promising, it falls short of characterising robust NMJ formation in this 3D co-culture model. Contractile and electrophysiological analysis will be required in order to investigate the functional capacity of the *in vitro* neuromuscular interactions observed here.

5. Analysis of myotube interaction with embryonic stem cell-derived motoneurons in 3D co-culture

5.1. Introduction

The results presented in Chapter 4 identify a clear limitation in the use of primary motoneurons in 3D co-culture with primary myotubes. Areas of co-localisation between pre- and post-synaptic markers are low in number, suggesting that few neuromuscular junctions (NMJs) are formed in these cultures. Given the poor level of co-localisation between pre- and post-synaptic markers in previously published work (Daniels *et al.*, 2000; Das *et al.*, 2010), it is not surprising that definitive immunocytochemical evidence for synaptic formation has also been difficult to obtain in this 3D system. Although attempts to improve both the frequency and reliability of putative neuromuscular contacts have been successful in this model to some extent, further improvements to the culture system, leading to greater levels of neuromuscular interaction, are necessary. Adaptations to the current co-culture model that will allow for the best possible chances of promoting substantial numbers of robust synaptic contacts in 3D are therefore needed to ensure that this 3D system adequately models neuromuscular interaction *in vitro*.

As discussed previously (see **Section 4.4.4.4.**), low levels of *ChAT* mRNA expression in 3D co-culture utilising primary motoneurons, compared with MDC only controls, indicates the relatively low number of motoneurons present in this system. This is likely to represent a major factor contributing to the low levels of synaptic contact observed within this culture model, and may well help to explain the relatively small improvement these cells are able to illicit in the maturation of the co-cultured MDCs. By drastically increasing the size of the motoneuron population within these cultures, it may be possible to significantly improve the level of

neuromuscular interaction and synaptic contact occurring within this *in vitro* model. Purification of primary motoneurons using methods described previously (Camu *et al.*, 1993), results in very small populations of cells and is therefore not suitable for use in a model of this size. Similarly, increasing the size of the unsorted ventral horn cell population in co-culture is impractical due to the number of cells reliably attainable from such protocols and the ability for the developed culture model to carry enough media to sustain such a large cell population.

Embryonic stem cell (ESc)-derived motoneurons represent an alternative source of motoneurons *in vitro* which are easily purified and available in relatively vast quantities. A yield of 10 million motoneurons is not uncommon from preparations of such cells while preparations from rat ventral horns usually yields just 2 to 3 million unsorted cells (Henderson *et al.*, 1995). Furthermore, the model developed in this Thesis so far is entirely restricted to animal models, since obtaining primary human motoneurons is not possible. Establishment of ESc-derived motoneurons within this culture model would open up the possibility of developing human motoneuron-myotube cultures in 3D. This would greatly expand the use and direct relevance of this model for future research since human muscle cultures are relatively easy to establish (Brady *et al.*, 2008; Mudera *et al.*, 2010). The ESc population is also far more reliable, originating from single clones instead of cells from the spinal cords of a number of litter mates, and such cells are ethically sounder since they require the sacrifice of far fewer animals to achieve similar results.

Most importantly however, work published recently has demonstrated, far more conclusively than studies using primary cells, that ESc-derived motoneurons are capable of forming well defined synaptic contacts *in vitro* (Miles *et al.*, 2004; Guo *et al.*, 2010). Given these significant advantages over primary motoneurons, ESc-

derived motoneurons represent an exciting possibility with regard to the further development of this 3D *in vitro* culture model.

5.1.1. Embryonic stem cell-derived motoneurons *in vitro*

Inducing pluripotent stem cells to differentiate into neural progenitors has been possible for a decade (Reubinoff *et al.*, 2001), and has since been suggested as a potential therapy for the treatment of neurodegenerative conditions such as Parkinson's disease and Amyotrophic Lateral Sclerosis (ALS) (Reubinoff *et al.*, 2001; Miles *et al.*, 2004). Although cultured embryonic stem cells are able to differentiate into neural progenitors relatively easily (Reubinoff *et al.*, 2001), the ability to generate ESc-derived neurons, which express markers characteristic of specific neuronal populations and accurately recapitulate normal programs of neurogenesis, is far more complex (Wichterle *et al.*, 2002).

In vivo, rostral neural progenitors develop into motoneurons in response to caudalizing signals, from molecules such as retinoic acid (RA), followed by the ventralizing activity of Sonic hedgehog (Shh) (Wichterle *et al.*, 2002). Understanding this developmental pathway has allowed the development of a protocol to promote motoneuron differentiation from EScs through timed exposure to RA and Shh (Wichterle *et al.*, 2002).

Cells differentiated in such a manner express the LIM homeodomain proteins Isl1, Lhx3 and Lim1, which are normally associated with spinal motoneurons, as well as the motoneuron specific homeobox transcription factor HB9, indicating the development of a specific spinal motoneuron phenotype from within this population (Wichterle *et al.*, 2002). Mouse ESc-derived motoneurons, differentiated using the same RA and Shh signals used by Wichterle *et al.* (2002), express cholineacetyl transferase (ChAT) and vesicular acetylcholine transporter (VAChT), indicating that

these cells are able to develop a cholinergic transmitter phenotype (Miles *et al.*, 2004). These cells also display passive membrane potentials comparable to those of E18 rat phrenic motoneurons and their electrophysiological responses to the neurotransmitters GABA, glycine and glutamate are likewise characteristic of embryonic motoneurons (Miles *et al.*, 2004). It appears then that EScs, exposed to RA and Shh at appropriate time points, are capable of differentiating into cells with many of the molecular and functional characteristics of *in vivo* spinal motoneurons (Miles *et al.*, 2004).

Bath application of glutamate has been shown to significantly increase both the number of large (>1.5 mV) endplate potentials and the frequency of twitch contractions recorded from myotubes when co-cultured with ESc-derived motoneurons (Miles *et al.*, 2004; Guo *et al.*, 2010). Such activity can be blocked by treatment with either tetrodotoxin (TTX) or D-tubocurarine, indicating that the excitability of the cultured myotubes is induced by neural activity and not spontaneously generated by the muscle cells themselves (Miles *et al.*, 2004; Guo *et al.*, 2010). Immunocytochemical studies illustrate that neurons within such cultures possess enlarged neurite terminals that are highly branched and in direct apposition to distinct acetylcholine receptor (AChR) clusters on the myotube membrane, providing further evidence for neuromuscular synaptogenesis *in vitro* (Miles *et al.*, 2004; Guo *et al.*, 2010).

Despite the ability to promote specific neural lineage differentiation, significant levels of heterogeneity usually persist in cultures of ESc-derived motoneurons (Placantonakis *et al.*, 2009). Recently, bacterial artificial chromosome (BAC) transgenesis has been identified as a useful tool for identifying specific populations of neurons from differentiated and heterogenous EScs, through introduction of the green fluorescent protein (GFP) gene coupled to the *HB9* promoter (Placantonakis

et al., 2009). Manipulations of BAC transgenesis methodology in future will likely lead to the development of techniques for purifying desired cells from a general population containing both undifferentiated precursors and other unwanted cell types (Placantonakis *et al.*, 2009). This advancement would not only be advantageous for *in vivo* experimentation, where implantation of undifferentiated cells usually leads to teratoma formation, but also for *in vitro* studies where purified motoneuron populations could be obtained and studied in isolation from other neural and supporting cell types (Placantonakis *et al.*, 2009).

5.1.2. Aims of this Chapter

In collaboration with Dr. Ivo Lieberam's group at King's College, London, the potential for ESc-derived motoneurons to form NMJs in 3D co-culture was investigated as part of a pilot study. The experiments described in this Chapter therefore represent a preliminary investigation into whether substantial increases in motoneuron cell numbers, through the use of ESc-derived motoneurons, leads to a significant improvement in the number of putative NMJs formed in 3D co-culture with primary MDCs.

1. Do mouse ESc-derived motoneurons survive in 3D co-culture with primary rat MDCs?
2. Do ESc-derived motoneurons form neuromuscular contacts with co-cultured myotubes in 3D culture?
3. Are more neuromuscular contacts formed in this system when using ESc-derived motoneurons than when using primary motoneurons?

5.2. Materials and Methods

5.2.1. Cell Culture

5.2.1.1. Embryonic stem cell-derived motoneurons

Mouse ESc-derived motoneurons were kindly provided by Dr. Ivo Lieberam's group from King's College, London. An Mnx1(HB9)::CD14-IRES-GFP BAC (Figure 5.1), was stably transfected into these cells, allowing for the purification of motoneurons away from undifferentiated precursors and other cell types by magnetic-activated cell sorting (MACS) for the CD14 surface tag. Cells purified in this manner and investigated for GFP positivity (Figure 5.2) were found to be over 90% GFP positive (data provided by Dr. Ivo Lieberam's group), indicating the high level of motoneuron purity achievable in these cultures.

5.2.1.2. Establishment and maintenance of ESc-derived motoneurons with MDCs in 3D co-culture

Primary MDCs were isolated from the hind limbs of P1 neonatal rat pups and seeded within 3D collagen constructs at a density of 5 million MDCs/ ml as described previously (see **Section 2.1.7.2.**). After 4 days in culture, media was switched to CNB+ in order to promote myoblast fusion. After 7 days *in vitro*, constructs were switched to a media containing a 1:1 mix of CNB and ADFNK, supplemented with IGF-1 at 10 ng/ ml, GDNF at 10 ng/ ml, 200 pM agrin and Wnt-3 recombinant protein at 20 ng/ µl (CNB/ ADFNK+). ESc-derived motoneurons were then plated on top of these constructs at a density of 1 million cells per construct. Co-culture constructs were returned to the incubator and maintained for a further 4-14 days before being prepared for analysis; media was changed daily throughout the culture period. Parallel control cultures were also established using an identical method, but without addition of ESc-derived motoneurons after 7 days *in vitro*.

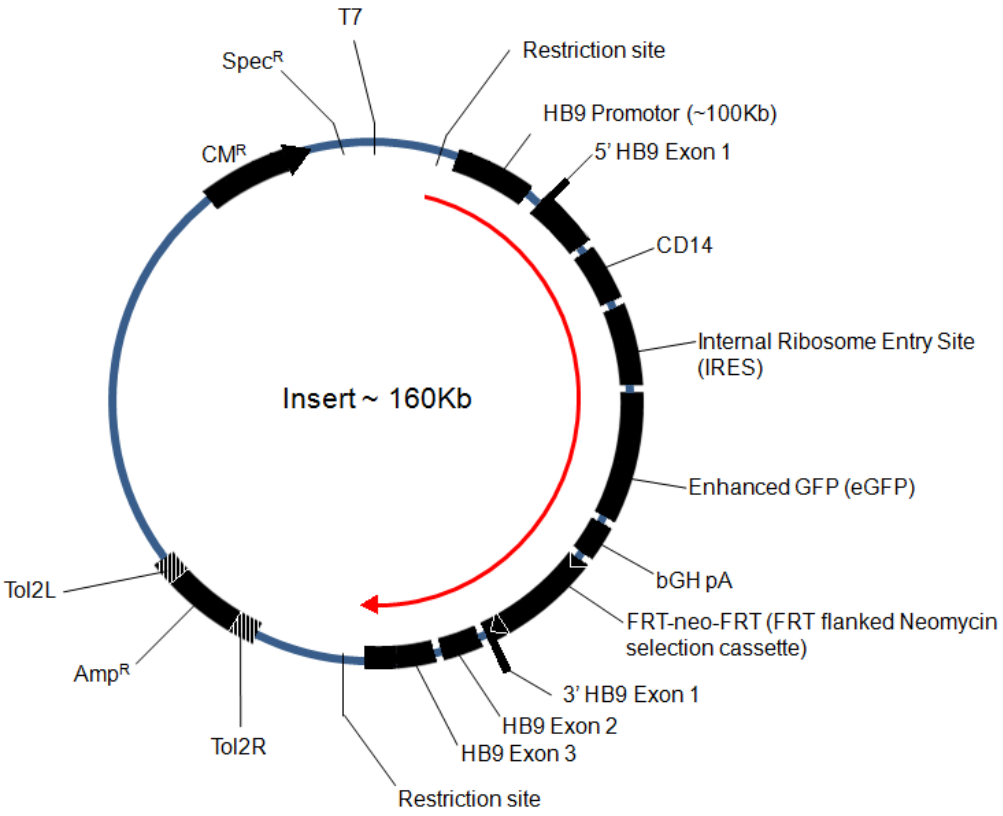

Figure 5.1: Diagram illustrating the structure of the BAC construct inserted into the ESc-derived motoneurons used in this study. The IRES sequence allows for independent expression of both CD14 and eGFP, under control of the HB9 promoter, in successfully transfected cells.

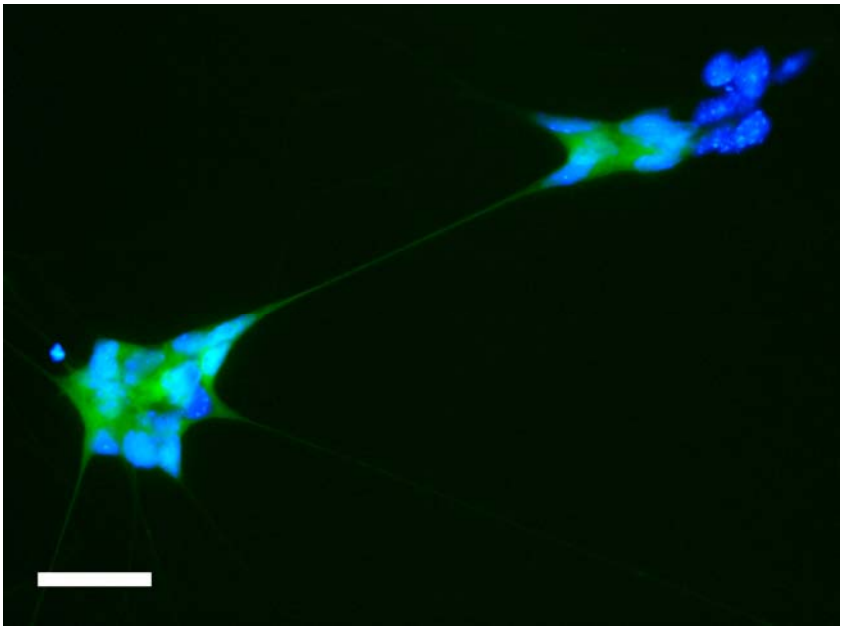

Figure 5.2: Unsorted ESc-derived motoneurons cultured on glass cover slips. Cells successfully differentiated into motoneurons express HB9, and therefore eGFP, allowing them to be identified in mixed culture with undifferentiated cells and other cell types. Scale bar = 20 μm.

5.2.2. Immunocytochemistry

MDC and ESc-derived motoneuron 3D co-cultures were immunostained for either microtubule-associated protein-2 (MAP-2) and desmin or synaptic vesicle protein 2 (SV-2) and acetylcholine receptors (AChRs) in order to observe the interactions between the 2 cell types (Table 2.1). Fixation and staining was carried out using the protocol detailed in Chapter 2 (see **Section 2.2.**).

5.2.3. Quantitative PCR analysis

Cultures designated for quantitative PCR (qPCR) analysis were homogenised in TRIzol reagent and the RNA isolated according to the protocol described previously (see **Section 2.3.1.**). RNA was then converted to cDNA using the protocol described previously (see **Section 2.3.2.**).

QPCR was performed using the Rotor-Gene Q real-time PCR cycler (Qiagen). The PCR reaction mixture (0.15 µl forward primer, 0.15 µl reverse primer, 0.2 µl nuclease free water , 10 µl 2x SYBR Green PCR mix (Qiagen) and 9.5 µl sample cDNA at 7.3 ng/ µl) was prepared for each gene to be analysed in duplicate micro-centrifuge tubes using the QIAgility automated PCR setup machine and accompanying software (Qiagen). Tubes were transferred to the Rotor-Gene Q and incubated at 95^{o}C for 5 minutes before being cycled 50 times at 95^{o}C for 10 seconds and 60^{o}C for 30 seconds. This protocol was designed by Qiagen for use with the QuantiFast SYBR Green 2 step PCR kit and so no optimisation of the thermal cycling parameters was necessary. The primers utilised in this analysis were the same as those used previously (see **Section 4.2.4.** and Table 2.2).

The threshold cycle (C_T) was defined as the fractional cycle number at which the fluorescence generated by binding of the SYBR green molecule to double stranded

DNA exceeded a fixed threshold above the baseline. To quantitate the amount of each target gene presented, the comparative C_T method was used, as outlined in the Qiagen "Analysis of real-time PCR" bulletin (Qiagen). The mean C_T value from duplicate reactions for each sample was determined and normalised to that of the endogenous housekeeping gene (RPII). The amount of target amplification relative to the endogenous control was calculated using the formula $2^{-\Delta\Delta C_T}$.

5.3. Results

Co-cultures of primary rat MDCs and mouse ESc-derived motoneurons were established in 3D utilising parameters optimised in Chapters 3 and 4, and based on advice from Dr. Ivo Lieberam's group at King's College, London. MDCs were maintained in co-culture with ESc-derived motoneurons for 4, 9 and 14 days before being prepared for analysis. Assessment of the cultured cells was undertaken using immunocytochemical (ICC) microscopy and qPCR analysis.

Due to time constraints, only 1 set of constructs was prepared for co-cultures examined at different time points. Further investigation will therefore be required in order to validate any conclusions drawn. The data collected here is a preliminary investigation to assess the suitability of ESc-derived motoneurons for future use in this culture model.

5.3.1. Neuromuscular interaction between primary MDCs and ESc-derived motoneurons in 3D culture

As was the case for 3D co-cultures utilising primary neurons, the clustering of MAP-2 positive cells, coupled with the extremely high MDC seeding density, made realistic cell counts impossible. This in turn made accurately estimating levels of ESc-derived motoneuron survival difficult. After 4 days in co-culture the number of surviving neurons appeared to be substantial however, with a large number of MAP-2 positive cell clusters visible on the surface of the construct (Figure 5.3). Neurites could be seen extending from these clusters, indicating the ability of these cells to extend exploratory neurites out into the surrounding matrix.

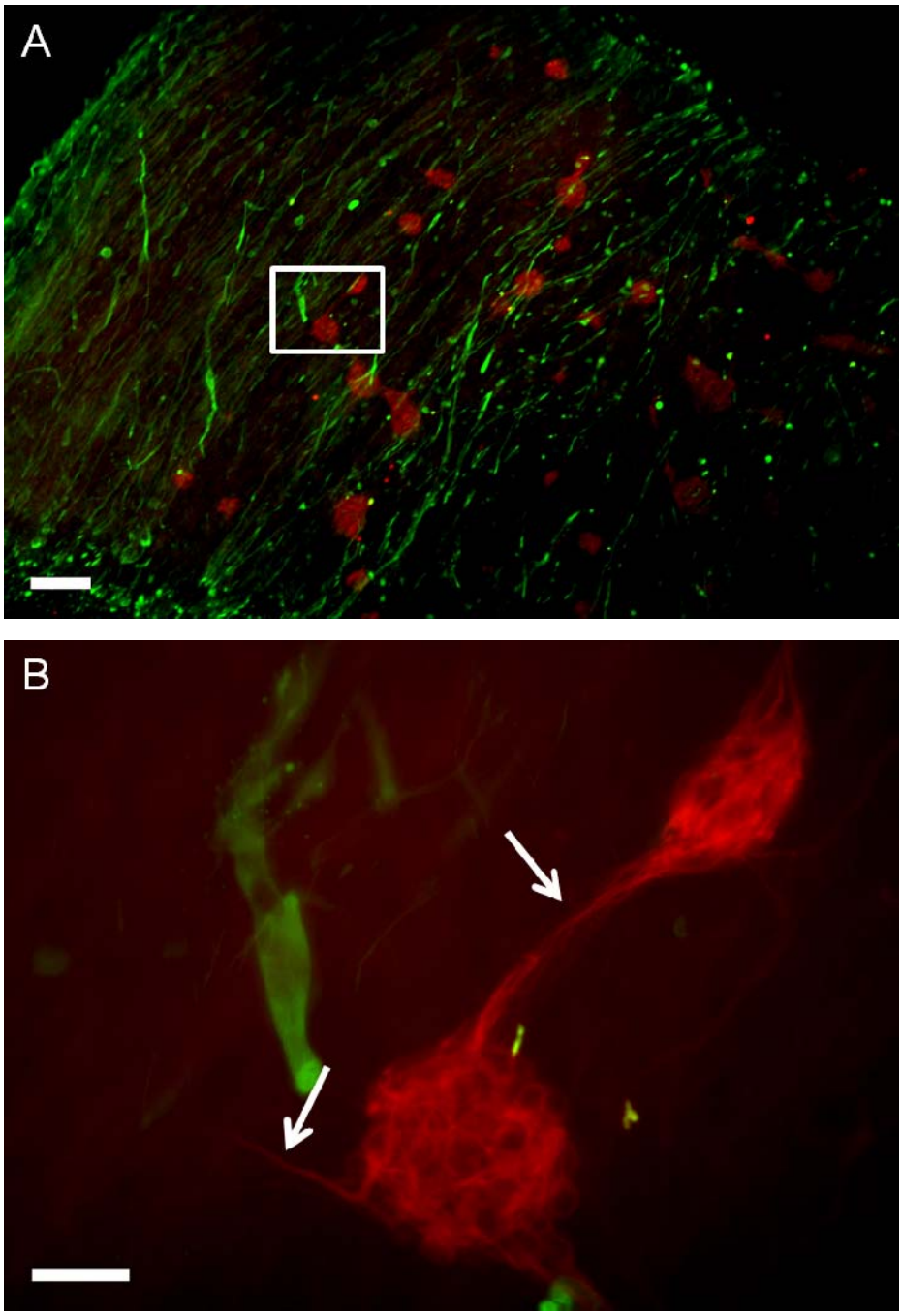

Figure 5.3: ESc-derived motoneurons in 3D co-culture with primary rat MDCs. (A) 3D construct seeded with 5 million primary rat MDCs, co-cultured with 1 million purified ESc-derived motoneurons for 4 days and immunostained for MAP-2 (red) and desmin (green). (B) Magnification of the highlighted area in A. Note the extension of exploratory neurites out from MAP-2 positive cell clusters (white arrows). Scale bar = 100 μm in A and 20 μm in B.

The number of MAP-2 positive cell clusters on the construct surface appeared much lower in 9 day co-culture, compared with 4 day co-culture. In 14 day co-culture almost all MAP-2 positivity was lost, indicating significant levels of ESc-derived motoneuron cell death in these co-cultures over a 2 week period.

Immunostaining of 30 μm construct sections for SV-2 demonstrated the ability for ESc-derived motoneurons to promote neurite growth into the exogenous collagen matrix (Figure 5.4). Intense SV-2 staining correlated with clusters of cell bodies when co-stained with MAP-2, as was the case for primary motoneuron cultures. These bright foci of SV-2 staining largely disappeared in 14 day co-culture, providing further evidence for a lack of motoneuron survival following this length of time *in vitro*.

Despite low overall levels of positive MAP-2 and SV-2 immunostaining in 14 day co-culture, some immuno-reactivity was observed within this culture model. Furthermore, some co-localisation of AChRs and SV-2 immuno-reactivity was also observed (Figure 5.5). As was the case in primary cells, the incidence of co-localisation in 3D co-culture was low in overall number and a decrease in the number of co-localisations/ mm^2 with increasing duration of co-culture appeared to be a general trend (Table 5.1). The greatest number of co-localisations observed when using ESc-derived motoneurons was 2.67/ mm^2 and was achieved after 4 days in co-culture. Primary cultures examined after 14 days in co-culture in Chapter 4 (see **Section 4.3.5.2.**) were found to possess 4.24 co-localisations/ mm^2 (± 2.69, n=3), While the maximum number of co-localisations observed in ESc-derived motoneuron cultures was lower than this value, it should be noted that this is just n=1 at present and the data point recorded does fall within 1 standard error of the mean value obtained from analysis of primary cultures.

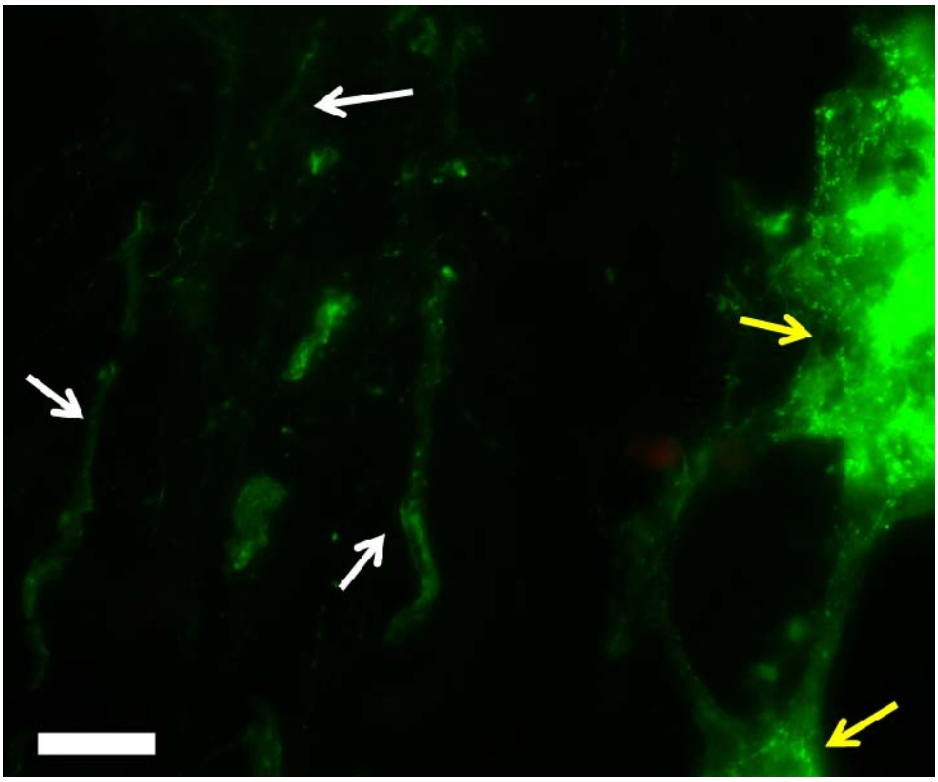

Figure 5.4: Neurite infiltration into a 3D collagen matrix. A 30 μm section from a 3D construct seeded with 5 million primary rat MDCs, co-cultured with 1 million purified ESc-derived motoneurons for 9 days and immunostained for SV-2 (green). SV-2 projections (white arrows) indicated the ability for neurites to penetrate the exogenous matrix. Foci of bright SV-2 staining (yellow arrows), indicative of neuronal cell body clusters, were entirely absent from sections of 14 day co-culture constructs. Scale bar = 20 μm.

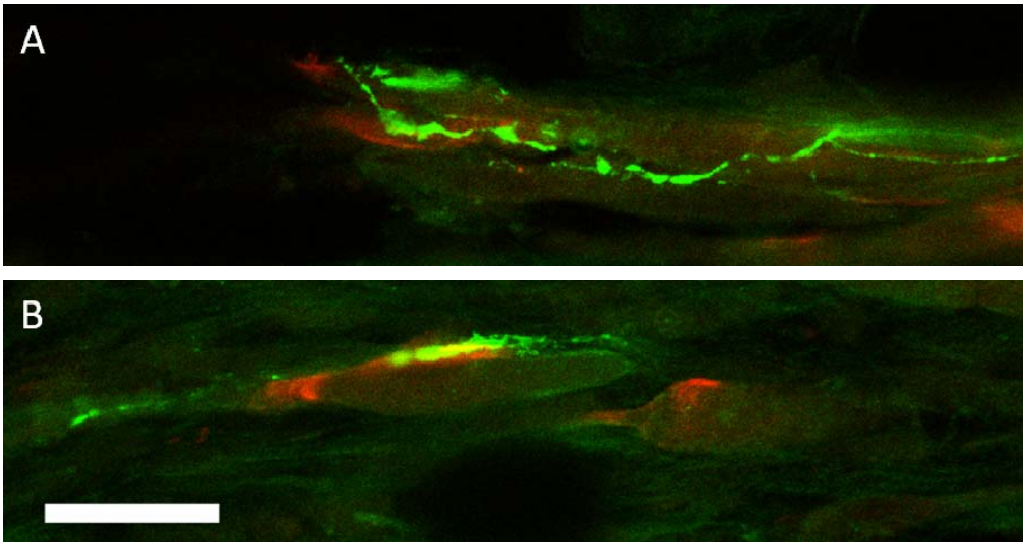

Figure 5.5: Neuromuscular interaction in 3D co-culture using ESc-derived motoneurons. Images of 30 μm sections from constructs seeded with 5 million primary rat MDCs, co-cultured with 1 million purified ESc-derived motoneurons for 14 days and immunostained for AChRs (red) and SV-2 (green). Scale bar = 20 μm.

Days in co-culture	Total co-localisations counted	Area of section analysed (mm^2)	Co-localisations/ mm^2
4 days	24	9	2.67
9 days	5	12.5	0.4
14 days	8	4.5	1.78

Table 5.1: Analysis of the number of AChR/ SV-2 co-localisations observed in 3D co-culture of MDCs and ESc-derived motoneurons. Constructs were cultured for different durations before analysis, n=1 for each time point.

Primary cells took 2 weeks in co-culture to develop 4.24 co-localisations/ mm^2 while the greatest level of co-localisation was recorded in ESc-derived cells after just 4 days. Analysis of primary constructs maintained for 7 days in co-culture during preliminary investigation of primary motoneurons in 3D produced just 0.04 co-localisations/ mm^2 (see **Section 4.3.3.**). Taken together, these data appear to indicate that use of ESc-derived motoneurons does not lead to a significant increase in the number of appositions of pre- and post-synaptic structures within this 3D co-culture model, but the formation of such structures does appear more rapid than equivalent cultures utilising primary motoneurons. The collected data also suggest that ESc-derived motoneuron survival within this model drops sharply over the first 2 weeks *in vitro*, indicating the unsuitability of the culture model, in its current form, for promoting ESc-derived motoneuron survival over significant lengths of time.

5.3.2. Gene expression in MDC constructs cultured with and without ESC-derived motoneurons

Quantitative PCR analysis of MDC and ESc-derived motoneuron 3D co-cultures indicated a substantial upregulation of *ChAT* in co-culture compared with MDC only controls. The expression level of *ChAT* was 8220.44 times higher in 4 day co-culture than in MDC only controls. After 9 days in co-culture, *ChAT* expression was just 0.00016 of that recorded in MDC only controls. Similarly, in 14 day co-culture, expression of *ChAT* had dropped to 0.000066 of that measured in the control construct. This data supports ICC evidence for substantial motoneuron survival following 4 days in 3D co-culture with MDCs as well as extensive cell death, over the next 10 days *in vitro*, leaving very few motoneurons in culture after 2 weeks.

QPCR data for markers of muscle maturation and NMJ formation indicate the positive effect ESc-derived motoneuron presence has on MDC maturation within this

3D co-culture model (Figure 5.6). An upregulation of myosin heavy chain genes *MYH3*, *MYH7, MYH8,* as well as mRNAs for troponin T1 and AChRε, was observed in constructs maintained in co-culture for 4 days. Expression in 9 day and 14 day co-culture appeared to be close to 1 for all genes, indicating that, at these time points, the expression of these genes was roughly equal in co-culture and MDC only controls. This demonstrates the plasticity in MDC gene expression when neurons are removed from culture.

Data from 4 day co-culture also indicates the ability for ESc-derived motoneurons to promote maturation of the cultured MDCs towards a more adult phenotype. By far the most substantial increase in MYHC expression was observed in *MYH7*, the myosin isoform expressed in slow adult fibres. Increased expression of adult myosin isoforms indicates the movement of the seeded cells towards a more mature phenotype. Moreover, the only MYHC gene not to show an increase in expression in co-culture at any time point was *MYH1*, the adult fast myosin isoform. This, coupled with the apparent upregulation of *MYH7*, indicates not only a movement of cultured MDCs towards a more developmentally mature configuration, but also the specific switching of fibres towards a predominantly slow phenotype.

As with all other genes examined, expression of AChRε mRNA was found to steadily decrease with increasing length of co-culture. These data suggest a decreasing level of NMJ development in MDCs from cultures maintained in co-culture for increasing lengths of time. This phenomenon is in line with ICC analysis indicating a decrease in the level of motoneuron survival and numbers of AChR/ SV-2 co-localisations in co-cultures of increasing length.

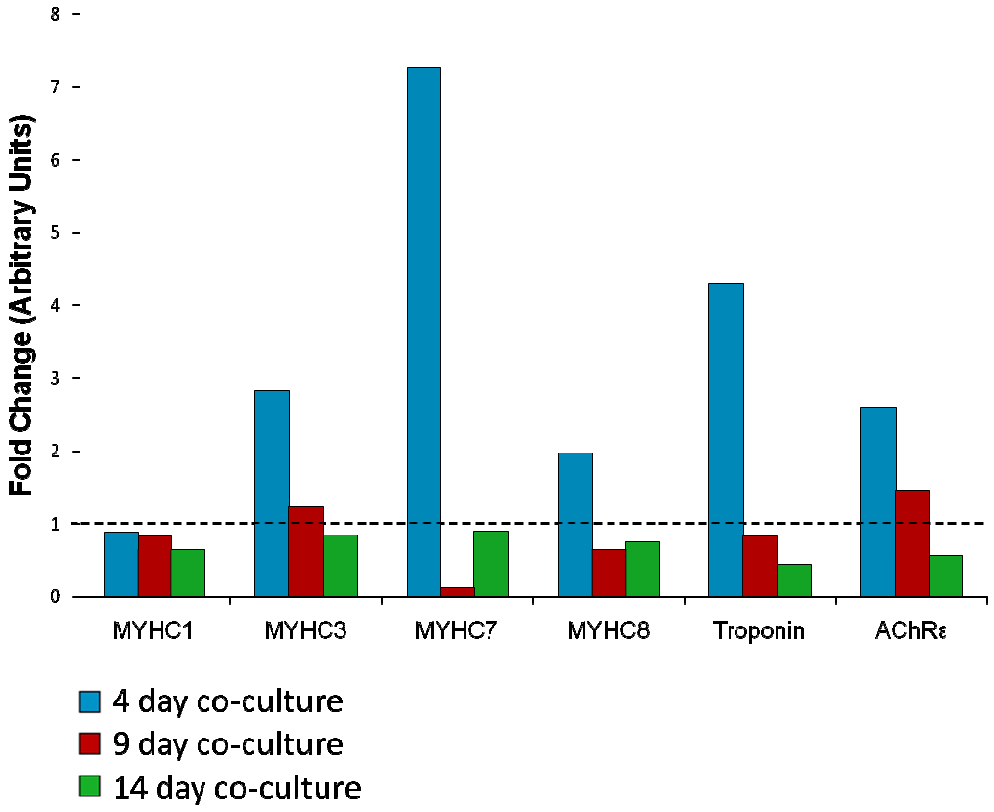

Figure 5.6: Fold change in mRNA expression levels for markers of muscle maturation and NMJ formation from 3D MDC constructs co-cultured with ESc-derived motoneurons. C_T values were normalised to an internal house-keeping gene (RPII) and expressed relative to levels recorded for 3D constructs without motoneurons at equivalent time points. n=1.

5.4. Discussion

The use of ESc-derived motoneurons in co-culture with primary MDCs within this 3D model holds great potential for the development and relevance of this *in vitro* culture system. Adaptation of the culture model to allow for the successful incorporation of these cells into this system first requires assessment of their ability to survive and interact with cultured myotubes within the current culture parameters. ICC and qPCR analysis have therefore been performed as a basic investigation of mouse ESc-derived motoneuron behaviour in 3D co-culture with primary rat MDCs.

5.4.1. ESc-derived motoneuron survival in 3D co-culture with primary rat MDCs

Immunostaining for the neuronal markers MAP-2 and SV-2, indicated very low levels of motoneuron survival following 2 weeks in co-culture. While substantial clusters of neurons were visible on construct surfaces after 4 and even 9 days in co-culture, motoneurons were all but entirely absent from older constructs. Communication with Dr. Ivo Lieberam's group at Kings College suggested that ESc-derived motoneurons, differentiated in this manner and cultured on Matrigel in 2D, typically lasted only 3-4 days *in vitro*. Previously published work using cells similar to those used in this study were only ever cultured for 3-7 days *in vitro* (Wichterle *et al.*, 2002; Miles *et al.*, 2004), perhaps indicating poor survival of these cells over longer time frames. According to published data (Wichterle *et al.*, 2002), the number of surviving ESc-derived motoneurons following 3 days *in vitro,* was found to be less than 25% of the cells plated, thus providing further evidence for poor *in vitro* survival rates in these cells.

Primary motoneurons are likewise difficult to maintain *in vitro* for long periods (Henderson *et al.*, 1995), which would perhaps explain the apparent difficulty in sustaining ESc-derived motoneuron survival in culture. If ESc-derived motoneurons possess a phenotype truly mimicking that of the *in vivo* spinal motoneuron, then it is logical to assume survival rates *in vitro* will mirror those observed in the primary cells. Survival of primary motoneurons from mixed ventral horn populations co-cultured with MDCs over 2 weeks (see **Section 4.3.5.2.**), likely indicates the positive effect that glial cell presence has on motoneuron survival *in vitro* (Ang *et al.*, 1992; Taylor *et al.*, 2007).

More long-term survival of ESc-derived motoneuron and MDC co-cultures has been reported. Guo *et al.* (2010) successfully maintained human ESc-derived motoneurons and primary rat MDCs for at least 13 days *in vitro* using a defined and specialised co-culture medium. While there may be inherent differences in the *in vitro* survival capacities of ESc-derived motoneurons from different donor species, the possibility also exists that improved motoneuron survival could be achieved through application of a more thoroughly investigated medium composition.

In this study, a 1:1 mix of CNB and ADFNK media was used, in the hope that a mixture of the media used in Chapter 4 and the media used at King's College for growing ESc-derived motoneurons would provide all the necessary supplements to facilitate both primary MDC and ESc-derived motoneuron survival. While positive staining indicated this media was capable of maintaining both cell types in the short term, the apparent loss of most ESc-derived motoneurons over 2 weeks perhaps suggests this media is insufficient or incapable of supporting long term ESc-derived motoneuron survival. More careful examination of requirements of the cultured cells may therefore lead to the development of a media better suited to maintaining these co-cultures in the medium to long term.

5.4.2. Transcription profile of MDCs co-cultured with ESc-derived motoneurons

Addition of ESc-derived motoneurons for 4 days led to substantial increases in expression of mRNAs for sarcomere contractile machinery (Figure 5.6), suggesting a positive effect from ESc-derived motoneuron presence on the contractile ability of the cultured myotubes. The sharp drop in expression of these genes in co-cultures maintained for longer periods is in line with the apparent death of the majority of the motoneuron population during this time. This in turn indicates that removal of the neuronal influence *in vitro* has an effect on the cultured myotubes, mirroring the atrophy of *in vivo* muscle fibres that is observed following denervation (Condon *et al.*, 1990; Midrio, 2006).

In 4 day co-culture, the largest increase in expression was observed for *MYH7.* Conversely, at every time point examined, *MYH1* expression decreased in co-culture compared with MDC only controls. These data not only indicate a level of maturation of the cultured myotubes towards a more adult phenotype, but also the apparent preferential selection of a slow fibre type. As described previously (see **Section 1.3.3.**), data from denervation studies suggests innervation is required to maintain a slow muscle phenotype *in vivo* (Condon *et al.*, 1990; Midrio, 2006). Should this observation hold up to repeat experimentation, it would therefore indicate a high level of cross talk between the cultured myotubes and ESc-derived motoneurons and the development of a physiologically correct adult phenotype within this *in vitro* co-culture model.

Increased expression of AChRε mRNA in MDCs co-cultured with ESc-derived motoneurons for 4 days suggests an increased development of the post-synaptic membrane compared with MDC only controls. A similar increase was observed in

co-cultures with primary motoneurons, suggesting roughly equal levels of post-synaptic differentiation within the two culture models. However, the occurrence of this upregulation, coupled with comparable levels of AChR/ SV-2 co-localisation (see **Section 5.4.3.**), after just 4 days *in vitro,* compared with 2 weeks in primary co-culture, suggests a capacity for more rapid synaptic differentiation in this model. The drop off in AChRε mRNA expression at later time points is in line with other collected data suggesting motoneuron cell death in longer co-cultures.

Expression levels of *ChAT* after 4 day co-culture indicated a vast upregulation in expression of the gene; thousands of times higher than the expression levels recorded in MDC only controls. This is logical since *ChAT* is synthesised in the neuron and the significant drop in expression levels over time correlates to the apparent motoneuron cell death observed in ICC data from co-cultures maintained for longer periods.

Of significant interest is the difference in expression levels of *ChAT* in co-cultures utilising ESc-derived motoneurons and those utilising primary mixed ventral horn cells. While primary co-cultures showed only a 3 fold increase in levels of *ChAT* mRNA expression (see **Section 4.3.5.4.**), the upregulation recorded in ESc-derived motoneuron co-culture was thousands of times greater than in controls. Some of this difference is perhaps attributable to differences in the efficiencies of the 1 step qPCR protocol used for primary co-cultures and the 2 step protocol utilised here. However, the fact that levels of MYHC, troponinT1 and AChRε mRNA upregulation were all in the same order of magnitude in both models, suggests an inherent difference in the level of *ChAT* expression in primary and ESc-derived motoneurons.

This difference likely correlates to the substantial difference in the size of the motoneuron population between the two culture models. The data obtained clearly

indicates that, after 4 days in co-culture, the size of the ESc-derived motoneuron population is vast, which in turn appears to have a strong positive effect on the transcriptional profile of the cultured myotubes. Conversely, *ChAT* data from primary motoneurons suggests low cell numbers but these cells are able to survive for several weeks in this co-culture environment. As mentioned previously, this is likely attributable to the presence of supporting glial cell types in mixed ventral horn cultures.

5.4.3. Neurite outgrowth and neuromuscular junction formation

Immunostaining for SV-2 indicated extensive neurite infiltration into areas of the collagen matrix surrounding motoneuron clusters (Figure 5.4). This mirrors positive staining from primary co-cultures, and suggests both cell types are capable of promoting significant levels of neurite infiltration into the exogenous matrix.

Levels of SV-2 co-localisation with AChRs in ESc-derived motoneuron co-culture were not found to be drastically improved over primary motoneuron co-cultures. The maximum number recorded was 2.67 co-localisations/ mm^2 and was observed following 4 days in co-culture. Comparing this observation to co-localisation data for mixed ventral horn cells after 7 and 14 days in co-culture with MDCs, indicates that the number of putative NMJs formed when using ESc-derived motoneurons is not improved. However, there is some indication that formation of putative NMJs may occur more quickly than when using primary cells. AChR/ SV-2 co-localisation frequencies appeared to decrease with increasing length of co-culture as a general trend and is logical given the apparent motoneuron cell death observed over time *in vitro*.

High levels of ESc-derived motoneuron survival in 4 day co-culture, and concurrent low levels of AChR/ SV-2 co-localisation, suggests that low motoneuron cell number

was not the cause of the low level of synapse formation in these 3D cultures, as was hypothesised from analysis of data from Chapter 4 (see **Section 5.1.**). Previous work has demonstrated that 4 days *in vitro* should be sufficient for ESc-derived motoneurons to promote NMJ formation with primary myotubes (Miles *et al.*, 2004). The collected data therefore implies that the collagen matrix may possibly be inconducive to promoting significant levels of NMJ assembly *in vitro*, since the 3D matrix is the most substantial difference between cultures established in this study and those from previously published work (Miles *et al.*, 2004).

However, even taking into account the fact that this observation is only n=1 at present, this conclusion requires much further investigation. It is possible that the 4 day culture period apparently available to these ESc-derived motoneurons *in vitro* is far too short a time frame to allow significant levels of synapse formation within this 3D model. As already discussed (see **Section 5.4.1.**), media used in this study was not fully optimised and it may also be the case that a lack of appropriate media supplementation had an inhibitory effect on NMJ assembly within this model. Investigation into alternative media compositions and additional supplementation may therefore have a substantial positive effect on synapse formation as well as ESc-derived motoneuron survival within this 3D culture model.

Another factor to consider in this analysis is the fact that the current set-up of this model allows for only a limited supply of media to the densely seeded constructs. In total, 16 million cells were present in each optimised co-culture examined in this study, and the chamber size meant only about 5 mls of media could be added to sustain them. Although media was changed daily throughout the culture period, this was not frequent enough to prevent the media turning yellow, indicating the build up of an acidic environment and the depletion of media supplements. Neurotrophic factors such as BDNF, GDNF and CNTF are all known to play crucial roles in

regulating neuromuscular synaptic connections, and are believed to be involved in regulating synapse elimination in early postnatal poly-innervated muscle fibres (Nguyen & Lichtman, 1996; Ribchester, 2009). It seems plausible therefore that fluctuations in media composition as the cultured cells rapidly deplete the surrounding media could well have a significant effect on neuromuscular interaction within these cultures. Development of a culture system incorporating either larger culture chambers or a form of media perfusion is something that should be investigated as a means to increase the reliability and suitability of this system for investigating neuromuscular interaction in 3D.

5.5. Conclusions

Although the data presented in this Chapter represents a small pilot study, with minimal results, analysis of the collected data indicates that ESc-derived motoneurons survive only for a short period in 3D co-culture with primary rat MDCs. During this time, these cells do not promote greater levels of synaptic contact with cultured myotubes than primary mixed ventral horn cells. However, there is some evidence that ESc-derived motoneuron presence has a strong positive effect on MDC development in 3D co-culture, in terms of myotube transcription profiles, suggesting increased motoneuron numbers do have a positive effect on construct maturation. Given the discussed limitations coupled to the use of these cells in the current model, further investigation is necessary before strong conclusions regarding the effect of increased motoneuron cell number on NMJ formation in this 3D co-culture system can be made.

6. General Discussion

The data collected and analysed in this Thesis represents an attempt to co-culture motoneurons with muscle derived cells within a three dimensional culture environment. It covers the steps taken to optimise culture conditions to promote maximal levels of neuromuscular interaction within this *in vitro* system, and observations regarding the development and maturation of the cultured cells over several weeks.

Successful development of a truly biomimetic culture environment, capable of promoting the formation of robust synaptic contacts between these 2 cell types would be of great potential benefit to the *in vitro* study of skeletal muscle and neuromuscular development. It would provide the means to measure the functional capacity of skeletal muscle, in an entirely controlled environment, in response to physical, chemical and pathological challenge. Moreover, the optimisation of a standardised protocol for establishing such models may help significantly reduce investigators' reliance on animal models, thereby greatly improving the ethical position of such work in future.

6.1. Development of a 3D model for the *in vitro* co-culture of muscle derived cells and motoneurons

A substantial amount of work utilising muscle derived cells (MDCs) within an exogenous collagen matrix has focused on use of the culture force monitor (CFM) system (Cheema *et al.*, 2003; Brady *et al.*, 2008; Mudera *et al.*, 2010). The use of this technique somewhat limits its broader application as an *in vitro* culture model, since the open nature of the construct environment prevents the long term maintenance of the cultured cells, which typically become infected after roughly 72

hours *in vitro*. The work presented in this Thesis has adapted the CFM protocol to allow for the development of a more physiologically relevant *in vitro* model, capable of being maintained in culture for weeks. Furthermore, it demonstrates the improvement such a model represents to standard 2D tissue culture techniques which has been discussed in previous work (Vandenburgh *et al.*, 1988), but never publically investigated in any great detail.

The data obtained here indicates that differentiation of myoblasts into primary myotubes can occur at equivalent levels in both 2D and 3D systems, provided culture conditions are appropriately optimised. Although both systems appear equally capable of promoting myoblast formation, 3D constructs hold significant advantage over 2D cultures since the application of a uniaxial, mechanical signal promotes alignment of seeded cells along the lines of principal strain. This leads to the formation of unbranched and parallel aligned myotubes capable of performing directed work. This system is not only more biologically representative of the *in vivo* tissue but, unlike 2D culture, the flexibility of the exogenous matrix allows for the maintenance of densely packed, differentiated myotubes in culture for extended periods.

The development of optimised culture conditions for primary rat cells in this system and comparison to previous work (Cheema *et al.*, 2003; Mudera *et al.*, 2010), demonstrates the plasticity of the model for culturing a variety of primary cell types and cell lines. However, inherent differences in optimal seeding densities, when establishing cultures from different donor sources, do exist. This observation advocates careful application of the culture conditions, developed in this study, in future work, since donor cell type is likely to have an impact on construct development.

Successful development of a long term 3D culture model for MDCs has allowed for progression into the investigation of motoneuron influence on the development of the model. The work presented in this Thesis has demonstrated that motoneurons derived from both primary tissue and embryonic stem cells (EScs) are capable of surviving within this system and developing exploratory neurites able to penetrate the surrounding exogenous matrix.

Primary motoneurons are capable of surviving for several weeks in 3D co-culture with primary MDCs. However, the total size of this cell population is relatively small, hence the level of MDC maturation is poor and the level of apparent synaptic contact infrequent. Never-the-less, evidence collected so far suggests a small but positive effect on the maturation of MDCs cultured in this 3D environment in terms of contractile protein machinery mRNA transcription, overall construct contraction and differentiation of the post-synaptic membrane compared with MDC only controls.

Preliminary data from constructs established with primary rat MDCs and co-cultured with ESc-derived motoneurons suggests the positive effect these neurons have on MDC maturation may be greater than primary motoneurons. However, the level of putative synaptic contact that occurs in this model remains low. ESc-derived motoneuron survival in this 3D co-culture model also appears to be problematic, and further investigation is required to validate initial observations and to ascertain whether or not culture of these cells for longer periods is at all possible.

Results from primary motoneuron studies suggested low levels of motoneuron survival in this culture model which was in turn predicted to be the cause of the low levels of NMJ formation observed. However, substantial increases in motoneuron number, through the use of ESc-derived motoneuron culture techniques, did not lead to a noticeable improvement in the levels of pre- and post-synaptic structure

apposition. This is possibly attributable to a number of factors including media composition, issues with consistent media supply and ESc-derived motoneuron survival time *in vitro*. Maturation of these 3D constructs leads to increasing collagen fibril density and fibroblast proliferation rates (Hadjipanayi *et al.*, 2009), and it is also possible that this has an inhibitory effect on synaptic development in this system through the matrix becoming increasingly dense and impenetrable over time.

These observations suggest a shift into alternative matrices, such as the fibrin based model discussed previously (see **Section 3.1.2.1.**), would be pertinent for future investigation since such models utilise far fewer cells, and therefore have smaller nutrient demands, and do not generate increasingly dense matrices over time. However, work in this lab has demonstrated that primary rat MDCs seeded within fibrin constructs do not survive past 7-10 days *in vitro* since they rapidly contract and degrade the matrix, leading to the construct snapping or disintegrating. It appears the rigidity of the collagen matrix is required in order to maintain such metabolically active cells for significant periods. The most logical choice moving forward is therefore to investigate the possibility of more complex matrices, containing collagen along with other ECM components, to reduce construct rigidity and promote greater levels of myotube-neurite interaction. This should be coupled with investigation into alternative media delivery methods and compositions in order to promote ESc-derived motoneuron survival for more significant periods. Such steps will in turn allow for a more in depth analysis of the effect of increased motoneuron density on synapse formation and myotube maturation within this 3D culture system.

6.2. Limitations of the current experimental technique

Apart from the conclusions regarding alterations to the developed model for use in future work discussed above, a number of limitations preclude more in depth analysis of the developed constructs and are discussed here.

Although data pertaining to the cross talk of myotubes and motoneurons is apparent within the current co-culture model, the work to date falls short of demonstrating the formation of robust and functional neuromuscular junctions (NMJs) in this 3D system. This is largely due to difficulties in applying conventional biochemical analytical technique to this bespoke system.

Previously published work has relied on electrophysiological data and observation of myotube twitch responses to demonstrate the functionality of *in vitro* synapses (Miles *et al.*, 2004; Guo *et al.*, 2010). Unfortunately, the dense nature of the exogenous collagen matrix makes resolving myotubes difficult, which in turn makes patch clamp recording extremely challenging within this system. Recent data has shown that collagen matrices are remodelled to a greater extent than fibrin based scaffolds when culturing MDCs in 3D (Hinds *et al.*, 2011). The construct is remodelled to a far greater degree, and the subsequent level of contractile force measured is lower (Hinds *et al.*, 2011). Given this observation, it is not surprising that very little twitch contraction was observed within the developed model across all 112 sets of constructs established during this study. The rigidity of the collagen matrix, when contracted down in mature constructs, makes the likelihood of observing myotube twitching low. That is not to say that cultured myotubes within this system do not contract, but rather that observation of these events is difficult to resolve.

Given the inherent difficulty in utilising either electrophysiological recording or twitch observation to test NMJ functionality in the collagen model, the best surrogate measure is likely to be recording peak twitch and tetanic myotube contraction, in response to treatment with a motoneuron stimulant such as glutamate, as has been used previously in 2D co-culture models (Miles *et al.*, 2004). Once the construct has matured within the chamber slide system, it should be possible to return the anchored gel to the CFM system, so that recording of generated force can be made. However, the CFM in its current format is only capable of making 1 reading per second (Eastwood *et al.*, 1996), which is insufficient for recording twitch responses in cultured myotubes. Published work utilising fibrin based constructs have demonstrated a method of recording twitch responses using custom built force transducers capable of recording force data in the millisecond range (Khodabukus & Baar, 2009; Hinds *et al.*, 2011). Development of such a system for use with the collagen model is currently ongoing in this group and is the next logical step in attempting to assess the functionality of the neuromuscular interaction indicated in this study.

The large amount of extracellular collagen, as has been discussed already, also poses a problem to accurate measurement of cellular protein levels within this system. Enzyme-linked immunosorbent assay (ELISA) represents a viable solution to this problem since it should allow for far greater sensitivity when examining protein concentration from 3D co-culture samples.

An alternative methodology would be to use a Cytometric Bead Array (BD Bioscience, Oxford, UK). This protocol involves a flow cytometry application in conjunction with antibody bound beads each possessing a different fluorescence intensity. By incorporating antibodies for multiple antigens of interest, this system allows for the quantification of multiple proteins from a single sample

simultaneously. Regardless of the technique used, development of a fully reliable protocol for measuring changes in protein levels between MDC only culture and motoneuron co-culture would be invaluable in characterising the effect of motoneuron presence. Such a technique would also widen the uses of the collagen model as a generalised 3D *in vitro* culture system.

6.3. Future work

Although the data collected in this Thesis represents a substantial step forward in the development of a 3D *in vitro* culture system for neuromuscular interaction, this model is still very much in development. Future work needs to therefore focus on refining the developed techniques and investigating new methods for analysing the constructs produced.

First and foremost, repeats of the experiments in Chapter 5 should be carried out in order to draw more robust conclusions regarding the survival of ESc-derived motoneurons in 3D co-culture and their interaction with cultured MDCs. It would be prudent to carry this out in conjunction with development of altered culture dishes or media perfusion systems, to allow more continuous media presence and eliminate chances of media depletion during culture.

Further media supplementation may well assist ESc-derived motoneuron survival and a more thorough investigation of appropriate media compositions may have a strong positive effect on the life span of these 3D co-cultures as well as levels of synapse formation *in vitro*. Should it only prove possible to maintain ESc-derived motoneurons for 3-7 days *in vitro*, regardless of media supplementation, an alternative solution may be to include astroglia in the co-culture environment, since these cells are known to improve motoneuron survival *in vitro* through the release of positive neurotrophic factors (Ang *et al.*, 1992; Taylor *et al.*, 2007). Another

possibility would be to investigate altering the time point at which ESc-derived motoneurons are added to the culture model. MDCs cultured for 2 weeks in CNB+IGF-1 should allow sufficient time for myotube formation and construct maturation. ESc-derived motoneurons could then be added at this time point and the co-culture maintained for just 7 days. No significant difference in fusion efficiencies between co-cultures and MDC only controls suggests this protocol should yield an equal number of myotubes to those developed in the presence of motoneurons. Previously published work suggests a co-culture of this time frame should also be sufficient for allowing NMJ formation *in vitro* when using ESc-derived motoneurons and primary MDCs (Miles *et al.*, 2004).

As discussed already (see **Section 6.1.**), the increase in collagen fibril density in highly contracted constructs may have a negative impact on the formation of robust synaptic contacts in this model. The incorporation of other molecules into the collagen scaffold should therefore be investigated as a means to improve neurite outgrowth and neuromuscular synapse formation. Maturation and maintenance of nerve terminals *in vivo* is believed to rely on the presence of laminin β2 as well as synaptic collagens α3 and α6 (Wu *et al.*, 2010). Incorporation of such proteins into the exogenous matrix, or use of Matrigel as a surrogate for basement membrane presence, could well have a drastic effect on neuromuscular interaction within this *in vitro* system. Increased complexity of the model in this manner not only stands to potentially improve cellular interaction and maturation but also the biomimicity of the construct as a whole, moving it closer to being truly representative of the *in vivo* niche.

Once appropriate conditions for motoneuron co-culture with primary MDCs in 3D have been identified, measurement of putative NMJ functionality should be assessed. This will require the development of appropriate force transducers in

order to examine the contractile function of cultured myotubes in response to neuronal stimulation through bath application of glutamate.

Coupled with this is the possible development of protocols for long term electrical stimulation of co-culture constructs and its effect on NMJ maturation. Maintenance of NMJs *in vivo* is known to be activity dependent (Akaaboune *et al.*, 1999), which raises the possibility that the low level of pre- and post-synaptic apposition and motoneuron survival in this culture model may be improved through repetitive and controlled stimulation patterns. Other groups have developed electrical stimulation rigs for the stimulation of 3D MDC constructs in the medium to long term (Donnelly *et al.*, 2010), and adaptation of such equipment for use with this model represents an exciting possibility for future development.

A final point for consideration is the delivery method of the motoneurons in this model. A monolayer on top of the MDC seeded construct, as was employed throughout this study, made sense initially as it created the smallest distance for neurites to traverse in order to interact with underlying myotubes. However, such a system is not representative of the *in vivo* condition and it may well be practical to investigate alternative methods for delivering the cells. For example, use of clustered neurons, in an optimised matrix, would allow for precise and directed application of the neuronal element. This would then allow for more accurate assessment of neurite outgrowth and direction, and come closer to emulating the compartmentalisation of the cells as is seen *in vivo.*

6.4. Conclusions

The development of organised, long term 3D constructs for the co-culture of primary rat MDCs and motoneurons is possible using the protocols developed in this Thesis. Such constructs promote high levels of organised myotube development and represent a significant advantage over conventional culture systems in terms of modelling the *in vivo* tissue. The presented data indicate that primary and ESc-derived motoneuron survival is possible within this system. Motoneurons develop exploratory neurites which appear to interact with underlying myotubes, promoting varying levels of MDC maturation, as well as providing some evidence for synapse formation in these co-cultures.

This work demonstrates the possibilities of this 3D system for the *in vitro* investigation of neuromuscular interaction, and highlights the potential benefit to myotube maturation that incorporation of a biologically correct neural input has on the cultured cells. More work is now required to further develop both the biomimicity of this system as well as the means to effectively analyse the developed constructs. Continued optimisation and development of this culture system will likely be of substantial benefit to the future investigation of neuromuscular development, maturation and pathology *in vitro*.

7. References

Abou Neel, E. A., Cheema, U., Knowles, J. C., Brown, R. A. & Nazhat, S. N. (2006). Use of multiple unconfined compression for control of collagen gel scaffold density and mechanical properties. *Soft Matter* **2**, 986.

Akaaboune, M., Culican, S. M., Turney, S. G. & Lichtman, J. W. (1999). Rapid and reversible effects of activity on acetylcholine receptor density at the neuromuscular junction in vivo. *Science* **286**, 503-507.

Alberts, B., Johnson, A., Lewis, J., Raff, M., Roberts, K. & Walter, P. (2002). *Molecular Biology of the Cell*, 4th edn. Garland Science.

Alessandri-Haber, N., Paillart, C., Arsac, C., Gola, M., Couraud, F. & Crest, M. (1999). Specific distribution of sodium channels in axons of rat embryo spinal motoneurones. *J Physiol (Lond)* **518 (Pt 1)**, 203-214.

Allen, R. E., Rankin, L. L., Greene, E. A., Boxhorn, L. K., Johnson, S. E., Taylor, R. G. & Pierce, P. R. (1991). Desmin is present in proliferating rat muscle satellite cells but not in bovine muscle satellite cells. *J Cell Physiol* **149**, 525-535.

de Almeida, F. L. A., Pessotti, N. S., Pinhal, D., Padovani, C. R., Leitão, N. de J., Carvalho, R. F., Martins, C., Portella, M. C. & Dal Pai-Silva, M. (2010). Quantitative expression of myogenic regulatory factors MyoD and myogenin in pacu (Piaractus mesopotamicus) skeletal muscle during growth. *Micron* **41**, 997-1004.

Anderson, M. J. & Cohen, M. W. (1977). Nerve-induced and spontaneous redistribution of acetylcholine receptors on cultured muscle cells. *J Physiol* **268**, 757-773.

Ang, L. C., Bhaumick, B., Munoz, D. G., Sass, J. & Juurlink, B. H. (1992). Effects of astrocytes, insulin and insulin-like growth factor I on the survival of motoneurons in vitro. *J Neurol Sci* **109**, 168-172.

Arce, V., Pollock, R. A., Philippe, J. M., Pennica, D., Henderson, C. E. & deLapeyrière, O. (1998). Synergistic effects of schwann- and muscle-derived factors on motoneuron survival involve GDNF and cardiotrophin-1 (CT-1). *J Neurosci* **18**, 1440-1448.

Arsenijevic, Y. & Weiss, S. (1998). Insulin-Like Growth Factor-I Is a Differentiation Factor for Postmitotic CNS Stem Cell-Derived Neuronal Precursors: Distinct Actions from Those of Brain-Derived Neurotrophic Factor. *The Journal of Neuroscience* **18**, 2118 -2128.

Aviss, K. J., Gough, J. E. & Downes, S. (2010). Aligned electrospun polymer fibres for skeletal muscle regeneration. *Eur Cell Mater* **19**, 193-204.

Bach, A. D., Beier, J. P. & Stark, G. B. (2003). Expression of Trisk 51, agrin and nicotinic-acetycholine receptor epsilon-subunit during muscle development in a novel three-dimensional muscle-neuronal co-culture system. *Cell Tissue Res* **314**, 263-274.

Bailey, A. J., Shellswell, G. B. & Duance, V. C. (1979). Identification and change of collagen types in differentiating myoblasts and developing chick muscle. *Nature* **278**, 67-69.

Baldwin, K. M. & Haddad, F. (2001). Effects of different activity and inactivity paradigms on myosin heavy chain gene expression in striated muscle. *J Appl Physiol* **90**, 345-357.

Bárány, M. (1967). ATPase Activity of Myosin Correlated with Speed of Muscle Shortening. *J Gen Physiol* **50**, 197-218.

Baroffio, A., Aubry, J. P., Kaelin, A., Krause, R. M., Hamann, M. & Bader, C. R. (1993). Purification of human muscle satellite cells by flow cytometry. *Muscle Nerve* **16**, 498-505.

Beauchamp, J. R., Heslop, L., Yu, D. S., Tajbakhsh, S., Kelly, R. G., Wernig, A., Buckingham, M. E., Partridge, T. A. & Zammit, P. S. (2000). Expression of CD34 and Myf5 defines the majority of quiescent adult skeletal muscle satellite cells. *J Cell Biol* **151**, 1221-1234.

Bell, G., Emslie-Smith, D. & Patterson, C. (1980). *Textbook of Physiology*, 10th edn. New York: Churchill Livingstone.

Bergamin, E., Hallock, P. T., Burden, S. J. & Hubbard, S. R. (2010). The cytoplasmic adaptor protein Dok7 activates the receptor tyrosine kinase MuSK via dimerization. *Mol Cell* **39**, 100-109.

Bian, W. & Bursac, N. (2008). Tissue engineering of functional skeletal muscle: challenges and recent advances. *IEEE Eng Med Biol Mag* **27**, 109-113.

Bian, W., Liau, B., Badie, N. & Bursac, N. (2009). Mesoscopic hydrogel molding to control the 3D geometry of bioartificial muscle tissues. *Nat Protoc* **4**, 1522-1534.

Bischoff, R. (1974). Enzymatic liberation of myogenic cells from adult rat muscle. *Anat Rec* **180**, 645-661.

Bitar, M., Salih, V., Brown, R. A. & Nazhat, S. N. (2007). Effect of multiple unconfined compression on cellular dense collagen scaffolds for bone tissue engineering. *J Mater Sci Mater Med* **18**, 237-244.

Bladt, F., Riethmacher, D., Isenmann, S., Aguzzi, A. & Birchmeier, C. (1995). Essential role for the c-met receptor in the migration of myogenic precursor cells into the limb bud. *Nature* **376**, 768-771.

Blanton, J. R., Jr, Grant, A. L., McFarland, D. C., Robinson, J. P. & Bidwell, C. A. (1999). Isolation of two populations of myoblasts from porcine skeletal muscle. *Muscle Nerve* **22**, 43-50.

Bloch-Gallego, E., Huchet, M., el M'Hamdi, H., Xie, F. K., Tanaka, H. & Henderson, C. E. (1991). Survival in vitro of motoneurons identified or purified by novel antibody-based methods is selectively enhanced by muscle-derived factors. *Development* **111**, 221 -232.

Boonen, K. J. M., Langelaan, M. L. P., Polak, R. B., van der Schaft, D. W. J., Baaijens, F. P. T. & Post, M. J. (2010). Effects of a combined mechanical stimulation protocol: Value for skeletal muscle tissue engineering. *J Biomech* **43**, 1514-1521.

Borges, L. S., Yechikhov, S., Lee, Y. I., Rudell, J. B., Friese, M. B., Burden, S. J. & Ferns, M. J. (2008). Identification of a Motif in the Acetylcholine Receptor β Subunit Whose Phosphorylation Regulates Rapsyn Association and Postsynaptic Receptor Localization. *The Journal of Neuroscience* **28**, 11468 -11476.

Borschel, G. H., Dow, D. E., Dennis, R. G. & Brown, D. L. (2006). Tissue-Engineered Axially Vascularized Contractile Skeletal Muscle. *Plastic and Reconstructive Surgery* **117**, 2235-2242.

Brady, M. A., Lewis, M. P. & Mudera, V. (2008). Synergy between myogenic and non-myogenic cells in a 3D tissue-engineered craniofacial skeletal muscle construct. *J Tissue Eng Regen Med* **2**, 408-417.

Brand-Saberi, B., Gamel, A. J., Krenn, V., Müller, T. S., Wilting, J. & Christ, B. (1996). N-cadherin is involved in myoblast migration and muscle differentiation in the avian limb bud. *Dev Biol* **178**, 160-173.

Buckingham, M. & Relaix, F. (2007). The role of Pax genes in the development of tissues and organs: Pax3 and Pax7 regulate muscle progenitor cell functions. *Annu Rev Cell Dev Biol* **23**, 645-673.

Budnik, V. & Salinas, P. C. (2011). Wnt signaling during synaptic development and plasticity. *Curr Opin Neurobiol* **21**, 151-159.

Burridge, K. & Chrzanowska-Wodnicka, M. (1996). Focal adhesions, contractility, and signaling. *Annu Rev Cell Dev Biol* **12**, 463-518.

Camu, W., Bloch-Gallego, E. & Henderson, C. E. (1993). Purification of Spinal Motoneurons from Chicken and Rat Embryos by Immunopanning. *Neuroprotocols* **2**, 191-199.

Charge, S. B. P. & Rudnicki, M. A. (2004). Cellular and Molecular Regulation of Muscle Regeneration. *Physiological Reviews* **84**, 209 -238.

Cheema, U., Yang, S.-Y., Mudera, V., Goldspink, G. G. & Brown, R. A. (2003). 3-D in vitro model of early skeletal muscle development. *Cell Motil Cytoskeleton* **54**, 226-236.

Cheema, U., Brown, R., Mudera, V., Yang, S. Y., McGrouther, G. & Goldspink, G. (2005). Mechanical signals and IGF-I gene splicing in vitro in relation to development of skeletal muscle. *J Cell Physiol* **202**, 67-75.

Chen, F., Qian, L., Yang, Z.-H., Huang, Y., Ngo, S. T., Ruan, N.-J., Wang, J., Schneider, C., Noakes, P. G., & other authors. **(2007).** Rapsyn interaction

with calpain stabilizes AChR clusters at the neuromuscular junction. *Neuron* **55**, 247-260.

Christ, B. & Brand-Saberi, B. (2002). Limb muscle development. *Int J Dev Biol* **46**, 905-914.

Clow, C. & Jasmin, B. J. (2010). Brain-derived Neurotrophic Factor Regulates Satellite Cell Differentiation and Skeltal Muscle Regeneration. *Mol Biol Cell* **21**, 2182-2190.

Condon, K., Silberstein, L., Blau, H. M. & Thompson, W. J. (1990). Differentiation of fiber types in aneural musculature of the prenatal rat hindlimb. *Dev Biol* **138**, 275-295.

Cooper, S. T., Maxwell, A. L., Kizana, E., Ghoddusi, M., Hardeman, E. C., Alexander, I. E., Allen, D. G. & North, K. N. (2004). C2C12 co-culture on a fibroblast substratum enables sustained survival of contractile, highly differentiated myotubes with peripheral nuclei and adult fast myosin expression. *Cell Motil Cytoskeleton* **58**, 200-211.

Cornelison, D. D. & Wold, B. J. (1997). Single-cell analysis of regulatory gene expression in quiescent and activated mouse skeletal muscle satellite cells. *Dev Biol* **191**, 270-283.

Cosgrove, B. D., Sacco, A., Gilbert, P. M. & Blau, H. M. (2009). A home away from home: challenges and opportunities in engineering in vitro muscle satellite cell niches. *Differentiation* **78**, 185-194.

Cossu, G. & Borello, U. (1999). Wnt signaling and the activation of myogenesis in mammals. *EMBO J* **18**, 6867-6872.

Daniels, M. P., Lowe, B. T., Shah, S., Ma, J., Samuelsson, S. J., Lugo, B., Parakh, T. & Uhm, C. S. (2000). Rodent nerve-muscle cell culture system for studies of neuromuscular junction development: refinements and applications. *Microsc Res Tech* **49**, 26-37.

Das, M., Rumsey, J. W., Gregory, C. A., Bhargava, N., Kang, J.-F., Molnar, P., Riedel, L., Guo, X. & Hickman, J. J. (2007). Embryonic motoneuron-skeletal muscle co-culture in a defined system. *Neuroscience* **146**, 481-488.

Das, M., Rumsey, J. W., Bhargava, N., Gregory, C., Riedel, L., Kang, J. F. & Hickman, J. J. (2009). Developing a novel serum-free cell culture model of skeletal muscle differentiation by systematically studying the role of different growth factors in myotube formation. *In Vitro Cell Dev Biol Anim* **45**, 378-387.

Das, M., Rumsey, J. W., Bhargava, N., Stancescu, M. & Hickman, J. J. (2010). A defined long-term in vitro tissue engineered model of neuromuscular junctions. *Biomaterials* **31**, 4880-4888.

Dee, K., Freer, M., Mei, Y. & Weyman, C. M. (2002). Apoptosis coincident with the differentiation of skeletal myoblasts is delayed by caspase 3 inhibition and abrogated by MEK-independent constitutive Ras signaling. *Cell Death Differ* **9**, 209-218.

deLapeyrière, O. & Henderson, C. E. (1997). Motoneuron differentiation, survival and synaptogenesis. *Current Opinion in Genetics & Development* **7**, 642-650.

Dennis, R. G. & Kosnik, P. E. (2000). Excitability and Isometric Contractile Properties of Mammalian Skeletal Muscle Constructs Engineered in vitro. *In Vitro Cellular & Developmental Biology Animal* **36**, 327-335.

Dennis, R. G., Kosnik, P. E., Gilbert, M. E. & Faulkner, J. A. (2001). Excitability and contractility of skeletal muscle engineered from primary cultures and cell lines. *American Journal of Physiology - Cell Physiology* **280**, C288 -C295.

Dhawan, V., Lytle, I. F., Dow, D. E., Huang, Y.-C. & Brown, D. L. (2007). Neurotization improves contractile forces of tissue-engineered skeletal muscle. *Tissue Eng* **13**, 2813-2821.

Dobbins, G. C., Luo, S., Yang, Z., Xiong, W. C. & Mei, L. (2008). alpha-Actinin interacts with rapsyn in agrin-stimulated AChR clustering. *Mol Brain* **1**, 18.

Donnelly, K., Khodabukus, A., Philp, A., Deldicque, L., Dennis, R. G. & Baar, K. (2010). A novel bioreactor for stimulating skeletal muscle in vitro. *Tissue Eng Part C Methods* **16**, 711-718.

Duan, C., Ren, H. & Gao, S. (2010). Insulin-like growth factors (IGFs), IGF receptors, and IGF-binding proteins: Roles in skeletal muscle growth and differentiation. *General and Comparative Endocrinology* **167**, 344-351.

Eastwood, M., Porter, R., Khan, U., McGrouther, G. & Brown, R. (1996). Quantitative analysis of collagen gel contractile forces generated by dermal fibroblasts and the relationship to cell morphology. *J Cell Physiol* **166**, 33-42.

Eastwood, M., Mudera, V. C., McGrouther, D. A. & Brown, R. A. (1998). Effect of precise mechanical loading on fibroblast populated collagen lattices: morphological changes. *Cell Motil Cytoskeleton* **40**, 13-21.

Eisen, J. S. (1998). Genetic and molecular analyses of motoneuron development. *Current Opinion in Neurobiology* **8**, 697-704.

Faraut, B., Ravel-Chapuis, A., Bonavaud, S., Jandrot-Perrus, M., Verdière-Sahuqué, M., Schaeffer, L., Koenig, J. & Hantaï, D. (2004). Thrombin

reduces MuSK and acetylcholine receptor expression along with neuromuscular contact size in vitro. *Eur J Neurosci* **19**, 2099-2108.

Fear, J. (1977). Observations on the fusion of chick embryo myoblasts in culture. *J Anat* **124**, 437-444.

Finn, A. J., Feng, G. & Pendergast, A. M. (2003). Postsynaptic requirement for Abl kinases in assembly of the neuromuscular junction. *Nat Neurosci* **6**, 717-723.

Fischbach, G. D. (1970). Synaptic potentials recorded in cell cultures of nerve and muscle. *Science* **169**, 1331-1333.

Fischbach, G. D. (1972). Synapse formation between dissociated nerve and muscle cells in low density cell cultures. *Developmental Biology* **28**, 407-429.

Florini, J. R., Ewton, D. Z. & Coolican, S. A. (1996). Growth hormone and the insulin-like growth factor system in myogenesis. *Endocr Rev* **17**, 481-517.

Forcales, S. V. & Puri, P. L. (2005). Signaling to the chromatin during skeletal myogenesis: novel targets for pharmacological modulation of gene expression. *Semin Cell Dev Biol* **16**, 596-611.

Furuno, K., Goodman, M. N. & Goldberg, A. L. (1990). Role of different proteolytic systems in the degradation of muscle proteins during denervation atrophy. *J Biol Chem* **265**, 8550-8557.

Gamble, H. J., Fenton, J. & Allsopp, G. (1978). Electron microscope observations on human fetal striated muscle. *J Anat* **126**, 567-589.

Gershman, L. C., Dreizen, P. & Stracher, A. (1966). Subunit structure of myosin, II. Heavy and light alkali components. *Proc Natl Acad Sci U S A* **56**, 966-973.

Ghazanfari, N., Fernandez, K. J., Murata, Y., Morsch, M., Ngo, S. T., Reddel, S. W., Noakes, P. G. & Phillips, W. D. (2011). Muscle Specific Kinase: Organiser of synaptic membrane domains. *The International Journal of Biochemistry & Cell Biology* **43**, 295-298.

Gilmore, K. J., Kita, M., Han, Y., Gelmi, A., Higgins, M. J., Moulton, S. E., Clark, G. M., Kapsa, R. & Wallace, G. G. (2009). Skeletal muscle cell proliferation and differentiation on polypyrrole substrates doped with extracellular matrix components. *Biomaterials* **30**, 5292-5304.

Goldspink, D. F. (1976). The effects of denervation on protein turnover of rat skeletal muscle. *Biochem J* **156**, 71-80.

Gomes, A. V., Potter, J. D. & Szczesna-Cordary, D. (2002). The role of troponins in muscle contraction. *IUBMB Life* **54**, 323-333.

Gorza, L., Gundersen, K., Lømo, T., Schiaffino, S. & Westgaard, R. H. (1988). Slow-to-fast transformation of denervated soleus muscles by chronic high-frequency stimulation in the rat. *The Journal of Physiology* **402**, 627 -649.

Grefte, S., Kuijpers-Jagtman, A. M., Torensma, R. & Von den Hoff, J. W. (2007). Skeletal muscle development and regeneration. *Stem Cells Dev* **16**, 857-868.

Grill, S. E. & Rymer, W. Z. (1987). Beta-contributions to fusimotor action in triceps surae muscles of decerebrated cats. *J Neurophysiol* **57**, 574-595.

Grinnell, A. D. (1995). Dynamics of nerve-muscle interaction in developing and mature neuromuscular junctions. *Physiol Rev* **75**, 789-834.

Guo, X., Das, M., Rumsey, J., Gonzalez, M., Stancescu, M. & Hickman, J. (2010). Neuromuscular junction formation between human stem-cell-derived

motoneurons and rat skeletal muscle in a defined system. *Tissue Eng Part C Methods* **16**, 1347-1355.

Hadjipanayi, E., Mudera, V. & Brown, R. A. (2009). Close dependence of fibroblast proliferation on collagen scaffold matrix stiffness. *J Tissue Eng Regen Med* **3**, 77-84.

Hadjipanayi, E., Cheema, U., Mudera, V., Deng, D., Liu, W. & Brown, R. A. (2011). First implantable device for hypoxia-mediated angiogenic induction. *J Control Release*.

Henderson, C., Bloch-Gallego, E. & Camu, W. (1995). Purified Embryonic Motorneurons. In *Nerve Cell Culture: A Practical Approach*, pp. 69-81. Oxford University Press.

Henríquez, J. P. & Salinas, P. C. (2011). Dual roles for Wnt signalling during the formation of the vertebrate neuromuscular junction. *Acta Physiol (Oxf)*.

Henriquez, J. P., Webb, A., Bence, M., Bildsoe, H., Sahores, M., Hughes, S. M. & Salinas, P. C. (2008). Wnt signaling promotes AChR aggregation at the neuromuscular synapse in collaboration with agrin. *Proceedings of the National Academy of Sciences* **105**, 18812 -18817.

Hinds, S., Bian, W., Dennis, R. G. & Bursac, N. (2011). The role of extracellular matrix composition in structure and function of bioengineered skeletal muscle. *Biomaterials* **32**, 3575-3583.

Houenou, L. J., Haverkamp, L. J., McManaman, J. L. & Oppenheim, R. W. (1991). The regulation of motoneuron survival and differentiation by putative muscle-derived neurotrophic agents: neuromuscular activity and innervation. *Development* **Suppl 2**, 149-155.

Huang, N. F., Patel, S., Thakar, R. G., Wu, J., Hsiao, B. S., Chu, B., Lee, R. J. & Li, S. (2006). Myotube assembly on nanofibrous and micropatterned polymers. *Nano Lett* **6**, 537-542.

Hughes, S. M. & Salinas, P. C. (1999). Control of muscle fibre and motoneuron diversification. *Curr Opin Neurobiol* **9**, 54-64.

Irintchev, A., Zeschnigk, M., Starzinski-Powitz, A. & Wernig, A. (1994). Expression pattern of M-cadherin in normal, denervated, and regenerating mouse muscles. *Dev Dyn* **199**, 326-337.

Jagla, K., Dolle, P., Mattei, M.-G., Jagla, T., Schuhbaur, B., Dretzen, G., Bellard, F. & Bellard, M. (1995). Mouse Lbx1 and human LBX1 define a novel mammalian homeobox gene family related to the Drosophila lady bird genes. *Mechanisms of Development* **53**, 345-356.

Janz, R., Goda, Y., Geppert, M., Missler, M. & Südhof, T. C. (1999). SV2A and SV2B Function as Redundant Ca2+ Regulators in Neurotransmitter Release. *Neuron* **24**, 1003-1016.

Jing, L., Lefebvre, J. L., Gordon, L. R. & Granato, M. (2009). Wnt Signals Organize Synaptic Prepattern and Axon Guidance through the Zebrafish unplugged/MuSK Receptor. *Neuron* **61**, 721-733.

Jones, S. P. & Ridge, R. M. (1987). Motor units in a skeletal muscle of neonatal rat: mechanical properties and weak neuromuscular transmission. *J Physiol* **386**, 355-375.

Kääriäinen, M., Järvinen, T., Järvinen, M., Rantanen, J. & Kalimo, H. (2000). Relation between myofibers and connective tissue during muscle injury repair. *Scand J Med Sci Sports* **10**, 332-337.

Kalmar, B. & Greensmith, L. (2009). Activation of the heat shock response in a primary cellular model of motoneuron neurodegeneration-evidence for neuroprotective and neurotoxic effects. *Cell Mol Biol Lett* **14**, 319-335.

Kanning, K. C., Kaplan, A. & Henderson, C. E. (2010). Motor neuron diversity in development and disease. *Annu Rev Neurosci* **33**, 409-440.

Kassar-Duchossoy, L., Gayraud-Morel, B., Gomes, D., Rocancourt, D., Buckingham, M., Shinin, V. & Tajbakhsh, S. (2004). Mrf4 determines skeletal muscle identity in Myf5:Myod double-mutant mice. *Nature* **431**, 466-471.

Kaufman, S. J., George-Weinstein, M. & Foster, R. F. (1991). In vitro development of precursor cells in the myogenic lineage. *Dev Biol* **146**, 228-238.

Khodabukus, A. & Baar, K. (2009). Regulating fibrinolysis to engineer skeletal muscle from the C2C12 cell line. *Tissue Eng Part C Methods* **15**, 501-511.

Khodabukus, A., Paxton, J. Z., Donnelly, K. & Baar, K. (2007). Engineered muscle: a tool for studying muscle physiology and function. *Exerc Sport Sci Rev* **35**, 186-191.

Kjær, M. (2004). Role of Extracellular Matrix in Adaptation of Tendon and Skeletal Muscle to Mechanical Loading. *Physiological Reviews* **84**, 649 -698.

Kleinman, H. K. & Martin, G. R. (2005). Matrigel: basement membrane matrix with biological activity. *Semin Cancer Biol* **15**, 378-386.

Kostrominova, T. Y., Calve, S., Arruda, E. M. & Larkin, L. M. (2009). Ultrastructure of myotendinous junctions in tendon-skeletal muscle constructs engineered in vitro. *Histol Histopathol* **24**, 541-550.

Kovanen, V., Suominen, H. & Heikkinen, E. (1980). Connective tissue of “fast” and “slow” skeletal muscle in rats--effects of endurance training. *Acta Physiol Scand* **108**, 173-180.

Kummer, T. T., Misgeld, T. & Sanes, J. R. (2006). Assembly of the postsynaptic membrane at the neuromuscular junction: paradigm lost. *Current Opinion in Neurobiology* **16**, 74-82.

Langelaan, M. L. P., Boonen, K. J. M., Rosaria-Chak, K. Y., van der Schaft, D. W. J., Post, M. J. & Baaijens, F. P. T. (2010). Advanced maturation by electrical stimulation: Differences in response between C2C12 and primary muscle progenitor cells. *J Tissue Eng Regen Med*.

Lanuza, M. A., Garcia, N., Santafé, M., González, C. M., Alonso, I., Nelson, P. G. & Tomàs, J. (2002). Pre- and postsynaptic maturation of the neuromuscular junction during neonatal synapse elimination depends on protein kinase C. *J Neurosci Res* **67**, 607-617.

Lanuza, M. A., Gizaw, R., Viloria, A., González, C. M., Besalduch, N., Dunlap, V., Tomàs, J. & Nelson, P. G. (2006). Phosphorylation of the nicotinic acetylcholine receptor in myotube-cholinergic neuron cocultures. *J Neurosci Res* **83**, 1407-1414.

Larkin, L. M., Van der Meulen, J. H., Dennis, R. G. & Kennedy, J. B. (2006a). Functional evaluation of nerve-skeletal muscle constructs engineered in vitro. *In Vitro Cell Dev Biol Anim* **42**, 75-82.

Larkin, L. M., Calve, S., Kostrominova, T. Y. & Arruda, E. M. (2006b). Structure and Functional Evaluation of Tendon–Skeletal Muscle Constructs Engineered *in Vitro*. *Tissue Engineering* **12**, 3149-3158.

Leeson, T., Leeson, C. & Paparo, A. (1988). *Text/ Atlas of Histology*, 1st edn. London, UK: WB Saunders.

Levenberg, S., Rouwkema, J., Macdonald, M., Garfein, E. S., Kohane, D. S., Darland, D. C., Marini, R., van Blitterswijk, C. A., Mulligan, R. C., & other authors. **(2005).** Engineering vascularized skeletal muscle tissue. *Nat Biotechnol* **23**, 879-884.

Lewis, M. P., Tippett, H. L., Sinanan, A. C., Morgan, M. J. & Hunt, N. P. (2000). Gelatinase-B (matrix metalloproteinase-9; MMP-9) secretion is involved in the migratory phase of human and murine muscle cell cultures. *J Muscle Res Cell Motil* **21**, 223-233.

Lewis, M. P., Machell, J. R. A., Hunt, N. P., Sinanan, A. C. M. & Tippett, H. L. (2001). The extracellular matrix of muscle – implications for manipulation of the craniofacial musculature. *European Journal of Oral Sciences* **109**, 209-221.

Liao, H. & Zhou, G.-Q. (2009). Development and progress of engineering of skeletal muscle tissue. *Tissue Eng Part B Rev* **15**, 319-331.

Li, H. & Capetanaki, Y. (1993). Regulation of the mouse desmin gene: transactivated by MyoD, myogenin, MRF4 and Myf5. *Nucleic Acids Res* **21**, 335-343.

Lindon, C., Albagli, O., Pinset, C. & Montarras, D. (2001). Cell density-dependent induction of endogenous myogenin (myf4) gene expression by Myf5. *Dev Biol* **240**, 574-584.

Lin, W., Burgess, R. W., Dominguez, B., Pfaff, S. L., Sanes, J. R. & Lee, K.-F. (2001). Distinct roles of nerve and muscle in postsynaptic differentiation of the neuromuscular synapse. *Nature* **410**, 1057-1064.

Li, X.-M., Dong, X.-P., Luo, S.-W., Zhang, B., Lee, D.-H., Ting, A. K. L., Neiswender, H., Kim, C.-H., Carpenter-Hyland, E., & other authors. **(2008).** Retrograde regulation of motoneuron differentiation by muscle beta-catenin. *Nat Neurosci* **11**, 262-268.

Lowey, S. & Risby, D. (1971). Light Chains from Fast and Slow Muscle Myosins. *Nature* **234**, 81-85.

Lumley, J. S. ., Craven, J. L. & Aitken, J. T. (1980). *Essential Anatomy*, 3rd edn. New York: Churchill Livingstone.

Luo, S., Zhang, B., Dong, X.-P., Tao, Y., Ting, A., Zhou, Z., Meixiong, J., Luo, J., Chiu, F. C. A., & other authors. **(2008).** HSP90 beta regulates rapsyn turnover and subsequent AChR cluster formation and maintenance. *Neuron* **60**, 97-110.

Luo, Z. G., Je, H.-S., Wang, Q., Yang, F., Dobbins, G. C., Yang, Z.-H., Xiong, W. C., Lu, B. & Mei, L. (2003). Implication of geranylgeranyltransferase I in synapse formation. *Neuron* **40**, 703-717.

Machida, S., Spangenburg, E. E. & Booth, F. W. (2004). Primary rat muscle progenitor cells have decreased proliferation and myotube formation during passages. *Cell Prolif* **37**, 267-277.

Manzano, R., Toivonen, J. M., Calvo, A. C., Miana-Mena, F. J., Zaragoza, P., Muñoz, M. J., Montarras, D. & Osta, R. (2011). Sex, fiber-type and age

dependent in vitro proliferation of mouse muscle satellite cells. *J Cell Biochem*.

di Maso, N. A., Caiozzo, V. J. & Baldwin, K. M. (2000). Single-fiber myosin heavy chain polymorphism during postnatal development: modulation by hypothyroidism. *Am J Physiol Regul Integr Comp Physiol* **278**, R1099-1106.

Masuko, S., Kuromi, H. & Shimada, Y. (1979). Isolation and culture of motoneurons from embryonic chicken spinal cords. *Proc Natl Acad Sci U S A* **76**, 3537-3541.

McKeon-Fischer, K. D. & Freeman, J. W. (2010). Characterization of electrospun poly(L-lactide) and gold nanoparticle composite scaffolds for skeletal muscle tissue engineering. *J Tissue Eng Regen Med*.

McKeon, K. D., Lewis, A. & Freeman, J. W. (2010). Electrospun poly(D,L-lactide) and polyaniline scaffold characterization. *J Appl Polym Sci* **115**, 1566-1572.

Midrio, M. (2006). The denervated muscle: facts and hypotheses. A historical review. *Eur J Appl Physiol* **98**, 1-21.

Miles, G. B., Yohn, D. C., Wichterle, H., Jessell, T. M., Rafuse, V. F. & Brownstone, R. M. (2004). Functional Properties of Motoneurons Derived from Mouse Embryonic Stem Cells. *The Journal of Neuroscience* **24**, 7848 - 7858.

Mittaud, P., Camilleri, A. A., Willmann, R., Erb-Vogtli, S., Burden, S. J. & Fuhrer, C. (2004). A Single Pulse of Agrin Triggers a Pathway That Acts To Cluster Acetylcholine Receptors. *Mol Cell Biol* **24**, 7841-7854.

Molnar, G., Ho, M. L. & Schroedl, N. A. (1996). Evidence for multiple satellite cell populations and a non-myogenic cell type that is regulated differently in regenerating and growing skeletal muscle. *Tissue Cell* **28**, 547-556.

Mudera, V., Smith, A. S. T., Brady, M. A. & Lewis, M. P. (2010). The effect of cell density on the maturation and contractile ability of muscle derived cells in a 3D tissue-engineered skeletal muscle model and determination of the cellular and mechanical stimuli required for the synthesis of a postural phenotype. *J Cell Physiol* **225**, 646-653.

Navarrette, R. & Vrbová, G. (1993). Activity-dependent interactions between motoneurones and muscles: their role in the development of the motor unit. *Prog Neurobiol* **41**, 93-124.

Nguyen, Q. T. & Lichtman, J. W. (1996). Mechanism of synapse disassembly at the developing neuromuscular junction. *Current Opinion in Neurobiology* **6**, 104-112.

Nicolas-Bolnet, C. & Dieterlen-Lievre, F. (1995). In vitro survival and multiplication of chicken myeloblasts promoted for several weeks by chick embryo extract. *Poult Sci* **74**, 942-950.

Okada, K., Inoue, A., Okada, M., Murata, Y., Kakuta, S., Jigami, T., Kubo, S., Shiraishi, H., Eguchi, K., & other authors. **(2006).** The muscle protein Dok-7 is essential for neuromuscular synaptogenesis. *Science* **312**, 1802-1805.

Pette, D. & Staron, R. S. (2000). Myosin isoforms, muscle fiber types, and transitions. *Microsc Res Tech* **50**, 500-509.

Pette, D. & Vrbová, G. (1999). What does chronic electrical stimulation teach us about muscle plasticity? *Muscle Nerve* **22**, 666-677.

Placantonakis, D. G., Tomishima, M. J., Lafaille, F., Desbordes, S. C., Jia, F., Socci, N. D., Viale, A., Lee, H., Harrison, N., & other authors. **(2009).** BAC transgenesis in human embryonic stem cells as a novel tool to define the human neural lineage. *Stem Cells* **27**, 521-532.

Prockop, D. J. & Kivirikko, K. I. (1995). Collagens: molecular biology, diseases, and potentials for therapy. *Annu Rev Biochem* **64**, 403-434.

Qian, Y. K., Chan, A. W. S., Madhavan, R. & Peng, H. B. (2008). The function of Shp2 tyrosine phosphatase in the dispersal of acetylcholine receptor clusters. *BMC Neurosci* **9**, 70.

Relaix, F., Rocancourt, D., Mansouri, A. & Buckingham, M. (2005). A Pax3/Pax7-dependent population of skeletal muscle progenitor cells. *Nature* **435**, 948-953.

Reubinoff, B. E., Itsykson, P., Turetsky, T., Pera, M. F., Reinhartz, E., Itzik, A. & Ben-Hur, T. (2001). Neural progenitors from human embryonic stem cells. *Nat Biotech* **19**, 1134-1140.

Ribchester, R. R. (2009). Neuromuscular Junction: Synapse Elimination. In *Encyclopedia of Neuroscience*, pp. 663-670. Oxford: Academic Press.

Rouger, K., Fornasari, B., Armengol, V., Jouvion, G., Leroux, I., Dubreil, L., Feron, M., Guevel, L. & Cherel, Y. (2007). Progenitor Cell Isolation from Muscle-derived Cells based on Adhesion Properties. *Journal of Histochemistry & Cytochemistry* **55**, 607 -618.

Rudnicki, M. A., Schnegelsberg, P. N., Stead, R. H., Braun, T., Arnold, H. H. & Jaenisch, R. (1993). MyoD or Myf-5 is required for the formation of skeletal muscle. *Cell* **75**, 1351-1359.

Sanes, J. R. & Lichtman, J. W. (2001). Induction, assembly, maturation and maintenance of a postsynaptic apparatus. *Nat Rev Neurosci* **2**, 791-805.

Savolainen, J., Väänänen, K., Puranen, J., Takala, T. E., Komulainen, J. & Vihko, V. (1988). Collagen synthesis and proteolytic activities in rat skeletal muscles: effect of cast-immobilization in the lengthened and shortened positions. *Arch Phys Med Rehabil* **69**, 964-969.

Saxena, A. K., Marler, J., Benvenuto, M., Willital, G. H. & Vacanti, J. P. (1999). Skeletal muscle tissue engineering using isolated myoblasts on synthetic biodegradable polymers: preliminary studies. *Tissue Eng* **5**, 525-532.

Saxena, A. K., Willital, G. H. & Vacanti, J. P. (2001). Vascularized three-dimensional skeletal muscle tissue-engineering. *Biomed Mater Eng* **11**, 275-281.

Schmalbruch, H. (1990). Growth and denervation response of skeletal muscle fibers of newborn rats. *Muscle & Nerve* **13**, 421-432.

Schultz, E., Jaryszak, D. L., Gibson, M. C. & Albright, D. J. (1986). Absence of exogenous satellite cell contribution to regeneration of frozen skeletal muscle. *J Muscle Res Cell Motil* **7**, 361-367.

Sciote, J. J. & Morris, T. J. (2000). Skeletal muscle function and fibre types: the relationship between occlusal function and the phenotype of jaw-closing muscles in human. *J Orthod* **27**, 15-30.

Shafit-Zagardo, B. & Kalcheva, N. (1998). Making sense of the multiple MAP-2 transcripts and their role in the neuron. *Mol Neurobiol* **16**, 149-162.

Shefer, G., Van de Mark, D. P., Richardson, J. B. & Yablonka-Reuveni, Z. (2006). Satellite-cell pool size does matter: defining the myogenic potency of aging skeletal muscle. *Dev Biol* **294**, 50-66.

Sinanan, A. C. M., Hunt, N. P. & Lewis, M. P. (2004). Human adult craniofacial muscle-derived cells: neural-cell adhesion-molecule (NCAM; CD56)-expressing cells appear to contain multipotential stem cells. *Biotechnol Appl Biochem* **40**, 25-34.

Sinanan, A. C. M., Buxton, P. G. & Lewis, M. P. (2006). Muscling in on stem cells. *Biol Cell* **98**, 203-214.

Singh, A., Nelson-Moon, Z. L., Thomas, G. J., Hunt, N. P. & Lewis, M. P. (2000). Identification of matrix metalloproteinases and their tissue inhibitors type 1 and 2 in human masseter muscle. *Arch Oral Biol* **45**, 431-440.

Slater, C. R. (1976). Control of myogenesis in vitro by chick embryo extract. *Dev Biol* **50**, 264-284.

Smith, A. S. T., Shah, R., Hunt, N. P. & Lewis, M. P. (2010). The Role of Connective Tissue and Extracellular Matrix Signaling in Controlling Muscle Development, Function, and Response to Mechanical Forces. *Seminars in Orthodontics* **16**, 135-142.

Smith, C. K., 2nd, Janney, M. J. & Allen, R. E. (1994). Temporal expression of myogenic regulatory genes during activation, proliferation, and differentiation of rat skeletal muscle satellite cells. *J Cell Physiol* **159**, 379-385.

Spangenburg, E. E. & Booth, F. W. (2003). Molecular regulation of individual skeletal muscle fibre types. *Acta Physiol Scand* **178**, 413-424.

Strohman, R. C., Bayne, E., Spector, D., Obinata, T., Micou-Eastwood, J. & Maniotis, A. (1990). Myogenesis and Histogenesis of Skeletal Muscle on Flexible Membranes in vitro. *In Vitro Cellular & Developmental Biology* **26**, 201-208.

Tajbakhsh, S. (2009). Skeletal muscle stem cells in developmental versus regenerative myogenesis. *Journal of Internal Medicine* **266**, 372-389.

Tang, H., Veldman, M. B. & Goldman, D. (2006). Characterization of a muscle-specific enhancer in human MuSK promoter reveals the essential role of myogenin in controlling activity-dependent gene regulation. *J Biol Chem* **281**, 3943-3953.

Taylor, A. R., Gifondorwa, D. J., Newbern, J. M., Robinson, M. B., Strupe, J. L., Prevette, D., Oppenheim, R. W. & Milligan, C. E. (2007). Astrocyte and muscle-derived secreted factors differentially regulate motoneuron survival. *J Neurosci* **27**, 634-644.

Ten Broek, R. W., Grefte, S. & Von den Hoff, J. W. (2010). Regulatory factors and cell populations involved in skeletal muscle regeneration. *Journal of Cellular Physiology* **224**, 7-16.

Vandenburgh, H., Del Tatto, M., Shansky, J., Lemaire, J., Chang, A., Payumo, F., Lee, P., Goodyear, A. & Raven, L. (1996). Tissue-engineered skeletal muscle organoids for reversible gene therapy. *Hum Gene Ther* **7**, 2195-2200.

Vandenburgh, H. H., Karlisch, P. & Farr, L. (1988). Maintenance of highly contractile tissue-cultured avian skeletal myotubes in collagen gel. *In Vitro Cell Dev Biol* **24**, 166-174.

Vandenburgh, H. H., Shansky, J., Karlisch, P. & Solerssi, R. L. (1993). Mechanical stimulation of skeletal muscle generates lipid-related second messengers by phospholipase activation. *J Cell Physiol* **155**, 63-71.

Vandenburgh, H., Shansky, J., Benesch-Lee, F., Barbata, V., Reid, J., Thorrez, L., Valentini, R. & Crawford, G. (2008). Drug-screening platform based on the contractility of tissue-engineered muscle. *Muscle Nerve* **37**, 438-447.

Vrbova, G., Gordon, T. & Jones, R. (1995). *Nerve-Muscle Interaction*, 2nd edn. London, UK: Chapman & Hall.

Weiss, A. & Leinwand, L. A. (1996). The mammalian myosin heavy chain gene family. *Annu Rev Cell Dev Biol* **12**, 417-439.

Weiss, A., Schiaffino, S. & Leinwand, L. A. (1999). Comparative sequence analysis of the complete human sarcomeric myosin heavy chain family: implications for functional diversity. *Journal of Molecular Biology* **290**, 61-75.

Weston, C., Gordon, C., Teressa, G., Hod, E., Ren, X.-D. & Prives, J. (2003). Cooperative regulation by Rac and Rho of agrin-induced acetylcholine receptor clustering in muscle cells. *J Biol Chem* **278**, 6450-6455.

Whitesides, G. M., Ostuni, E., Takayama, S., Jiang, X. & Ingber, D. E. (2001). Soft lithography in biology and biochemistry. *Annu Rev Biomed Eng* **3**, 335-373.

Wichterle, H., Lieberam, I., Porter, J. A. & Jessell, T. M. (2002). Directed Differentiation of Embryonic Stem Cells into Motor Neurons. *Cell* **110**, 385-397.

Wu, H., Xiong, W. C. & Mei, L. (2010). To build a synapse: signaling pathways in neuromuscular junction assembly. *Development* **137**, 1017-1033.

Xie, Z. P. & Poo, M. M. (1986). Initial events in the formation of neuromuscular synapse: rapid induction of acetylcholine release from embryonic neuron. *Proc Natl Acad Sci USA* **83**, 7069-7073.

Yablonka-Reuveni, Z. & Rivera, A. J. (1994). Temporal expression of regulatory and structural muscle proteins during myogenesis of satellite cells on isolated adult rat fibers. *Dev Biol* **164**, 588-603.

Yablonka-Reuveni, Z., Day, K., Vine, A. & Shefer, G. (2008). Defining the transcriptional signature of skeletal muscle stem cells. *Journal of Animal Science* **86**, E207 -E216.

Yasin, R., Van Beers, G., Nurse, K. C., Al-Ani, S., Landon, D. N. & Thompson, E. J. (1977). A quantitative technique for growing human adult skeletal muscle in culture starting from mononucleated cells. *J Neurol Sci* **32**, 347-360.

Zammit, P. & Beauchamp, J. (2001). The skeletal muscle satellite cell: stem cell or son of stem cell? *Differentiation* **68**, 193-204.

Zhang, B., Luo, S., Wang, Q., Suzuki, T., Xiong, W. C. & Mei, L. (2008). LRP4 serves as a coreceptor of agrin. *Neuron* **60**, 285-297.

8. Appendices

8.1. Appendix A

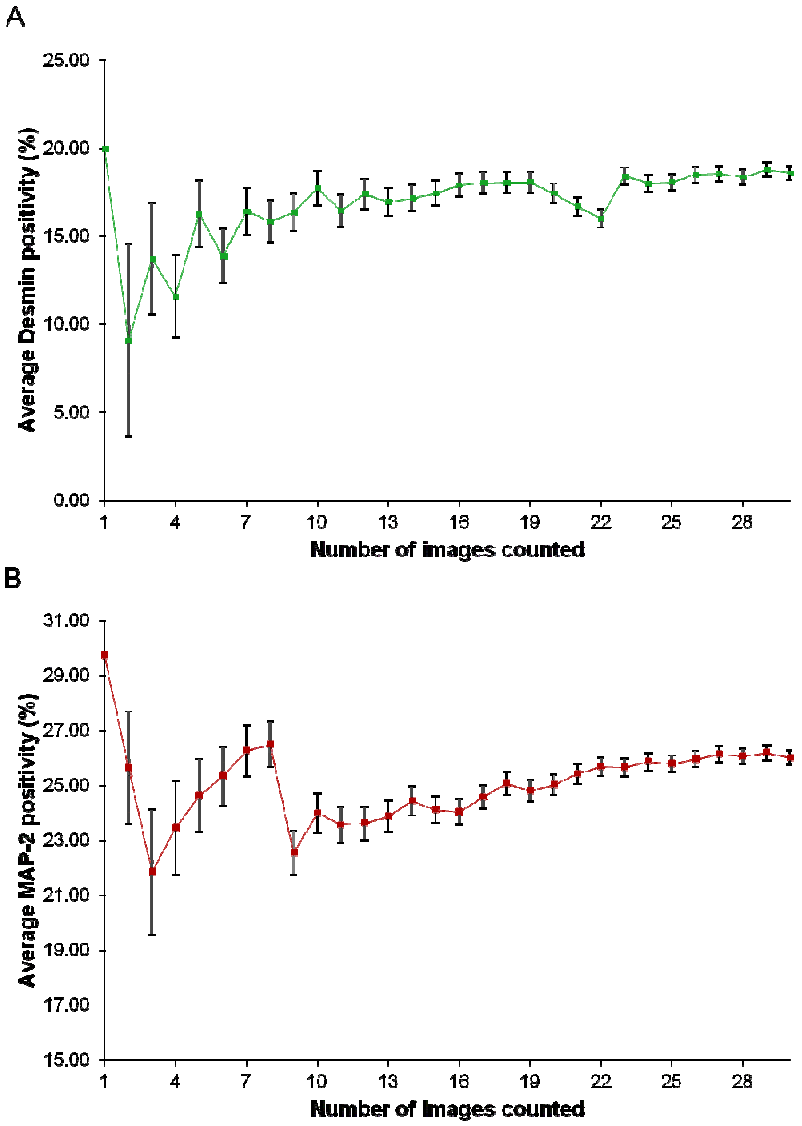

Appendix A: Cumulative frequency analysis in 2D culture. (A) Example of a cumulative frequency study measuring desmin positivity from 2D cultures of primary rat MDCs. (B) Example of cumulative frequency study measuring MAP-2 positvity from 2D cultures of mixed ventral horn cells. In each case a running total was recorded and used to calculate the mean after each new image was analysed. The process continued until fluctuations in the mean levelled out. Error bars = standard error of the mean.

8.2. Appendix B

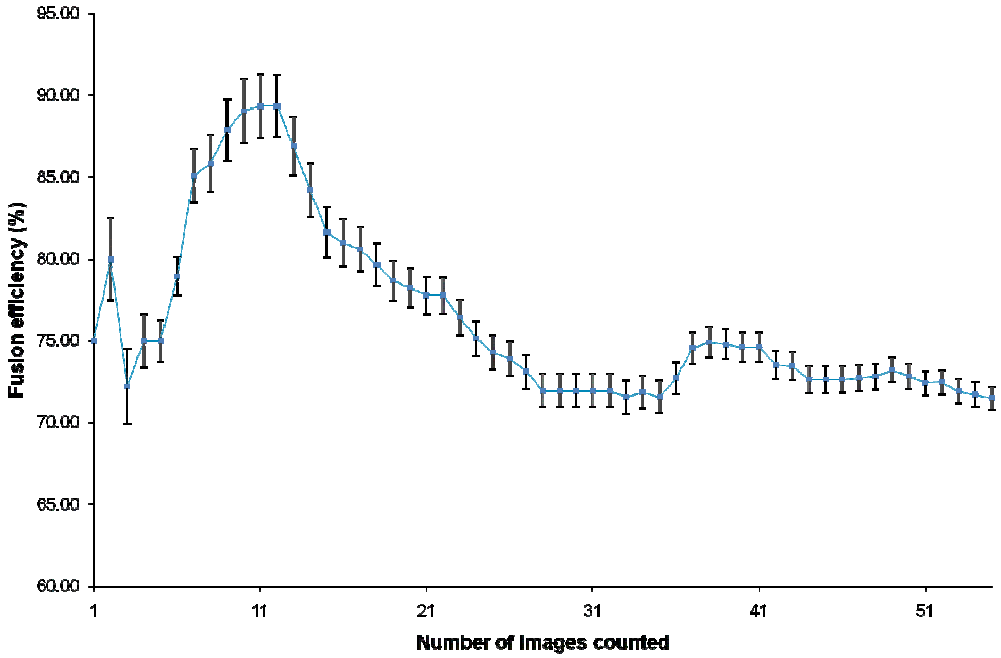

Appendix B: Cumulative frequency analysis in 3D culture. Example of a cumulative frequency study measuring the fusion efficiency from a 3D culture of primary rat MDCs. A running total was recorded and used to calculate the mean after each new image was analysed. The process continued until fluctuations in the mean levelled out. Error bars = standard error of the mean.

8.3. Appendix C

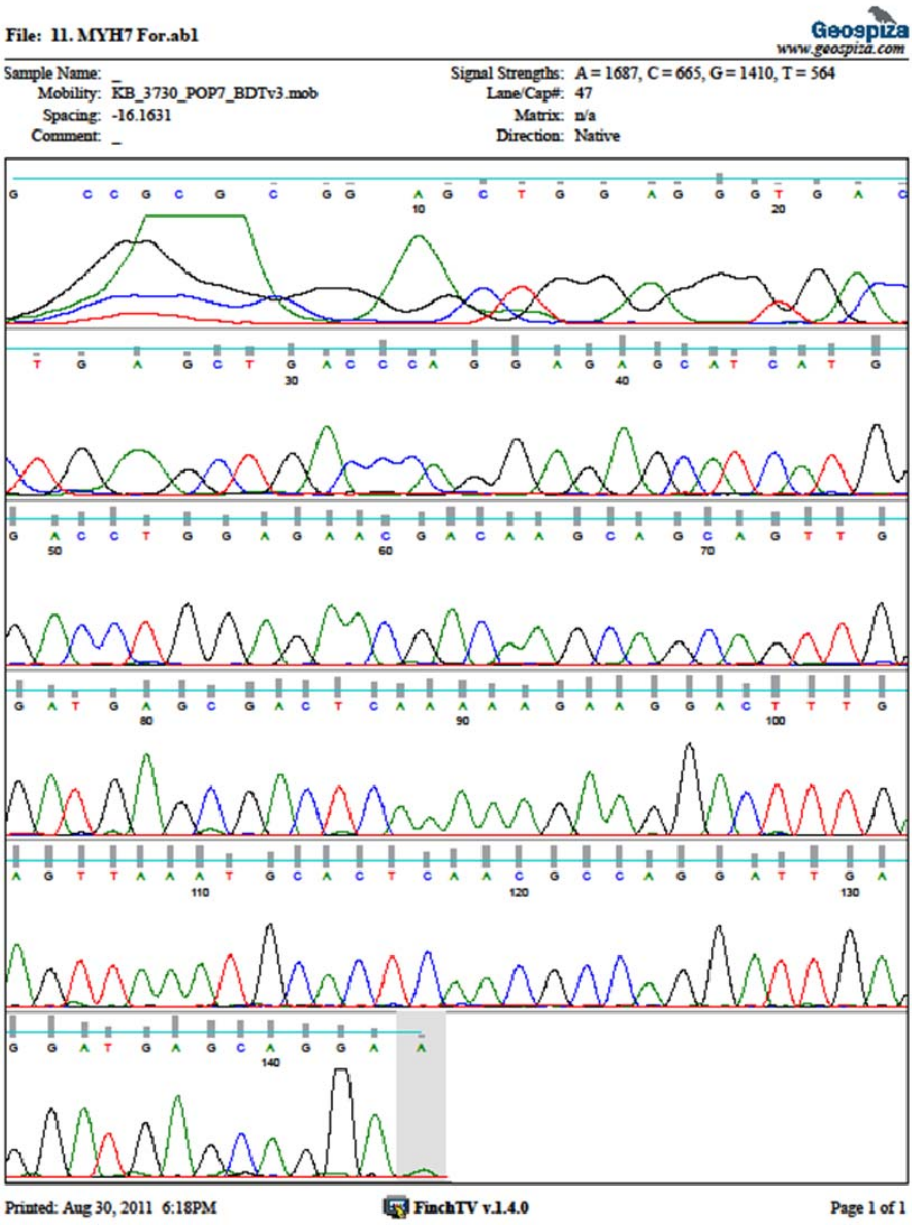

Appendix C: An example of the sequence data provided by GeneService. The data for the *MYH7* forward primer is shown. All returned sequences were compared to the known gene sequence, in order to confirm the validity of the designed primers for use in PCR and qPCR analysis.